

UNIVERZITA KARLOVA
Lékařská fakulta v Hradci Králové

DISERTAČNÍ PRÁCE

Doktorský studijní program
Lékařská chemie a biochemie

***In vitro* studium mechanismu protinádorového účinku
montaninových alkaloidů čeledi Amaryllidaceae**

***In vitro* study of anticancer effect of Amaryllidaceae montanine
alkaloids**

Mgr. Darja Koutová

Školitel: RNDr. Radim Havelek, Ph.D.

Prohlášení autora

Prohlášení:

Prohlašuji tímto, že jsem doktorskou disertační práci zpracovala samostatně, a že jsem uvedla všechny použité informační zdroje. Zároveň dávám souhlas k tomu, aby tato práce byla uložena v Lékařské knihovně Lékařské fakulty v Hradci Králové a zde užívána ke studijním účelům za předpokladu, že každý, kdo tuto práci použije pro svou publikační nebo přednáškovou činnost, se zavazuje, že bude tento zdroj informací řádně citovat.

Souhlasím se zpřístupněním elektronické verze mé práce v informačním systému Univerzity Karlovy, Praha.

Tato práce byla finančně podporována granty Lékařské fakulty v Hradci Králové: SVV260543 a PROGRES Q40/1

Hradec Králové, 2022

Darja Koutová

PODĚKOVÁNÍ

Velmi si vážím jakékoliv pomoci, které se mi během mého doktorského studia dostalo. Nebýt významné ochoty mých kolegů a přátel z Ústavu lékařské biochemie Lékařské fakulty v Hradci Králové kdykoliv mi poskytnout cenné rady a pomocnou ruku, nebylo by možné obsáhnout veškeré požadavky, které si tato práce nárokovala splnit. Rovněž by tato práce nevznikla bez vysoce odborného, komplexního a ochotného přístupu kolegů z Katedry farmaceutické botaniky Farmaceutické fakulty Univerzity Karlovy v Hradci Králové.

Mé díky patří především:

Panu školiteli RNDr. Radimovi Havelkovi, Ph.D. za vynikající odborné a systematické vedení mé doktorské práce a předávání cenných zkušeností, rad i konstruktivních postřehů, které významnou měrou přispěly nejen ke vzniku této práce, ale také ke kvalitě publikací, jež během mého studia vznikly. A neméně významně bych rovněž chtěla poděkovat za trpělivý a přátelský postoj, který toto úsilí provázel.

Paní přednostce prof. MUDr. Martině Řezáčové, Ph.D. za expertní, profesionální a zároveň přátelský přístup, cenné rady, odborné konzultace a vytvoření dokonalých podmínek k mému studiu i profesnímu růstu.

Paní prof. Ing. Lucii Cahlíkové, Ph.D. jež se se svou bohatou zkušeností a erudicí podílela na vzniku a designu tohoto díla a svými cennými kritickými připomínkami, odborným dohledem i tvůrčí publikační činností přispěla k vysoké kvalitě publikovaných prací.

Paní PharmDr. Kateřině Hradiské Breiterové, Ph.D. a paní Mgr. Negar Maafi, které se podílely na izolaci a charakterizaci alkaloidů čeledi Amaryllidaceae a za jejich spolupráci při řešení dílčích publikačních a experimentálních úkolů.

Paní Nadě Mazánkové a paní Boženě Jánské za usilovnou a pečlivou technickou spolupráci při řešení experimentálních úkolů.

Celému kolektivu Ústavu lékařské biochemie, jmenovitě pak paní Mgr. Martině Majorošové, Ph.D. a paní PharmDr. Darině Muthné, Ph.D. za předání jejich cenných zkušeností a za jejich vytrvalou, obětavou pomoc při řešení nejen pracovních úkolů.

Zvláštní poděkování pak patří mému manželovi, dětem a rodičům, neb bez jejich podpory, úsměvu, vytrvalé pomoci a oběti by tato práce také nevznikla.

OBSAH

PODĚKOVÁNÍ	4
OBSAH	5
SEZNAM POUŽITÝCH ZKRATEK	6
SOUHRN	8
SUMMARY	10
1 CÍLE DISERTAČNÍ PRÁCE	12
2 SEZNAM PUBLIKACÍ A PŘÍSPĚVEK AUTORA V JEDNOTLIVÝCH PUBLIKACÍCH	13
2.1 CHEMICAL AND BIOLOGICAL ASPECTS OF MONTANINE-TYPE ALKALOIDS ISOLATED FROM PLANTS OF THE AMARYLLIDACEAE FAMILY	13
2.2 ALKALOID PROFILING OF <i>HIPPEASTRUM</i> CULTIVARS BY GC-MS, ISOLATION OF AMARYLLIDACEAE ALKALOIDS AND EVALUATION OF THEIR CYTOTOXICITY	13
2.3 AMARYLLIDACEAE ALKALOIDS OF DIFFERENT STRUCTURAL TYPES FROM <i>NARCISSUS</i> L. CV. PROFESSOR EINSTEIN AND THEIR CYTOTOXIC ACTIVITY	14
2.4 PANCRACINE, A MONTANINE-TYPE AMARYLLIDACEAE ALKALOID, INHIBITS PROLIFERATION OF A549 LUNG ADENOCARCINOMA CELLS AND INDUCES APOPTOTIC CELL DEATH IN MOLT-4 LEUKEMIC CELLS	15
3 ÚVOD DO PROBLEMATIKY	16
3.1 BUNĚČNÝ CYKLUS	16
3.2 ZÁSTAVA V KONTROLNÍM BODĚ G1/S	17
3.3 ZÁSTAVA V KONTROLNÍM BODĚ G2/M	18
3.4 TYPY BUNĚČNÉ SMRTI	19
3.4.1 Apoptóza	19
3.4.2 Autofagie	21
3.4.3 Nekróza	22
3.5 MOLEKULÁRNÍ MECHANISMY VEDOUcí K AKTIVACI MITOGENY AKTIVOVANÝCH PROTEINKINÁZ	22
3.6 SIGNÁLNÍ DRÁHA FOSFATIDYLINOSITOL-3-KINÁZY PI3K A KINÁZY AKT	22
4 KOMENTOVANÉ PUBLIKACE	24
4.1 CHEMICAL AND BIOLOGICAL ASPECTS OF MONTANINE-TYPE ALKALOIDS ISOLATED FROM PLANTS OF THE AMARYLLIDACEAE FAMILY	24
4.2 ALKALOID PROFILING OF <i>HIPPEASTRUM</i> CULTIVARS BY GC-MS, ISOLATION OF AMARYLLIDACEAE ALKALOIDS AND EVALUATION OF THEIR CYTOTOXICITY	46
4.3 AMARYLLIDACEAE ALKALOIDS OF DIFFERENT STRUCTURAL TYPES FROM <i>NARCISSUS</i> L. CV. PROFESSOR EINSTEIN AND THEIR CYTOTOXIC ACTIVITY	54
4.4 PANCRACINE, A MONTANINE-TYPE AMARYLLIDACEAE ALKALOID, INHIBITS PROLIFERATION OF A549 LUNG ADENOCARCINOMA CELLS AND INDUCES APOPTOTIC CELL DEATH IN MOLT-4 LEUKEMIC CELLS	68
5 DISKUZE	89
6 ZÁVĚR	93
7 SEZNAM PUBLIKACÍ NEZAHRNUTÝCH DO TÉMATU DISERTACE	94
8 SEZNAM CITACÍ POUŽITÉ LITERATURY	95

SEZNAM POUŽITÝCH ZKRATEK

14-3-3	regulační protein
Akt	též proteinkináza B, thymomas of AKR mice kinase
Apaf-1	apoptotic protease activating factor 1
ARTS	protein patřící do rodiny septinů
ATM	Ataxia telangiectasia mutated
ATR	Ataxia telangiectasia a rad-3-related
Bak	Bcl-2 antagonist/killer 1
Bax	Bcl-2 associated X protein
Bcl	protein regulující apoptózu, B-cell lymphoma 2
BH	Bcl-2 homologní doména
Bid	BH3 interacting domain death agonist
Bim	Bcl-2 interacting mediator of cell death
Cdc25A	cdc25A proteinfosfatáza
Cdk	cyklin dependentní kináza
CKI	inhibitor cyklin dependentních kináz
DNA	deoxyribonukleová kyselina
DP1	E2F dimerizační partner 1
DR4, 5	death receptor 4,5
E2F	transkripční faktor E2F
ERK	extracelulárními signály regulovaná kináza
Fas	apoptosis stimulating fragment
FasL	apoptosis stimulating fragment ligand
FoxO1/3	forkhead box O1/3 transkripční faktor
GADD45	growth arrest and DNA-damage-inducible protein
GP	růstové procento
HDAC	histondeacetyláza
Chk 1, 2	checkpoint kináza 1, 2
IC	inhibiční koncentrace
MAPK	mitogenem aktivovaná proteinkináza
Mcl	myeloid cell leukemia protein
MDM2, 4	mouse double minute homolog 2, 4

mTOR	mammalian target of rapamycin, Ser/Thr kináza
NF- κ B	nuclear factor kappa-B, jaderný faktor
NMR	nukleární magnetická rezonance
Noxa	phorbol-12-myristate-13-acetate-induced protein 1
p21	cyklin dependentní kinázy inhibující protein 21
p27	cyklin dependentní kinázy inhibující protein 27
p53	tumor supresorový protein 53
PI	propidium jodid
PI3K	fosfatidylinositol-3-kináza
pRb	fosforylovaný retinoblastomový protein
Puma	p53 upregulated modulator of apoptosis
Rb	retinoblastomový protein
SCF	ubikvitin ligáza SCF
Ser	serin
Smac/DIABLO	second mitochondria-derived aktivátor/ direct IAP-binding protein with low pI
TGF β	transformující růstový faktor β
Thr	threonin
TLC	metoda chromatografie na tenké vrstvě, thin layer chromatography
TNF/TNFR	tumour necrosis factor/TNF receptor
TRAIL	TNF-related apoptosis inducing ligand
Tyr	tyrosin

Možnosti současné terapie nádorových onemocnění jsou široké, přesto však tato onemocnění stále patří mezi nejčastější příčiny úmrtí. Dosavadní poznatky biomedicínského výzkumu se čím dál tím více uplatňují v léčebné strategii tohoto typu onemocnění. Pochopení molekulárních drah spojených se vznikem nádorových buněk, jejich progresí a metastází vedl k objevu nových protinádorových léčiv a rozvoji cílené léčby. Současně také poznání molekulárního mechanismu účinku protinádorových léčiv získaných z rostlin či jejich semisyntetických derivátů umožňuje rozšířit portfolio dosud používaných cytostatik.

Cílem disertační práce bylo studium cytotoxického a cytostatického účinku dosud neprozkoumaných isochinolinových alkaloidů montaninového typu *in vitro* s použitím panelu nádorových buněčných linií a nenádorové buněčné linie lidských plicních fibroblastů. V počáteční fázi studie byly základní typy montaninových alkaloidů - montanin a pankracin - izolovány, dále podrobeny screeningu cytotoxicity s použitím panelu devíti nádorových buněčných linií odlišného histotypu a jedné nenádorové buněčné linie plicních fibroblastů. Byly stanoveny hodnoty 50 % inhibiční koncentrace IC_{50} . Pankracin, parentní alkaloid čeledi Amaryllidaceae, byl komplexně prostudován s cílem pochopit molekulární mechanismus jeho účinku, především tedy vliv na viabilitu a proliferaci rezistentní buněčné linie adenokarcinomu plic A549 a leukemické linie MOLT-4. Jako součást detailnějšího studia molekulárních mechanismů účinku byly rovněž použity metody, které pomohly odkrýt vliv pankracinu na buněčný cyklus, vliv na indukci apoptózy a dále metody použité k detekci proteinů molekulárních drah vedoucí k antiproliferačnímu a cytotoxickému účinku. Nejprve byla zkoumána buněčná proliferace a viabilita nádorových buněk metodou barvení Trypanovou modří a detekcí proliferace v reálném čase systémem xCELLigence. Vliv na buněčný cyklus byl stanoven průtokovou cytometrií. Apoptóza byla stanovena pomocí značení Annexinem V/PI a také kvantifikací aktivity kaspáz (-3/7, -8 a -9). Proteiny účastníci se dějů spojených se zastavením růstu či iniciací apoptózy byly detekovány elektroforeticky a pomocí metody Western blot. Pankracin statisticky významně snížil viabilitu a proliferaci leukemické buněčné linie MOLT-4. Indukce apoptózy v buňkách MOLT-4 po ovlivnění pankracinem byla prokázána statisticky významně vyšší aktivitou kaspáz a rovněž detekcí fosfatidylserinu na mimobuněčné straně cytoplazmatické membrány leukemických buněk. Dalším důkazem indukce programované buněčné smrti vyvolané pankracinem je detekce tumor supresorového proteinu p53 fosforylovaného na serinu 392, proapoptotické MAP kinázy p38 fosforylované na

threoninu 180 a tyrosinu 182 a upregulace inhibitoru cyklin dependentních kináz, proteinu p27. Pankracin statisticky významně inhiboval proliferaci buněčné linie adenokarcinomu plic A549 a tento efekt přetrvával po dobu 96 h. Inhibice růstu rezistentního adenokarcinomu plic se projevila v důsledku zvýšení akumulace buněk v G1 fázi, tato zástava byla způsobena downregulací tumor supresorového proteinu Rb fosforylovaného na serinu 807 a 811, upregulací p27 a downregulací Akt kinázy fosforylované na threoninu 308. Závěrem lze tedy uvést, že redistribuce buněk v buněčném cyklu a indukce programované buněčné smrti jsou klíčové mechanismy působení pankracinu.

SUMMARY

The possibilities of current therapy of cancer diseases are wide, yet these diseases are still among the most common causes of death. The current findings of biomedical research are increasingly being applied in the treatment strategy of cancer. Understanding the molecular pathways associated with cancer cell formation, progression, and metastasis has led to the discovery of new anticancer drugs and the development of targeted therapies. Simultaneously, knowledge of the molecular mechanism of action of anticancer drugs derived from plants or their semisynthetic derivatives makes it possible to expand the portfolio of cytostatics used so far.

The aim of the dissertation was to study the cytotoxic effect of hitherto unexplored montanine-type isoquinoline alkaloids *in vitro* using a panel of cancer cell lines and a non-cancer cell line of human lung fibroblasts.

In the initial phase of the study, the basic types of montanine alkaloids, montanine and pancracine, were isolated, further subjected to cytotoxicity screening using a panel of 9 cancer cell lines of different histotype and one non-cancerous cell line formed by lung fibroblasts. Mean inhibitory concentrations IC_{50} values were determined. Pancracine, the parent alkaloid of the Amaryllidaceae family, has been comprehensively studied in order to understand the molecular mechanism of its action, especially the effect on viability and proliferation of the resistant lung adenocarcinoma cell line A549 and the leukemic cell line MOLT-4. As part of a more detailed study of the molecular mechanisms of action, methods have also been used that have shown its effect on cell cycle, replication, induction of apoptosis, and detection of molecular pathway proteins leading to antiproliferative and cytotoxic effects. First, cell proliferation and cancer cell viability were measured by Trypan blue staining assay and xCELLigence real-time proliferation system. The effect on the cell cycle was determined by flow cytometry. Apoptosis was determined by Annexin V / PI labelling and quantification of caspase activity (-3/7, -8 and -9). Proteins involved in growth arrest or apoptosis activation were detected by electrophoresis and western blotting. Pancracine significantly reduced the viability and proliferation of the leukemic cell line MOLT-4. The apoptosis-inducing effect of pancracine in MOLT-4 cells was demonstrated by a significantly higher caspase activity as well as by the detection of phosphatidylserine on the outer leaflet of the plasma membrane of leukemia cells. Further evidence of apoptosis is the detection of the p53 tumor suppressor protein phosphorylated at serine 392, the proapoptotic MAP kinase p38 phosphorylated at

threonine 180, and tyrosine 182, and the upregulation of the inhibitor of cyclin-dependent kinases p27. Pancracine significantly inhibited the proliferation of the A549 lung adenocarcinoma cell line and this effect persisted for 96 h. Growth inhibition of resistant lung adenocarcinoma was due to increased cell accumulation in the G1 phase, this G1 block was caused by downregulation of the tumor suppressor protein Rb phosphorylated at serine 807 and 811, upregulation of p27, and downregulation of Akt kinase phosphorylated at threonine 308.

In conclusion, cell cycle perturbation and induction of apoptotic cell death were considered to be the key mechanisms of pancracine action.

1 CÍLE DISERTAČNÍ PRÁCE

Cílem disertační práce bylo komplexně prostudovat cytostatickou a cytotoxickou aktivitu skupiny vybraných montaninových alkaloidů s použitím panelu nádorových buněčných linií odlišného histotypu a nenádorové lidské buněčné linie plicních fibroblastů. Zároveň si tato práce klade za cíl poodhalit molekulární mechanismus účinku vybraného montaninového alkaloidu. Konkrétně se věnuje těmto dílčím úkolům:

- Stanovení růstového procenta (GP) dosud netestovaných alkaloidů izolovaných z rostlin *Hippeastrum cultivars* v panelu 9 buněčných linií odvozených z histotypově odlišných nádorů a u jedné nenádorové linie lidských plicních fibroblastů.
- Stanovení hodnoty inhibiční koncentrace IC_{50} u těch izolovaných alkaloidů, jejichž jednodávková koncentrace $10 \mu\text{mol.l}^{-1}$ snížila GP pod 50 %.
- Stanovení růstového procenta (GP) dosud netestovaných alkaloidů izolovaných z rostliny *Narcissus* L. cv. Professor Einstein v panelu 9 buněčných linií odvozených z histotypově odlišných nádorů a u jedné nenádorové linie lidských plicních fibroblastů.
- Stanovení hodnoty inhibiční koncentrace IC_{50} u těch izolovaných alkaloidů, jejichž jednodávková koncentrace $10 \mu\text{mol.l}^{-1}$ snížila GP pod 50 %.
- Pomocí vhodné metody určit, zda je cytostatický účinek vybraného montaninového alkaloidu dlouhodobý a dávkově závislý.
- Posoudit, zda je cytostatický a cytotoxický účinek alkaloidu spojen s redistribucí buněčné populace v jednotlivých fázích buněčného cyklu.
- Zhodnotit, zda je cytotoxický účinek montaninového alkaloidu spojen s aktivací programované buněčné smrti a pomocí vybrané metody kvantifikovat počet apoptotických buněk v časně a pozdní fázi apoptózy.
- Detekovat a kvantifikovat klíčové proteiny účastníci se molekulárních dějů v pozadí cytostatického a cytotoxického účinku montaninového alkaloidu spojených se zástavou buněčného cyklu či indukci apoptózy.

2 SEZNAM PUBLIKACÍ A PŘÍSPĚVEK AUTORA V JEDNOTLIVÝCH PUBLIKACÍCH

Autorka publikovala celkem sedm původních prací v časopisech s impakt faktorem, z nichž 2 publikace jsou prvoautorské a pět publikací spoluautorských. Dále autorka publikovala 1 přehledový prvoautorský článek v časopise s impakt faktorem. Tato disertace je komentovaným souborem čtyř z těchto publikací věnujících se problematice montaninových alkaloidů. Seznam dalších publikací nezahrnutých do disertace je uveden v kapitole 7. Autorčin přínos v jednotlivých publikacích je následující:

2.1 Chemical and Biological Aspects of Montanine-Type Alkaloids Isolated from Plants of the Amaryllidaceae Family

Koutová, D.; Maafi, N.; Havelek, R.; Opletal, L.; Blunden, G.; Řezáčová, M.; Cahlíková, L. *Molecules* 2020, 25(10):2337.

IF2020 4,412, Q2 (Chemistry, Multidisciplinary: Molecules) dle AIS

Publikační příspěvek autorky disertační práce:

část biomedicínská

- rešerše týkající se především protinádorového účinku montaninových alkaloidů

část fytochemická

- rešerše věnující se přípravě nových syntetických derivátů s ohledem na jejich protinádorový účinek

Odborný dohled k fytochemické části a strukturně aktivním studiím zajišťovala prof. Ing. Lucie Cahlíková, Ph.D. z Katedry farmaceutické botaniky Farmaceutické fakulty Univerzity Karlovy v Hradci Králové.

2.2 Alkaloid profiling of *Hippeastrum* cultivars by GC-MS, isolation of Amaryllidaceae alkaloids and evaluation of their cytotoxicity

Al Shammari, L.; Al Mamun, A.; Koutová, D.; Majorošová, M.; Hulcová, D.; Šafratová, M.; Breiterová, K.; Maříková, J.; Havelek, R.; Cahlíková, L.

Rec. Nat. Prod. 2020, 14, 154–159.

IF2020 1,735, Q3 (Plant Sciences) dle AIS

Publikační příspěvek autorky disertační práce:

Experimentální

- Kultivace buněčných linií
- Screening cytotoxicity izolovaných látek z alkaloidního extraktu *Hippeastrum cultivars* metodou WST-1
- Stanovení hodnoty 50 % inhibiční koncentrace IC₅₀ montaninu u devíti nádorových a jedné nenádorové buněčné linie
- Statistické vyhodnocení výsledků cytotoxicity a hodnot IC₅₀

Publikační

- Část týkající se cytotoxicity alkaloidů nebo jejich derivátů

2.3 Amaryllidaceae alkaloids of different structural types from *Narcissus L. cv. Professor Einstein* and their cytotoxic activity

Breiterová, K.; Koutová, D.; Maříková, J.; Havelek, R.; Kuneš, J.; Majorošová, M.; Opletal, L.; Hošťálková, A.; Jenčo, J.; Řezáčová, M.

Plants 2020, 9, 137.

IF2020 3,935, Q1 (Plant Sciences) dle IF

Publikační příspěvek autorky disertační práce:

Experimentální

- Kultivace buněčných linií
- Stanovení cytotoxicity izolovaných alkaloidů čeledi Amaryllidaceae metodou WST-1
- Stanovení hodnoty 50 % inhibiční koncentrace IC₅₀ pankracinu u devíti nádorových a jedné nenádorové buněčné linie
- Statistické vyhodnocení výsledků cytotoxicity a hodnot IC₅₀

Publikační

- Část týkající se cytotoxicity alkaloidů nebo jejich derivátů

2.4 Pancracine, a Montanine-Type Amaryllidaceae Alkaloid, Inhibits Proliferation of A549 Lung Adenocarcinoma Cells and Induces Apoptotic Cell Death in MOLT-4 Leukemic Cells

Koutová, D.; Havelek, R.; Peterová, E.; Muthná, D.; Královec, K.; Breiterová, K.; Cahlíková, L.; Řezáčová M.

Int. J. Mol. Sci. 2021, 22(13):7014.

IF2020 5,923, Q2 (Biochemistry and Molecular Biology) dle AIS

Příspěvek autorky disertační práce:

Experimentální

- Kultivace buněčných linií
- Příprava experimentálních protokolů
- Stanovení viability a proliferace adherentní buněčné linie adenokarcinomu plic A549 a leukemické linie MOLT-4 metodou barvení Trypanovou modří
- Stanovení aktivity kaspáz
- Imunodetekce proteinů účastnících se molekulárních dějů v pozadí účinku pankracinu včetně denzitometrického stanovení
- Statistické vyhodnocení všech výsledků

Publikační

- Příprava designu studie a sepsání všech jeho částí

3 ÚVOD DO PROBLEMATIKY

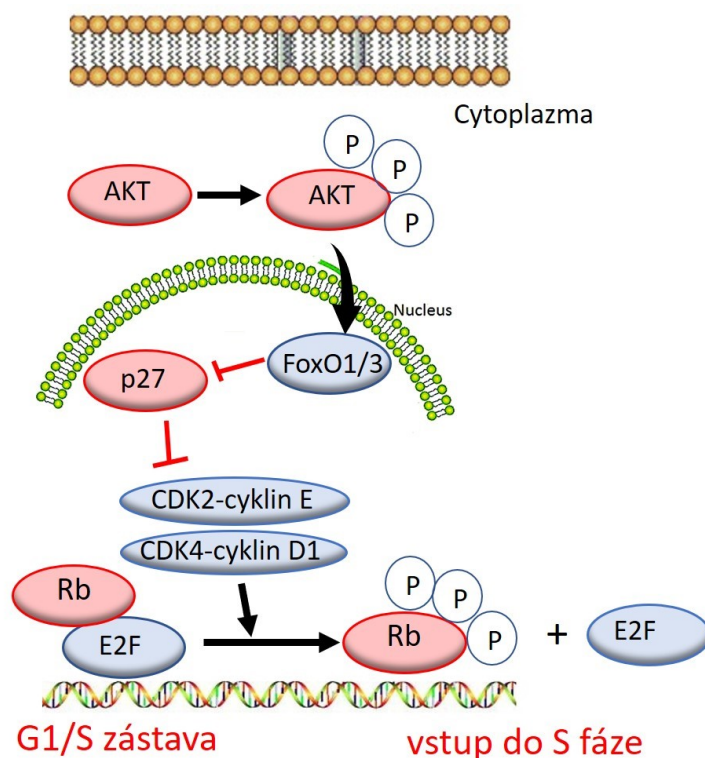
Přes značné vědecké a lékařské úsilí patří nádorová onemocnění mezi nejčastější příčiny úmrtí. Léčba v současné době zahrnuje chirurgické odstranění, radioterapii, chemoterapii, včetně hormonální terapie, neustále se rozvíjející imunoterapii a biologickou léčbu a samozřejmě kombinaci zmíněných. Hledání nových protinádorových léčiv v rovině základního výzkumu je možné chemickou *de novo* syntézou, kombinatorní chemií, purifikací nových protinádorových antibiotik, izolací a identifikací nových sloučenin rostlinného původu, případně přípravou semisyntetických derivátů vycházejících z látek přírodního původu (Klener a Klener 2010). Pochopení mechanismu účinku těchto látek v rovině základního výzkumu včetně jejich vlivu na buněčný cyklus a apoptózu je předpokladem úspěšného terapeutického zásahu.

3.1 Buněčný cyklus

Buněčný cyklus představuje sled vzájemně navazujících a souvisejících dějů, které vedou od jednoho buněčného dělení k následujícímu (Kovář 2000). Původně bylo buněčné dělení rozděleno do dvou fází: mitóza (M), tj. proces jaderného dělení; a interfázi, tedy přechod mezi dvěma M fázemi. Fáze mitózy zahrnují profázi, metafázi, anafázi a telofázi. Později se ukázalo, že i relativně klidná interfáze zahrnuje specifické děje, které se vymezily do fází G1, S a G2 (Vermeulen et al. 2003). Fáze G1 představuje časový úsek mezi ukončením předchozí mitózy a začátkem replikace DNA, součástí S fáze je tedy syntéza DNA. Ukončením S fáze začíná G2 fáze, což je časový úsek, ve kterém probíhá hlavní příprava na mitózu, tedy M fázi (Kovář 2000). Buňky v G1 mohou před zahájením replikace DNA vstoupit do klidového stavu zvaného G0. Buňky v G0 představují hlavní populaci nerostoucích, neproliferujících buněk v lidském těle (Vermeulen et al. 2003). Vzhledem k důležitosti procesů, které jsou součástí buněčného cyklu, je v rámci buněčného cyklu nastaven důmyslný systém kontroly. Kontrolní body buněčného cyklu jsou takové body progresu, kde se na základě endogenních i exogenních signálů rozhoduje o dalším postupu buňky buněčným cyklem (Kovář 2000). Hlavní rodiny regulačních proteinů, které hrají klíčovou roli v řízení progresu buněčného cyklu, jsou cykliny, cyklin dependentní kinázy (Cdk), jejich substrátové proteiny, inhibitory Cdk (CKI) a tumor supresorový genový produkt p53 a tumor supresorový fosforylovaný retinoblastomový protein pRb (Golias et al. 2004). Tyto rodiny tvoří základní regulační mechanismus zodpovědný za katalýzu přechodu buněčného cyklu a vstup kontrolními body (Golias et al. 2004).

3.2 Zástava v kontrolním bodě G1/S

U buněk nacházejících se v G1/S kontrolním bodě probíhá kontrola iniciace replikace DNA a tato kontrola se provádí v závěrečné části G1 fáze (Kovář 2000). Cyklin dependentní kinázy (Cdk) a cykliny buněčného cyklu tvoří aktivní komplexy. V této fázi buněčného cyklu jsou důležité 2 typy těchto komplexů, konkrétně Cdk4/6 ve vazbě s cyklinem D a Cdk2 ve vazbě s cyklinem E, jež vzájemně spolupracují na uvolnění transkripčního komplexu, který obsahuje Rb protein a transkripční faktor E2F (Bartek a Lukas 2001). Součástí tohoto inhibičního komplexu je hypofosforylovaný Rb protein ve vazbě na E2F-DP1 a histoneacetyláza HDAC. Fosforylací Rb proteinu komplexem Cdk4/6-cyklin D a Cdk2-cyklin E dojde k disociaci HDAC, čímž je umožněna transkripce genů potřebných pro replikaci DNA. Růstové faktory tuto kaskádu spustí aktivací Akt kinázy, která fosforyluje transkripční faktor FoxO1/3, tím jej inhibuje a zajišťuje tak přežití a proliferaci buněk. Faktorů a podnětů, které naopak zastaví celý tento proces, je celá řada, například poškození DNA, replikační stárnutí nebo snížená koncentrace růstových faktorů. Zvláštní úlohu v tomto procesu zajišťují inhibitory Cdk (CKI), rodina specifických členů INK4 nebo Kip/Cip, mezi které řadíme například protein p21 nebo p27 (Bartek a Lukas 2001). Zablokování replikace DNA na základě indukce inhibitoru p21 realizuje protein p53 v reakci na poškození DNA (Kovář 2000). K aktivaci inhibitoru p27 dochází prostřednictvím inhibičního růstového faktoru transforming growth factor β (TGF β) a také v důsledku kontaktu buněk. Substrátem p27 je Cdk2-cyklin E, ale také Cdk4/6-cyklin D. Zvýšená exprese p27 vede ke G1 bloku. TGF β kromě regulace CKI také inhibuje transkripci cdc25A, což je fosfatáza přímo vyžadována pro aktivaci Cdk. K inhibici cdc25A dochází také ubikvitinylací pomocí ubikvitin ligázy SCF v reakci na poškození DNA cestou přes Ataxia telangiectasia-mutated (ATM) kinázu, ATM and Rad3-related (ATR) kinázu a checkpoint kinázy Chk1/2. Aktivace signální dráhy Akt/p27/pRb iniciující zástavu v G1/S kontrolním bodě ilustruje obr. 1.

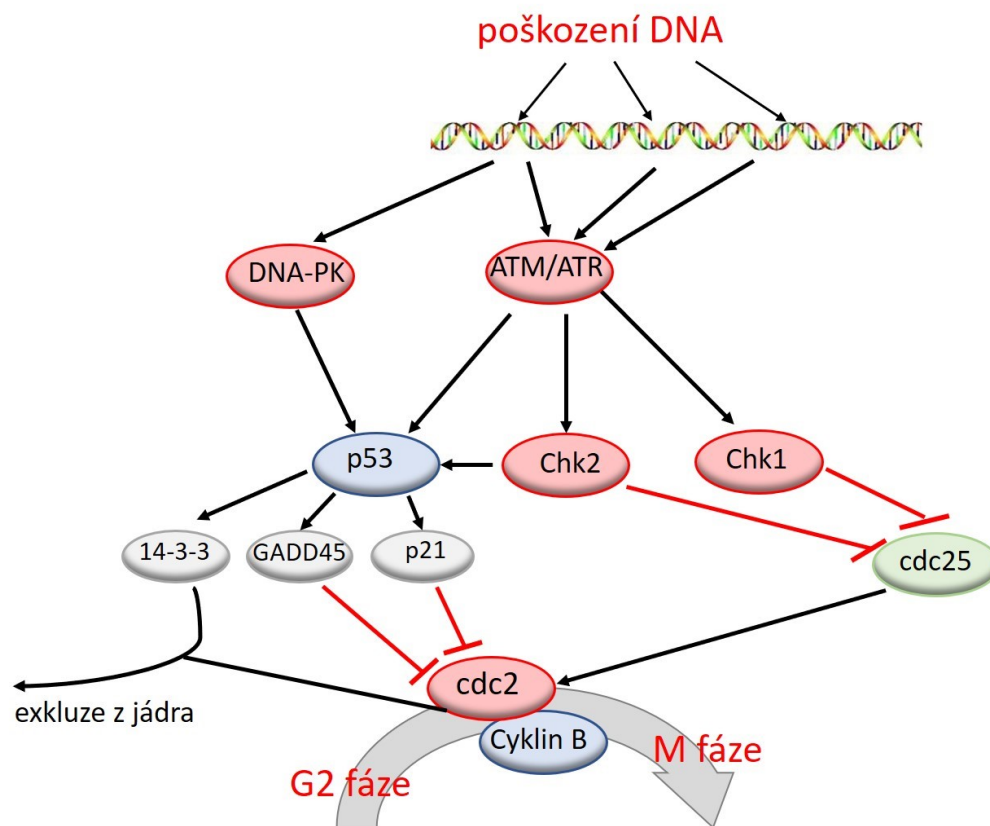


Obr. 1. Aktivace signální dráhy Akt/p27/pRb vedoucí k zástavě v kontrolním bodě G1/S, upraveno podle Bartek a Lukas 2001.

3.3 Zástava v kontrolním bodě G2/M

G2 kontrolní bod se nachází na přechodu G2 fáze do mitózy. Je spojen s aktivací Cdk2-cyklin B. Zablokování vstupu do mitózy způsobuje detekované poškození DNA, nedokončená replikace DNA a detekované poruchy duplikace centrozómu. Cdk2 je udržována v neaktivním stavu pomocí tyrosinkináz Wee1 a Myt1. Stopy poškození DNA vyvolané například ionizačním zářením vedou k aktivaci ATM/ATR kinázy, které spustí dvě paralelní kaskády, jež ve výsledku vedou k inaktivaci komplexu Cdk2-cyklin B. První kaskáda rychle inhibuje progresi do mitózy aktivací Chk1, která fosforylací inaktivuje cdc25, čímž se zabrání aktivaci Cdk2 (Řezáčová a Vávrová 2000). Druhá cesta vede přes tumor supresorový protein p53, jehož fosforylace umožní disociaci z MDM2 a MDM4 komplexu a to následně umožní aktivovat DNA vazebnou a transkripční regulační aktivitu p53. Transkripční aktivita p53 má dopad na gen 14-3-3, který se váže na fosforylovaný komplex Cdk2-cyklin B a exportuje ho z jádra, dále na gen GADD45, který váže a disociuje komplex Cdk2-cyklin B a p53 rovněž zvyšuje transkripční aktivitu pro protein p21, který je inhibítorem cyklin dependentních kináz včetně Cdk2 (Al-Ejeh et al. 2010). Až polovina solidních nádorů vykazuje strukturální defekty p53. Nejčastější funkční blokádu

p53 představuje zvýšení exprese MDM2 (Klener a Klener 2013). Schéma vybraných signálních drah vedoucí k zástavě v G2/M fázi ilustruje obr. 2.



Obr. 2. Schéma vybraných signálních cest vedoucí k zástavě v přechodu z G2 fáze do M fáze, upraveno podle Al-Ejeh et al. 2010.

3.4 Typy buněčné smrti

3.4.1 Apoptóza

Apoptóza neboli programovaná buněčná smrt je proces, který vede k řízené eliminaci přestárých, nefunkčních, nepotřebných, mutovaných, infikovaných či transformovaných buněk (Klener a Klener 2013). Jedná se o evolučně velmi starý mechanismus a obvykle nevede k rozvoji zánětlivé reakce. Je jisté, že jakékoliv omezení regulačních zásahů v procesu apoptózy vede k rozvoji různých patologických stavů, včetně nádorových onemocnění. Buňka umírající apoptózou vykazuje charakteristické morfologické změny, které ji odlišují od jiných typů buněčné smrti. Patří mezi ně kondenzace a fragmentace chromatinu v jádře, tvorba výběžků cytoplazmatické membrány, celkové zmenšení a zakulacení buňky a v pozdních fázích rozpad celé buňky do tzv. apoptotických tělísek (Ondroušková a Vojtěšek 2014). Rozlišujeme dvě

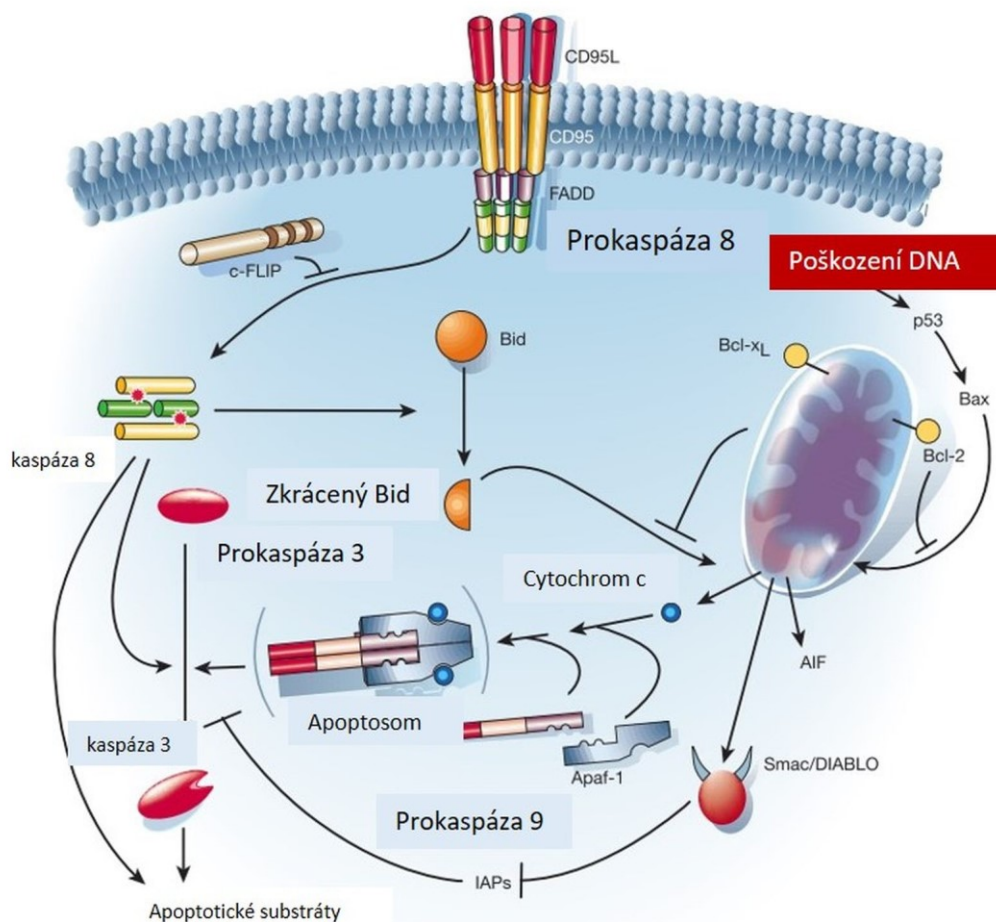
hlavní apoptotické dráhy, receptorovou (vnější, extrinsická) a mitochondriální (vnitřní, intrinsická).

Součástí obou těchto drah je aktivace cysteinových proteáz tzv. kaspáz a to štěpením neaktivních zymogenů, prokaspáz. Proces v obou případech vede ke spuštění efektorových kaspáz, které mají za úkol ireverzibilní strukturní změnu buněčných komponent a řízenou přeměnu buňky v apoptotická tělíska (Klener a Klener 2013). Apoptotická tělíska obsahují stále funkční organely, fragmenty kondenzovaného jádra a udržují si intaktní cytoplazmatickou membránu, která se od membrány zdravých buněk liší přítomností fosfatidylserinu na její vnější straně (Ondroušková a Vojtěšek 2014) a tím jsou rozpoznána a fagocytována makrofágy bez rozvoje zánětlivé reakce (Klener a Klener 2013).

K aktivaci vnější dráhy dochází vazbou ligandů smrti (TRAIL, FasL, TNF) na receptory smrti (DR4/DR5, Fas, TNFR atd.) vytvářející trimery. Následně spustí apoptotickou kaskádu dějů přes adaptorové proteiny, a to aktivací prokaspázy-8 nebo prokaspázy-10 (Ondroušková a Vojtěšek 2014).

K iniciaci apoptózy vnitřní mitochondriální cestou dochází zejména v případě neopravitelného poškození DNA. Pokud poškození DNA buňka neopraví, je odsouzena k záhubě. Hlavní roli v tomto procesu pak má tumor supresorový transkripční faktor p53. Mutace p53 či jiný defekt v rámci kontroly buněčné integrity, či defekt v apoptotické dráze může vést k přežívání buněčných klonů s mutovanou DNA. Selže-li apoptotická kontrola a překonají-li tyto buňky navíc ještě imunologický dohled, dochází k šíření nádorového onemocnění (Klener a Klener 2013). Regulaci apoptózy zajišťuje rodina Bcl-2 proteinů, které jsou přítomné v membráně mitochondrií nebo v cytoplazmě. Společným znakem těchto proteinů je přítomnost BH-domén v jejich struktuře (Řezáčová a Vávrová 2000). Rozlišujeme proapoptotické (Bax, Bak, Bid, Bim, Puma, Noxa) a antiapoptotické (Bcl-2, Bcl-XL, Mcl-1, Bcl-W, A1) Bcl-2 proteiny. Vzájemný poměr a interakce proapoptotických a antiapoptotických členů rodiny Bcl-2 rozhoduje o tom, zda bude apoptotická dráha inhibována nebo aktivována (Ondroušková a Vojtěšek 2014). K vzájemné interakci dochází právě pomocí BH-3 domén, dojde k vytvoření dimérů a tím se mohou navzájem inaktivovat (Ondroušková a Vojtěšek 2014). V procesu mitochondriální apoptotické cesty dochází k uvolnění cytochromu c z mezimembránového prostoru mitochondrií, ten se v cytoplazmě spojuje s proteinem Apaf-1 a prokaspázou-9, vytvoří se apoptozom a dochází ke štěpení prokaspázy-9 na aktivní kaspázu-9. Současně dochází k uvolnění dalších proteinů z mitochondrií (např. second mitochondria-derived aktivátor/ direct IAP-binding protein with low pI SMAC/DIABLO či protein patřící do rodiny

septinů ARTS apod.), které vážou a inaktivují antiapoptotické proteiny. Kaspáza-9 aktivuje efektorové kaspázy (kaspázy -3/-7), které v dalším procesu štěpí proteiny související s buněčnou adhezí, regulací apoptózy, strukturou jádra, buněčným cyklem a ve výsledku dojde k buněčné smrti (Ondroušková a Vojtěšek 2014). Schéma naznačující signální kaskádu vedoucí k programované buněčné smrti je znázorněno na obr. 3.



Obr. 3. Aktivace vnitřní a vnější apoptotické dráhy, upraveno podle Hengartner 2000.

3.4.2 Autofagie

Autofagie je proces, při kterém jsou buněčné komponenty (proteiny nebo dokonce celé orgány) směřovány do lyzozomů za účelem degradace (D'Arcy 2019). Lyzozomy jsou pak schopny tyto substráty štěpit, degradované složky mohou být buď recyklovány za vzniku nových buněčných struktur a/nebo organel, nebo alternativně mohou být dále zpracovány a použity jako zdroj energie. Autofagii může iniciovat řada stresorů, zejména nedostatek živin (kalorická restrikce) nebo může být výsledkem signálů přítomných během buněčné diferenciace a embryogeneze či na povrchu poškozených organel (D'Arcy 2019). Jedná se tedy o katabolický proces a je zachován u všech eukaryotických organismů (Saha et al. 2018). Pro

autofagii je charakteristický vysoký nárůst počtu autofagických vakuol v buňce, bez kondenzace jaderného chromatinu. Její role v nádorových buňkách je nejasná, v počátečních fázích autofagie spíše inhibuje rozvoj nádoru tím, že odstraňuje poškozené proteiny a organely, v pozdější fázi nejspíš pomáhá nádorovým buňkám vyrovnat se např. s nedostatkem živin nebo oxidativním stresem (Ondroušková a Vojtěšek 2014). Nejlépe prozkoumanou signální kaskádou regulující autofagii je dráha PI3K-Akt-mTOR-mTORC1/2 (Klener a Klener 2013).

3.4.3 Nekróza

Na rozdíl od apoptózy je nekróza alternativní nekontrolovanou formou buněčné smrti, která je vyvolána vnějším poškozením, jako je hypoxie nebo zánět (D'Arcy 2019). Tento proces často zahrnuje zvýšení hladiny různých prozánětlivých proteinů a sloučenin, jako je jaderný faktor NFκB. Dochází k ruptuře buněčné membrány způsobující rozlití buněčného obsahu do okolních oblastí, což má za následek rozvoj zánětu a poškození tkáně (D'Arcy 2019). Na rozdíl od apoptózy je nekróza energeticky nezávislou formou buněčné smrti, kde je buňka tak silně poškozena náhlým šokem (záření, teplo, chemikálie, hypoxie atd.), že není schopna fungovat. Buňka obvykle reaguje otokem, protože nedokáže udržet homeostázu s okolním prostředím (D'Arcy 2019).

3.5 Molekulární mechanismy vedoucí k aktivaci mitogeny aktivovaných proteinkináz

V důsledku poškození DNA jsou v buňce aktivovány mechanismy vedoucí k odstranění tohoto poškození nebo mechanismy vedoucí k přežití a proliferaci buňky, hlavní roli v tomto procesu hrají mitogenem aktivované proteinkinázy MAPK (Řezáčová a Vávrová 2000). Dosud bylo popsáno pět základních MAPK, z nichž extracelulárními signály regulované kinázy ERK1 a ERK2 mají význam spíše v signalizaci vedoucí k přežití buňky. Druhým typem jsou Jun N-terminální kinázy, JNK1, JNK2 a JNK3, dále mezi MAP kinázy řadíme p38 kinázy a ERK3/ERK4 a ERK5. Z těchto kináz jsou vzhledem k indukci signálů vedoucí ke smrti buňky nejdůležitější kinázy typu JNK a kináza p38, v literatuře je popisována spíše jejich proapoptotická úloha (Řezáčová a Vávrová 2000). Kináza p38 se rovněž podílí na zástavě buněčného cyklu (Muthná et al. 2010).

3.6 Signální dráha fosfatidylinositol-3-kinázy PI3K a kinázy Akt

Signální dráha zahrnující fosfatidylinositol-3-kinázu PI3K a kinázu Akt řídí buněčnou odpověď jako reakci na poškození buňky či v reakci na dostatek růstových faktorů a zajišťuje tak růst a přežití buněk a dále také metabolickou kontrolu a migraci (Faes a Dormond 2015).

Tato dráha se například aktivuje během G1/S přechodu buněčného cyklu a reguluje několik klíčových regulátorů buněčného cyklu, včetně stability proteinů p21, cyklinu D a p27 (Fresno-Vara et al. 2004). Klíčový mechanismus pro Akt modulaci specifické substrátové aktivity, jako jsou transkripční faktory β -catenin, p21, p27, MDM2 nebo Forkhead, zahrnuje regulaci jejich cytoplazmatické nebo jaderné lokalizace fosforylací. Dochází k indukci exprese několika genů, jako je např. gen cyklinu D1, který indukuje progresi buněčného cyklu prostřednictvím regulace hyperfosforylace a inaktivace proteinu Rb. Akt fosforyluje p27 a inhibuje jeho antiproliferační účinky tím, že jej zadržuje v cytoplazmě, podobný mechanismus byl popsán i pro protein p21 (Fresno-Vara et al. 2004).

Další část současného stavu poznání týkající se alkaloidů montaninového typu čeledi Amaryllidaceae a jejich potenciálního protinádorového účinku je shrnuta v přehledové publikaci, která je součástí spisu a je uvedena v kapitole 4.1.

4 KOMENTOVANÉ PUBLIKACE

4.1 Chemical and Biological Aspects of Montanine-Type Alkaloids Isolated from Plants of the Amaryllidaceae Family

Koutová, D.; Maafi, N.; Havelek, R.; Opletal, L.; Blunden, G.; Řezáčová, M.; Cahlíková, L.

Molecules 2020, 25(10):2337.

IF2020 4,412, Q2 (Biochemistry and Molecular Biology)

Cílem této rešerše bylo shrnout dosavadní poznatky o montaninových alkaloidech z pohledu biomedicínského a rovněž přinést recentní informace o výsledcích experimentální práce zaměřené na zefektivnění bioaktivity těchto isochinolinových alkaloidů přípravou nových semisyntetických derivátů, jelikož publikace takového rozsahu dosud zveřejněna nebyla.

Výzkum léků na bázi rostlin se týká především vývoje protinádorových léčiv z alkaloidů (Mondal et al. 2019), ačkoliv jejich biologické účinky jsou mnohem širší a rozmanitější. Intenzivní výzkum přírodních látek obohatil léčebnou strategii protinádorové terapie. Alkaloidy vinblastin, vinkristin a semisyntetické deriváty vinorelbin, vindesin a vinflunin získané studiem obsahových látek barvínku (*Catharanthus roseus*, *Vinca rosea* L.) představují významnou součást dnešní palety cytostatik (Klener a Klener 2010). Dále lze uvést například inhibitory topoizomerázy I inspirované alkaloidem kamptotecinem stromu *Camptotheca acuminata* (Gordaliza 2007). Rovněž je nutné zmínit taxany, látky izolované z kůry tisu, jež daly vzniknout inhibitorům depolymerace mikrotubulů a paletu cytostatik tak doplňuje paklitaxel a docetaxel (Klener a Klener 2013).

Do dnešního dne bylo izolováno přes 500 isochinolinových alkaloidů Amaryllidaceae s rozdílnou strukturou a biologickou aktivitou (Van Goietsenoven 2010). Ačkoliv některé látky jako Amaryllidaceae alkaloid pankratistatin (pankratistatinový strukturní typ) dosáhly po sérii podrobných studií procesu klinického hodnocení, většina isochinolinových alkaloidů je, co se týče úrovně inhibiční aktivity vůči růstu a viabilitě nádorových buněk, poznáním pouze na počátku preklinického vývoje (Qing et al. 2017). Negativum pro širší studium tak představuje absence detailnějších znalostí o mechanismu působení isochinolinových alkaloidů, cílové molekule nebo vlivu struktury na aktivitu, což potlačuje proces vedoucí k efektivnímu výběru kandidátního léčiva. Isochinolinové alkaloidy montaninového strukturního typu patřící do čeledi Amaryllidaceae nejsou zdaleka tak prozkoumány, ačkoliv již dříve byla publikována

první data naznačující cytotoxicitu montaninu, který je hlavním představitelem této skupiny látek (Silva et al. 2008).

Manthidin, koccinin, manthin a montanin byly první alkaloidy montaninového typu izolované Wildmanem a kol. v roce 1955 z rostliny rodu *Haemanthus* (Wildman a Kaufman 1955).

Doposud bylo identifikováno čtrnáct alkaloidů izolovaných z různých rostlin čeledi Amaryllidaceae, základní skelet tohoto strukturního typu tvoří pentacyklický 5,11-methanomorphanthridinový kruhový systém (Koutová et al. 2020). Byly započaty studie věnující se biologické aktivitě alkaloidů typu montaninu. Vzhledem k jejich významným inhibičním účinkům na růst nádorových buněčných linií patří dnes tyto struktury k nejintenzivněji zkoumaným (Masi et al. 2019, Al Shammari et al. 2020, Breiterová et al. 2020, Govindaraju et al. 2018). Bylo také prokázáno, že některé alkaloidy typu montaninu vykazují anxiolytické, antidepressivní a antikonvulzivní účinky včetně účinků imunomodulačních (da Silva et al. 2006). Samotný montanin byl studován také z hlediska inhibice acetylcholinesterázy jako potenciální zdroj léčiva Alzheimerovy choroby, potlačení revmatických onemocnění a terapeutického využití jeho antibakteriálních a antimykotických účinků (Farinon et al. 2017, Pagliosa et al. 2010, Evidente et al. 2004).

Prvním důkazem, že alkaloidy montaninového strukturního typu vykazují slibné *in vitro* cytotoxické účinky vůči nádorovým liniím, byla studie z roku 2008 popisující inhibiční efekt na růst nádorových buněk po aplikaci montaninu izolovaného z cibulí rostliny *Hippeastrum vittatum* (Silva et al. 2008). Od té doby se výzkum alkaloidů montaninového typu včetně izolace, přípravy semisyntetických derivátů a vlivu těchto látek na proliferaci a životaschopnost nádorových buněk rozšířil, stále však chybí data naznačující mechanismus tohoto působení.

Slibné antiproliferativní, cytotoxické a další významné biologické účinky některých zástupců Amaryllidaceae alkaloidů typu montaninu, zejména montaninu a pankracinu, vedly k přípravě a syntéze analogů těchto alkaloidů s cílem potencovat jejich účinek a zlepšit jejich vlastnosti. Alkaloidy typu montaninu zaujímají relativně malý kvantitativní podíl z celkového množství alkaloidů v rostlinném materiálu, dalo by se říct, že jsou spíše svým obsahovým zastoupením v extraktech v minoritním množství. Charakter jejich unikátních strukturálních vlastností a slibné biologické aktivity předurčují tyto molekuly k syntetickému úsilí (Guan et al. 2012, Maatwenko et al. 2008, Ishizaki et al. 1992, Bao et al. 2013, Hong et al. 2008, Jin et

al. 1997, Pearson et al. 1998, Banwell et al. 2001, Sha et al. 2001, Pandey et al. 2005, Yang et al. 2017).

Review

Chemical and Biological Aspects of Montanine-Type Alkaloids Isolated from Plants of the Amaryllidaceae Family

Darja Koutová ^{1,†}, Negar Maafi ^{2,†}, Radim Havelek ¹, Lubomír Opletal ², Gerald Blunden ³, Martina Řezáčová ¹ and Lucie Cahliková ^{2,*}

¹ Department of Medical Biochemistry, Faculty of Medicine in Hradec Králové, Charles University, Šimkova 870, 500 03 Hradec Králové, Czech Republic; koutova.darja@lfhk.cuni.cz (D.K.); havelekr@lfhk.cuni.cz (R.H.); rezacovam@lfhk.cuni.cz (M.Ř.)

² ADINACO Research Group, Department of Pharmaceutical Botany, Faculty of Pharmacy, Charles University, Heyrovského 1203, 500 05 Hradec Králové, Czech Republic; negarm@faf.cuni.cz (N.M.); opletal@faf.cuni.cz (L.O.)

³ School of Pharmacy and Biomedical Sciences, University of Portsmouth, Portsmouth, Hampshire P01 2DT, UK; gblunden10@gmail.com

* Correspondence: cahlikova@faf.cuni.cz

† These authors contributed equally to this work.

Academic Editors: Jaume Bastida and Strahil Berkov

Received: 24 April 2020; Accepted: 12 May 2020; Published: 16 May 2020



Abstract: Plants of the Amaryllidaceae family are promising therapeutic tools for human diseases and have been used as alternative medicines. The specific secondary metabolites of this plant family, called Amaryllidaceae alkaloids (AA), have attracted considerable attention due to their interesting pharmacological activities. One of them, galantamine, is already used in the therapy of Alzheimer's disease as a long acting, selective, reversible inhibitor of acetylcholinesterase. One group of AA is the montanine-type, such as montanine, pancracine and others, which share a 5,11-methanomorphanthridine core. So far, only 14 montanine-type alkaloids have been isolated. Compared with other structural-types of AA, montanine-type alkaloids are predominantly present in plants in low concentrations, but some of them display promising biological properties, especially in vitro cytotoxic activity against different cancerous cell lines. The present review aims to summarize comprehensively the research that has been published on the Amaryllidaceae alkaloids of montanine-type.

Keywords: alkaloids; Amaryllidaceae; biological activity; derivatives; montanine; montanine-type; pancracine

1. Introduction

Amaryllidaceae is a family of monocotyledonous plants that are widely distributed over the tropical and warm regions of the world, especially in the southern African region. Species of some genera are also found in the Mediterranean area and temperate regions of Asia [1,2]. The Amaryllidaceae is one of the 20 most important alkaloid containing plant families. Up to now, more than 600 structurally diverse alkaloids have been isolated from plants of this family with a wide range of interesting biological properties, including antitumor, antifungal, antibacterial, antiviral, antimalarial, analgesic, and antineurodegenerative activities [3–6].

Plants of the family Amaryllidaceae have a long history of usage as herbal remedies all over the world to cure different ailments and diseases [3,7–10]. For example, *Hymenocallis litorallis* has been used as a centuries-old remedy for cancer in the traditional medicine of the Mayan people of South

America [9]. A decoction of leaves of *Zephyranthes candida* has been utilized in South America as a remedy for diabetes mellitus [10], and the bulbs of *Boophone disticha* in southern Africa for cancer remediation by the indigenous Sotho, Xhosa and Zulu people [3,11]. The medicinal properties of these plants were already known in the fourth century B.C., when Hippocrates of Cos used oil from the daffodil *Narcissus poeticus* to treat uterine tumors [12,13]. Interestingly, this plant was also described in the Bible as a treatment of symptoms related to cancer [13].

Since the isolation of the first alkaloid, lycorine, from *N. pseudonarcissus* in 1877, Amaryllidaceae alkaloids (AA) have been attractive sources for chemical investigations, and many of them have been isolated, screened for different biological activities, and synthesized by a number of research groups. The most-known Amaryllidaceae alkaloid is galantamine, which is used in the form of its hydrobromide salt for the treatment of mild and severe stages of Alzheimer's disease [14].

2. Biosynthesis, Phytochemistry and Occurrence of Montanine-Type Alkaloids

Amaryllidaceae alkaloids are synthesized within the norbelladine pathway from the aromatic amino acids phenylalanine and tyrosine, which are used to produce key intermediates in the biosynthesis of 4'-O-methylnorbelladine [15]. This key intermediate is formed through the condensation of 3,4-dihydroxybenzaldehyde (also known as protocatechuic acid; 3,4-DHBA) produced from L-phenylalanine and tyramine formed from L-tyrosine (Figure 1). As the result of condensation of intermediates, a Schiff base is generated, which is reduced to norbelladine. The biosynthesis continues with methylation of norbelladine by 4'-O-methyltransferase to 4'-O-methylnorbelladine, as a central intermediate for the biosynthesis of most AA (Figure 1) [15–17]. This key intermediate undergoes three different types of intramolecular oxidative couplings: *ortho-para'*, *para-para'*, and *para-ortho'*, which lead to the formation of the basic structural types of AA: norbelladine, lycorine, homolycorine, galantamine, haemanthamine, crinine, narciclasine, tazettine and montanine (Figure 1). Generally, genes involved in the biosynthesis of AA are poorly studied and transcriptomic studies, as well as genome sequencing, were only recently initiated for this plant family [16,18–20].

Studies dealing with the biosynthesis of montanine type alkaloids are more or less controversial [21,22]. In the study reported in 1976, 11-hydroxyvittatine was suggested as the main precursor for montanine and haemanthamine biosynthesis in *Rhodophiala bifida*, mentioning the higher conversion ratio for haemanthamine in comparison with montanine caused by skipping the rearrangement step in the biogenesis of haemanthamine from 11-hydroxyvittatine. In this study, the rearrangement of 11-hydroxyvittatine to pancracine, and then 2-O-methylation of pancracine, was described as a possible pathway for the biosynthesis of montanine in this plant [23]. The proposed biosynthesis of montanine, and relationships within some AA of the crinine- haemanthamine and montanine-type described by Feinstein and Wildman, are summarized in Figure 2. A similar biosynthetic pathway for montanine-type alkaloids has been described, with slight modifications, in further studies [16,24].

Another biosynthetic pathway for montanine-type AA was described by Jin in 2007, who proposed the primary biosynthetic pathways of each type of AA [25]. These supposed the formation of cherylline-type AA by intramolecular addition to the *p'*-position of the electronic-rich aromatic ring to the benzylic position of the oxidized quinonoid form. Further addition of the secondary amine to the intermediate dienone provides montanine-type AA (Figure 3).

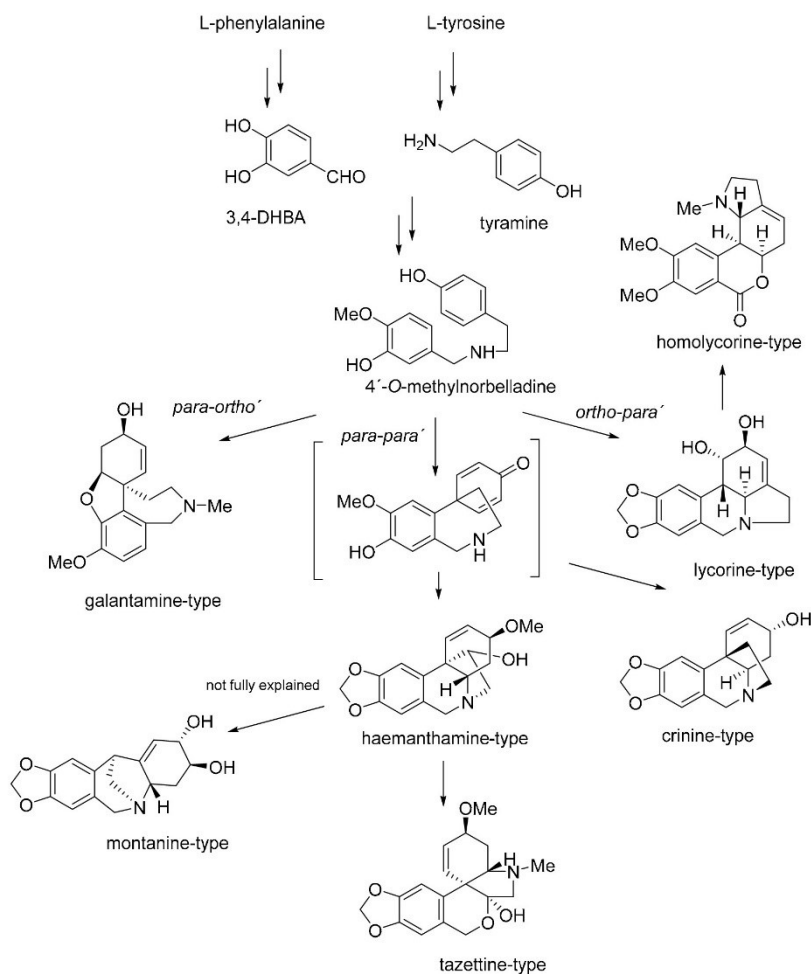


Figure 1. Biosynthetic pathway of main structural types of Amaryllidaceae alkaloids.

The first AA of montanine-type were isolated by Wildman et al. in 1955 from a *Haemanthus* species [26], namely coccinine, manthidine, manthine and montanine (Figure 4). Further congeners were identified and isolated from plants in the following decades (Table 1). Up to now, fourteen AA possessing an intriguing pentacyclic 5,11-*b*-methanomorphanthridine ring system as a core skeleton have been isolated from different Amaryllidaceae species (Figure 4, Table 1). According to the different position of the C=C double bond in the E ring of the alkaloid skeletons, they can be divided into two subgroups (Figure 4). Alkaloids from pancracine to montabuphine belonging to one of the representative subgroups possess the double bond between C1 and C11a. Most alkaloids within this subgroup differ from each other only in the configurations and oxygen-containing substitutions on stereocenters at C2 and C3 in ring E (Figure 4). Nangustine and 4-*O*-methylnangustine display different substituents in positions C3 and C4. Pancratinine B and pancratinine C (also known as squamigine), both isolated from *Pancreatum canariense* [27], are characterized by the presence of a double bond between C1 and C2 and with a hydroxy group at C11a (Figure 4). In 1995, Viladomat et

al. reported the isolation of montabuphine from bulbs of *B. flava*, describing the β -orientation for the methano-bridge for the first time [28]. This isolation has attracted attention, because this suggested that both enantiomeric forms of the montanine-type framework occur in nature. More recently, obtained data from the total synthesis of (+)-montabuphine found the previous spectroscopic published data to be controversial for the presented structure, and its legitimate structure is yet to be revised [29,30]. The overview of plants from which montanine-type AA have been isolated is summarized in Table 1.

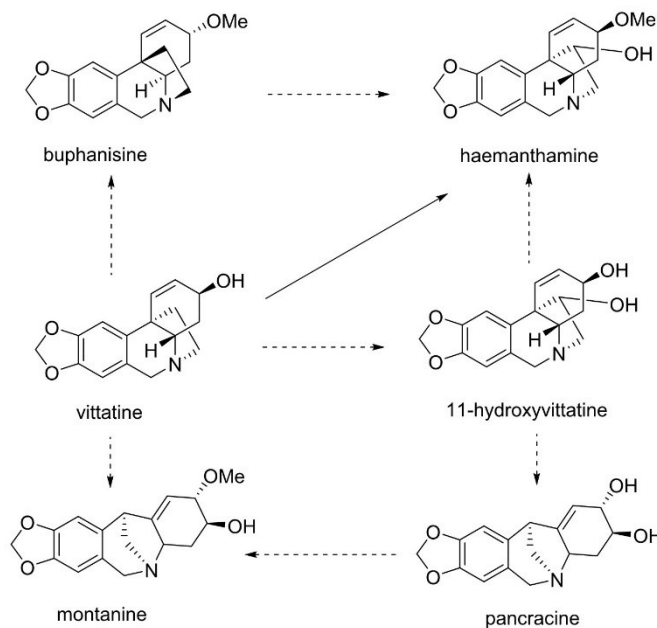


Figure 2. Proposed biosynthesis of montanine and pancracine, according to Feinstein and Wildman [23].

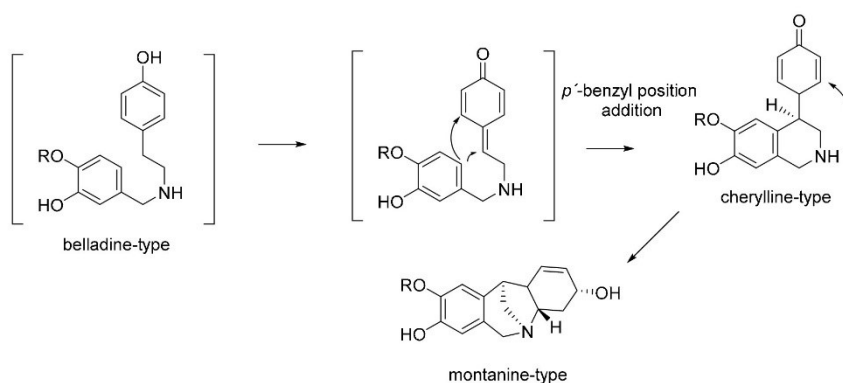


Figure 3. Proposed biosynthetic pathway for montanine-type, according to Jin [25].

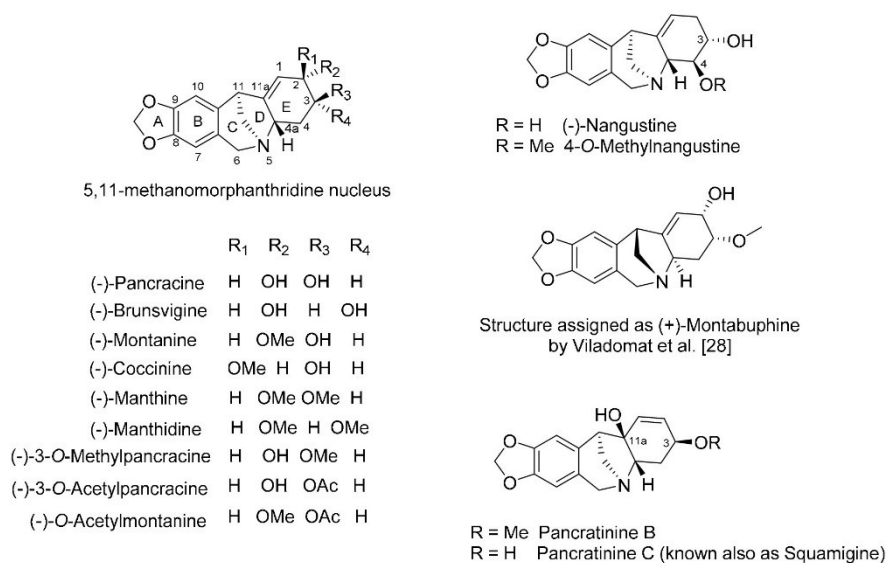


Figure 4. Chemical structures of montanine-type Amaryllidaceae alkaloids.

Table 1. Reported isolation and identification of montanine-type alkaloids in Amaryllidaceae plants.

Alkaloid	Amaryllidaceae Family Plants	References	Ref. for Spectroscopic Data (NMR, MS, UV, IR)
Montanine	<i>Rhodophiala bifida</i>	[16,31,32]	[33–40]
	<i>Haemanthus humilis</i>	[33]	
	<i>Haemanthus amarylloides</i>	[26]	
	<i>Haemanthus coccineus</i>	[26,34]	
	<i>Haemanthus montanus</i>	[26,34]	
	<i>Haemanthus sanguineus</i>	[34]	
	<i>Haemanthus paucifolius</i>	[41]	
	<i>Haemanthus deformis</i>	[41]	
	<i>Hippeastrum vittatum</i>	[35,42]	
	<i>Hippeastrum</i> cv. Ferrari	[43]	
	<i>Hippeastrum</i> cv. Double King	[43]	
	<i>Hippeastrum</i> cv. Pretty Nymph	[43]	
	<i>Hippeastrum</i> cv. Spartacus	[43]	
	<i>Hippeastrum argentinum</i>	[36]	
<i>Scadoxus multiflorus</i>	[37]		
Pancracine	<i>Rhodophiala bifida</i>	[16,32]	[36,39,40,44–46]
	<i>Pancreatium canariense</i>	[27,47]	
	<i>Pancreatium maritimum</i>	[44,45]	
	<i>Narcissus angustifolius</i> subsp. <i>transcarpathicus</i>	[46]	
	<i>Lycoris radiata</i>	[48]	
	<i>Hippeastrum</i> cv. Ferrari	[43]	
	<i>Hippeastrum</i> cv. Double King	[43]	
<i>Hippeastrum</i> cv. Pretty Nymph	[43]		
<i>Hippeastrum argentinum</i>	[36]		
Coccinine	<i>Haemanthus humilis</i>	[33]	[33,34,38–40]
	<i>Haemanthus amarylloides</i>	[26]	
	<i>Haemanthus coccineus</i>	[26]	
	<i>Haemanthus montanus</i>	[34]	
	<i>Haemanthus sanguineus</i>	[34]	
<i>Haemanthus deformis</i>	[41]		

Table 1. Cont.

Alkaloid	Amaryllidaceae Family Plants	References	Ref. for Spectroscopic Data (NMR, MS, UV, IR)
Manthine	<i>Haemanthus amarylloides</i>	[26]	[32,49]
	<i>Haemanthus montanus</i>	[34]	
	<i>Haemanthus tigrinus</i>	[50]	
Manthidine	<i>Haemanthus coccineus</i>	[26]	[40]
	<i>Haemanthus paucifolius</i>	[41]	
	<i>Haemanthus deformis</i>	[41]	
Brunsvigine	<i>Brunsvigia radulosa</i>	[50]	[40,49,51]
	<i>Brunsvigia cooperi</i>	[52]	
Panacratine B	<i>Panacratium canariense</i>	[27]	[27]
Panacratine C (reported also as Squamigine)	<i>Panacratium canariense</i>	[27]	[27,45]
	<i>Panacratium maritimum</i>	[45]	
	<i>Lycoris radiata</i>	[48]	
Nangustine	<i>Narcissus angustifolius</i> subsp. <i>transcarpathicus</i>	[46]	[46]
3-O-Methylpanacracine (reported also as isohaemanthamine)	<i>Lycoris radiata</i>	[48]	[32,49]
3-O-Acetylpanacracine	<i>Rhodophiala bifida</i>	[16]	[32]
4-O-Methylnangustine	<i>Hippeastrum argentinum</i>	[36]	[36]
Montabuphine	<i>Boophone flava</i>	[28]	[28–30]
O-Acetylmontanine	<i>Rhodophiala bifida</i>	[53]	[39]

3. Biological Activity of Montanine-Type Amaryllidaceae Alkaloids

Many studies have shown the antiproliferative, cytotoxic, antifungal, antibacterial, antimalarial, and anticholinesterase effects of AA [54–58]. The galantamine-type alkaloid galantamine is already used in the therapy of AD. Lycorine, haemanthamine, panacratistatin and narciclasine were found to display significant antiproliferative, cytotoxic and apoptotic properties across multiple cancer cell lines in vitro or the suppression of tumor growth in animal models of cancer in vivo [55,59–61]. As in the case of the potent pharmacological activities of lycorine-, haemanthamine- and narciclasine-type AA, the biological activities of montanine-type AA have also been studied, and today these structures belong to the most intensely investigated, since they have been reported to possess potent growth-inhibitory effects against diverse cancer cell lines [33,43,62,63]. It has also been shown that some montanine-type AA display anxiolytic, antidepressive and anticonvulsive activities, as well as immunomodulatory properties [42]. Moreover, montanine itself has also been studied for its acetylcholinesterase inhibition, and anti-rheumatic, antibacterial and antifungal effects [31,64,65].

3.1. Anticancer Potential of Montanine-Type Amaryllidaceae Alkaloids

The first evidence for montanine-type AA as an interesting group of plant-derived compounds that display growth inhibition and cytotoxicity to cancer cells in vitro was reported for montanine, isolated from bulbs of *Hippeastrum vittatum* in 2008 [35]. Since then, there have been other studies dealing with a group of montanine-type AA and their effect on proliferation and viability of cancer cells. Cytotoxicities, expressed as 50% inhibitory concentration (IC₅₀) values, for the antiproliferative activity of montanine-type AA in vitro against different cancer and non-cancer cell lines are summarized in Table 2. Either the IC₅₀ or GI₅₀ values quoted in the published works included in this table were determined using standard colorimetric assays, based on either the reduction of the tetrazolium salt WST-1 and MTT to formazan by mitochondrial dehydrogenases or an alternative quantitative assay based on the measurement of cellular protein content, using the protein-binding dye sulforhodamine B (SRB).

Table 2. Impact of montanine-type Amaryllidaceae alkaloids (AA) on proliferation of cancer and non-cancer cells using in vitro assays. Results are expressed as a (IC₅₀), or b (GI₅₀) in micromolar (μM) units, unless otherwise stated.

Montanine Type Alkaloid	Cell Line	Method of Assay/Time of Treatment	Value and Type of Half-Maximal Inhibitory Concentration		References
Montanine	Jurkat	WST-1/48 h	1.04 ± 0.14	a	[43]
	MOLT-4	WST-1/48 h	1.26 ± 0.11	a	[43]
	A549	WST-1/48 h	1.09 ± 0.31	a	[43]
	HT-29	WST-1/48 h	1.35 ± 0.47	a	[43]
	PANC-1	WST-1/48 h	2.30 ± 0.45	a	[43]
	A2780	WST-1/48 h	1.67 ± 0.29	a	[43]
	HeLa	WST-1/48 h	1.99 ± 0.22	a	[43]
	MCF-7	WST-1/48 h	1.39 ± 0.21	a	[43]
	SAOS-2	WST-1/48 h	1.36 ± 0.49	a	[43]
	MRC-5	WST-1/48 h	1.79 ± 0.50	a	[43]
	A549	MTT/48 h	1.9 ± 0.4	a	[33]
	HCT-15	MTT/48 h	6.8 ± 0.5	a	[33]
	SK-MEL-28	MTT/48 h	23.2 ± 1.9	a	[33]
	MCF-7	MTT/48 h	4.4 ± 0.4	a	[33]
	MDA-MB-231	MTT/48 h	3.4 ± 0.9	a	[33]
	Hs578T	MTT/48 h	3.6 ± 1.7	a	[33]
	HT-29	SRB/not specified	0.71 ± 0.1 μg/mL	a	[35]
	H460	SRB/not specified	0.57 ± 0.57 μg/mL	a	[35]
	RXF393	SRB/not specified	0.65 ± 0.01 μg/mL	a	[35]
	MCF7	SRB/not specified	0.74 ± 0.02 μg/mL	a	[35]
OVCAR3	SRB/not specified	0.84 ± 0.11 μg/mL	a	[35]	
Panracine	Jurkat	WST-1/48 h	5.07 ± 0.31	a	[62]
	MOLT-4	WST-1/48 h	2.71 ± 0.25	a	[62]
	A549	WST-1/48 h	2.29 ± 0.43	a	[62]
	HT-29	WST-1/48 h	2.60 ± 0.51	a	[62]
	A2780	WST-1/48 h	5.08 ± 0.43	a	[62]
	HeLa	WST-1/48 h	5.03 ± 0.36	a	[62]
	MCF-7	WST-1/48 h	2.68 ± 0.37	a	[62]
	SAOS-2	WST-1/48 h	2.20 ± 0.25	a	[62]
	MRC-5	WST-1/48 h	5.15 ± 0.34	a	[62]
	A2780	SRB/48 h	8.3 ± 0.5	b	[47]
	SW1573	SRB/48 h	4.3 ± 0.7	b	[47]
	T47-D	SRB/48 h	6.5 ± 2.5	b	[47]
	WiDr	SRB/48 h	9.1 ± 1.0	b	[47]
	Coccinine	A549	MTT/48 h	5.9 ± 0.8	a
HCT-15		MTT/48 h	16.8 ± 1.8	a	[33]
SK-MEL-28		MTT/48 h	>50	a	[33]
MCF-7		MTT/48 h	7.9 ± 0.9	a	[33]
MDA-MB-231		MTT/48 h	13.8 ± 0.8	a	[33]
Hs578T	MTT/48 h	5.3 ± 0.4	a	[33]	
Manthine	A549	MTT/72 h	3	b	[63]
	SKMEL-28	MTT/72 h	4	b	[63]
	U373	MTT/72 h	5	b	[63]
	MCF7	MTT/72 h	4	b	[63]
	Hs683	MTT/72 h	3	b	[63]
	B16F10	MTT/72 h	3	b	[63]

The previously mentioned work of Silva et al. [35] comparing montanine with vittatine reported the growth inhibitory activity of montanine against five human cell lines, colon adenocarcinoma HT29, non-small cell lung carcinoma H460, renal cell carcinoma RXF393, breast carcinoma MCF7 and epithelial ovarian cancer OVCAR3, with IC₅₀ values in the low μM range [35]. According to the study of Al Shammari et al. [43], montanine strongly decreased the growth of 7 different adherent cancer cell lines of several histotypes by treatment with a single 10 μM dose. Montanine was also

able to inhibit the cell growth of human leukemic cell lines MOLT-4 and Jurkat with a single dose of 10 μM , causing growth percentage GP values of 4% and 2%, respectively. All of these cell lines were tested for determination of IC_{50} values, using 48 hours' treatment and WST-1 assay. As can be seen in Table 2, Al Shammari et al. [43] used colon adenocarcinoma HT29 and breast carcinoma MCF7 cell lines and, similar to the study of Silva et al. [35]; values were in the low μM range (in the study of Silva et al. [35], 0.71 $\mu\text{g/mL}$ corresponds to 4.7 μM for HT-29, and 0.74 $\mu\text{g/mL}$ to 4.9 μM for MCF-7), although the second mentioned study does not specify the time interval over which montanine had been applied to the determined cell lines. Not only these, but also other adherent cancer cell lines used in the study (pancreatic carcinoma PANC-1, ovarian carcinoma A2780, cervix carcinoma HeLa, osteosarcoma SAOS-2), were very strongly inhibited by montanine treatment in low μM concentration. The concentration producing 50% inhibition of proliferation of a cancer cells model resistant to apoptosis (lung adenocarcinoma A549) is even lower and was $1.09 \pm 0.31 \mu\text{M}$ in this study [43]. Instead of these human adherent cancer cell lines, the IC_{50} values of leukemic Jurkat and MOLT-4 cell lines were very low, resulting in values of $1.04 \pm 0.14 \mu\text{M}$ and $1.26 \pm 0.11 \mu\text{M}$.

Another recent study of Masi et al. [33] confirmed the strong antiproliferative and cytotoxic effect of montanine on cancer cell death, using a panel of six cancer cell lines, including human breast carcinoma MCF-7, mammary gland Hs578T, adenocarcinoma MDA-MB-231, human colon carcinoma HCT-15, human lung carcinoma A549 and human melanoma SK-MEL-28 [33].

The study of Masi et al. [33] was also the first work reporting the cytotoxicity of coccinine, which was co-isolated with montanine from *Haemanthus humilis*. The antiproliferative effect of coccinine reported in this study revealed this montanine-type alkaloid as being the more promising anticancer agent. However, despite the promising observations on the activity of coccinine during the cell culture experiments, its overall cytotoxicity was less than that of montanine [33].

Another important montanine-type AA, pancracine, isolated from *N. cv. Professor Einstein*, displayed significant cytotoxic effects [62]. The first screening test for cytotoxicity revealed the ability of 10 μM pancracine treatment to reduce the viability of 9 cancer cell lines, including Jurkat, MOLT-4, A549, MCF-7, A2780, HT-29, PANC-1, HeLa and SAOS-2. Except for PANC-1, the IC_{50} values for all the remaining cell lines were determined; values ranged from 2.20 to 5.15 μM , as described in detail in Table 2 [62].

Antiproliferative activities were also achieved with pancracine isolated from *P. canariense* [47]. This structure-activity study was mentioned earlier in the section of derivatives of montanine type AA. Nevertheless, it is important to highlight the strong growth inhibitory effect of pancracine treatment observed in a mini-panel of human solid tumors derived from ovarian tissue (A2780), lung (SW1573), breast (T-47D) and colon (WiDr) [47]. As in the study of Breiterová et al. [66], A2780 had a similar IC_{50} value after 48 hours' treatment.

In vitro growth-inhibitory effects of another montanine type AA, manthine, against cancer cells resistant to (A549, SK-MEL-28, U373) and sensitive to (MCF-7, Hs683, B16F10) apoptosis suggest that manthine is capable of overcoming apoptosis resistance [63]. In the same study, manthine also significantly reduced the proliferation of the GSC22 cancer cell line at a concentration as low as 1 μM and also inhibited proliferation by 95% at concentrations of 10 and 30 μM . Manthine was, surprisingly enough, more efficient than haemanthamine [63].

From the papers published so far, it appears that montanine, the main representative of montanine-type AA, is the most effective in reducing the growth of cancer cell lines within this group of structurally related compounds. On the other hand, the relevance of this conclusion is uncertain, since only four of these compounds have been tested for cytotoxicity so far. It is evident from the results described that further efforts should be made to reveal the mechanism of the cytotoxic effect of these substances and a detailed mode of action can lead to better subsequent in vivo testing. Since many different types of solid and leukemic cancer cell lines have been used to study cytotoxicity, it can be concluded that montanine type AA are promising agents in the field of therapy of human cancer diseases.

3.2. Other Biological Activities of Montanine-Type Amaryllidaceae Alkaloids

As already mentioned above, montanine-type alkaloids are not abundant in plants, thus only a few pilot studies have been reported on other biological activities of these compounds.

Montanine and pancracine were screened for their antibacterial activity in two different studies [65,67]. Montanine was the more active of the two alkaloids against pathogenic *Escherichia coli*, *Pseudomonas aeruginosa*, *Staphylococcus aureus* and *S. epidermis*, giving values of 5, 20, 5 and 15 µg respectively, as minimum quantities required for activity [67]. The antibacterial and antifungal activity of pancracine has been studied using an agar diffusion technique against a Gram-positive-bacterium *S. aureus*, two Gram-negative bacteria *E. coli* and *P. aeruginosa*, and *Candida albicans* [65]. Pancracine displayed activity against *S. aureus* and *P. aeruginosa* and moderate activity against *C. albicans*, with a MIC of 188 µg/mL.

The in vitro antiparasitic activity of nangustine and pancracine isolated from *N. angustifolius* subsp. *transcarpathicus* against the protozoans *Trypanosoma brucei rhodesiense*, *T. cruzi*, *Leishmania donovani* and *P. falciparum* was reported in 2002 [46]. Pancracine showed a higher activity than nangustine against all four protozoan parasites tested (Table 3). While nangustine has been classified as inactive, pancracine showed weak activity against *T. brucei rhodesiense* and *T. cruzi*, but no activity against *L. donovani*. The IC₅₀ values of 0.75 and 0.70 µg/mL, respectively, for two strains of *Plasmodium falciparum*, represented the weak antimalarial activity of pancracine. No cytotoxic activity was demonstrated for either alkaloid against L-6 cells (rat skeletal myoblasts) within this study [46].

Table 3. In vitro activity of nangustine and pancracine against parasitic protozoa [46].

Parasite	<i>Trypanosoma brucei rhodesiense</i>	<i>Trypanosoma cruzi</i>	<i>Leishmania donovani</i>	<i>Plasmodium falciparum</i>	
Stage	Trypomastigote	Trypomastigote	Amastigotes	Erythrocytic form	
Strain	SIIB 900 IC ₅₀ (µg/mL)	Tulahuen C4 IC ₅₀ (µg/mL)	MHOM-ET-67/L82 IC ₅₀ (µg/mL)	K1 IC ₅₀ (µg/mL)	NF54 IC ₅₀ (µg/mL)
Nangustine	9.6	54.6	>30	2.14	2.93
Pancracine	0.7	7.1	>30	0.75	0.70

Montanine has also been studied for its antiarthritic activity in antigen-induced and collagen-induced arthritis models [31]. The alkaloid significantly attenuated the development of experimental arthritis in both acute and chronic models [31], dose-dependently, with the lower dose being more effective in arthritis severity and paw nociception. This finding hypothesized that increased availability of montanine leads to an acute activation that culminates in mechanisms of desensitization of the receptor, reducing the activation of receptor cell signaling and, consequently, decreasing the biological effect seen at lower doses [31]. The obtained results indicated that montanine has a potential as a drug for autoimmune diseases, such as arthritis.

Two studies concerning the unique insight into biosynthesis regulation of AA montanine in the *R. bifida* plant [16] and its anti-rheumatic effect [31] are followed by a patent granted to the scientific group of prof. Zuanazzi in 2020 [68]. The embodiment of US20200000798A1 patent invention describes in detail the method of extraction of the alkaloid montanine, which is much faster than the previously described methods of isolation of alkaloids from *R. bifida* plant dispensing with numerous changes of solvent in order to strain the plant. The importance of this alkaloid is then evaluated by in vivo and in vitro tests as very promising in the treatment of anti-inflammatory diseases such as rheumatoid arthritis, ulcerative colitis, sepsis, acute pulmonary disease, inflammatory infections; in particular, inflammatory and fibrosing diseases related to the lungs and kidneys, osteoporosis. These drug candidate bioactivities were determined through biologically significant effect on the nociception, migration and proliferation of fibroblasts and lymphocytes and without changing or depressing the immune system.

AA are relevant options for the treatment of neurological disorders and neurodegenerative diseases. Montanine has been characterized behaviorally and toxicologically in a search for therapeutic applications by da Silva [42]. It has been found that montanine reduces locomotor activity and has sedative, anxiolytic, anticonvulsant and antidepressant effects in mice. Da Silva et al. suggested that montanine may act on the benzodiazepine site of the GABA receptor in mouse brain, and thus the anxiolytic, hypnotic effects of montanine could be caused by its combined action on several neurotransmitter receptor systems, including GABA receptors [42]. To the best of our knowledge, there is only one in silico study describing an interaction between montanine and γ -amino butyric acid type-A receptor associated protein (GABARAP), which is the ubiquitin-like modifier implicated in the intracellular trafficking of the GABA receptor [66] to study alkaloids with potential antiepileptic activity. On the other hand, a study revealing the mechanism of this action is still missing. Extracts of three *Haemanthus* species, *H. coccineus*, *H. montanus* and *H. sanguineus*, and major alkaloid constituents, coccinine and montanine, were investigated in vitro for their affinity to the serotonin transporter protein SERT as potential antidepressants [34]. Both montanine and coccinine exhibited lower SERT affinity than estimated and did not explain the higher activity observed in the extracts.

Since galantamine, an AA, is used in the therapy of AD, AA and their semisynthetic derivatives have been intensively studied for their biological activity connected with the potential treatment of this disease [69–72]. So far, only two montanine-type alkaloids have been investigated for their potential to inhibit acetylcholinesterase. 4-O-Methylangustine, isolated from *H. argentinum*, was not able to inhibit acetylcholinesterase activity significantly [36]. The effect of montanine on acetylcholinesterase activity has been studied at concentrations of 1, 500 and 100 μ M. Montanine inhibited, in a dose-dependent manner, more than 50% of the enzyme at 1 mM concentration. With concentrations of 500 and 100 μ M, 30–45% inhibition of AChE activity was detected [64]. The IC_{50} value was not determined within the study, but, from the obtained results, it can be deduced that the IC_{50} of montanine is higher than 100 μ M. Compared with the IC_{50} value of galantamine ($1.7 \pm 0.1 \mu$ M [73]), montanine is recognized as a weak AChE inhibitor.

4. Preparation of Montanine-Type Alkaloids by Rearrangement of Haemanthamine-Type Ring System

The unique structural features and promising biological activities associated with montanine-type AA and their low content in plant material have attracted considerable synthetic efforts [29,30,39,40,49,74–91]. However, most synthetic approaches involve many steps and low yield. For example, Hong et al., in 2008, reported the total synthesis of (–)-manthine involving over 18 steps [49]. Since multigram isolation of haemanthamine from plant material has been developed and old reports describe a semisynthetic transformation of the haemanthamine-type skeleton to the montanine-type scaffold [50,92], the preparation of montanine-type AA from the haemanthamine-type seems to be an elegant route for production of these alkaloids in higher amount compared with their total synthesis. The possibility of transformation of the haemanthamine ring type to the montanine-type skeleton through an intramolecular rearrangement was reported for the first time by Inubushi et al. in 1960 [50], within a study to define the absolute configuration of the newly discovered montanine-type alkaloids. During an experiment designed to find a method for replacing the C11 hydroxyl in crinine-type alkaloids with hydrogen, haemanthamine and crinamine were reacted with mesylchloride in pyridine and hydrolyzed by alkalized water. The result was the generation of two new compounds with a montanine-type scaffold, isomeric, but not identical to montanine and coccinine [50]. Manthine was also synthesized by the rearrangement of haemanthamine through mesylation and the addition of sodium methoxide as a nucleophile [50]. In 2009, Cedrón et al. [92] reported an unexpected rearrangement of the haemanthamine skeleton to a montanine skeleton in the presence of different halogenating agents like thionyl chloride ($SOCl_2$), thionyl bromide and diethylaminosulfur trifluoride (DAST). Several experiments were performed to improve the yield. The different ratio of $SOCl_2$ and the presence of base in the reaction mixture have been studied. When 1.5 equiv. of $SOCl_2$ and 1.5

equiv. of pyridine were used, lower yields of products were obtained. The best results were achieved using a large excess of SOCl_2 . When 20 equiv. of SOCl_2 were used, the yield improved to 71% of the montanine-type skeleton [92]. In 2018, a series of synthetic analogues of montanine-type alkaloids was reported by Govindaraju et al. [63]. The mechanism of this rearrangement has been described recently in detail, explaining the mesylated hydroxyl group at C-11 as a good leaving group being attacked intramolecularly by an electron rich aromatic moiety to create a new bond between C-10a and C-11, leading to the appearance of a 7-membered ring (Figure 5) [50,63].

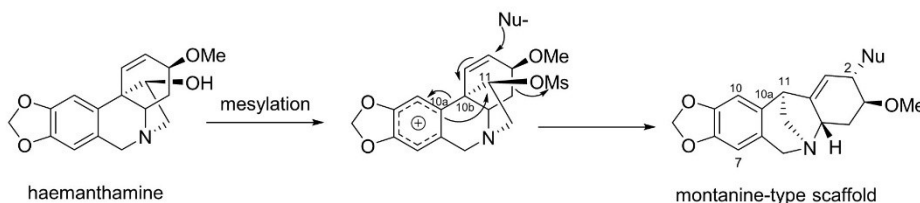


Figure 5. Tentative mechanism for haemanthamine-montanine skeletal rearrangement, according to Govindaraju et al. [63].

5. Preparation and Structure Activity Relationship Studies on Synthetic Analogues of Montanine Type Alkaloids

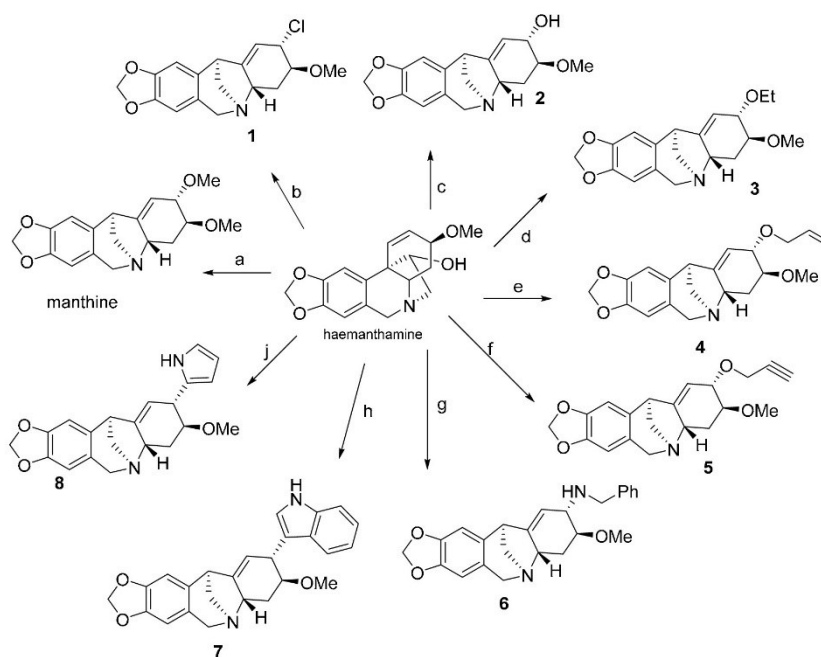
The promising antiproliferative properties of some representatives of montanine-type AA, primarily of montanine and pancracine, initiated the development of synthetic analogues of these alkaloids.

A series of montanine derivatives has been developed under different reaction conditions (Scheme 1, Scheme 2). Various C2-substituted derivatives were prepared through the rearrangement of the haemanthamine ring by using different nucleophiles. Compounds 3, 4 and 5 were prepared by using ethanol, allyl alcohol and propargyl alcohol respectively in tetrahydrofuran (THF) solution and treated with NaH. Compound 6 was prepared by substitution of the OH group at C2 using benzylamine. Compounds 7 and 8 were produced using indole and pyrrole dissolved in THF and alkalized with NaH. Compound 1 was formed through haemanthamine rearrangement using methansulfonyl chloride and then utilized in the synthesis of 9, 10, 11 and 12, to investigate the possible effect of different substitutions in ring B and on nitrogen (Scheme 2). The detailed preparation of these derivatives can be found in Govindaraju et al. [63]. Subsequently, montanine-type derivatives were screened for their antiproliferative activity on different cancer cell lines [63].

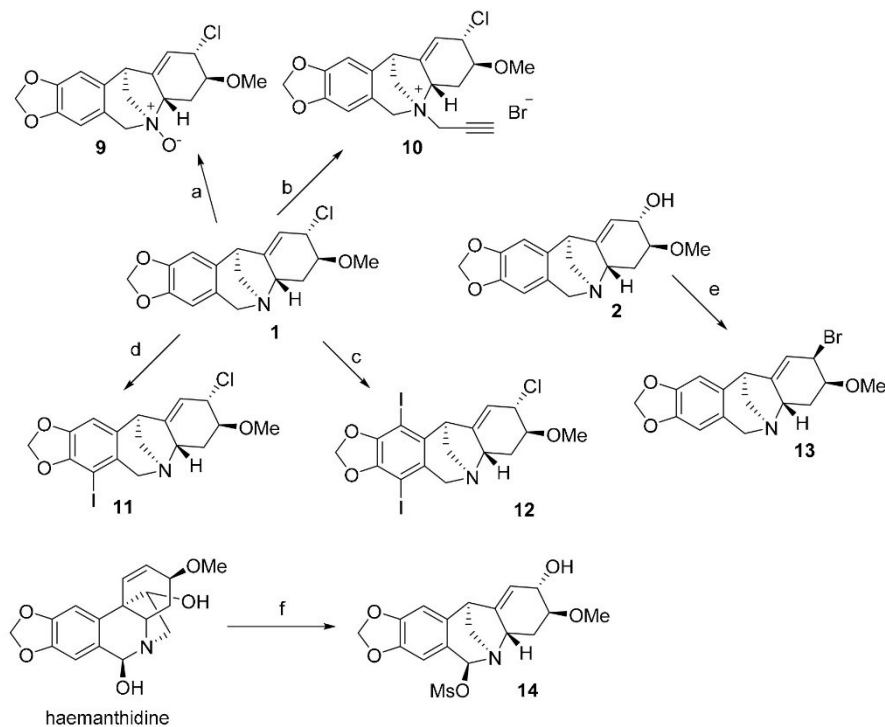
The antiproliferative properties of the synthesized compounds were evaluated *in vitro* using the MTT colorimetric assay on a panel of six cancer cell lines (A549, SKMEL-28, U373, MCF7, Hs683, B16F10); the results are summarized in Table 4. For the study of antiproliferative activity, the most explored position was C2, as the OH group is accessible for many chemical reactions. In the developed mini library, it has been demonstrated that the highest anticancer activity belongs to manthine, but a replacement of the methoxy group at position C2 by an ethoxy group, such as in 3, leads to reduction of antiproliferative activity, although other substitutions of a three-membered carbon chain with multiple unsaturated bonds regain the activity. Although compound 7 showed interesting antiproliferative activity against different cell lines while containing a large indole substituent at position C2, overall, a small molecule replacement at C2, like OH, Cl and Br, is preferred for anticancer activity and the stereochemical configuration of C2 replacement does not seem critical for maintenance of activity, as demonstrated for derivatives 1, 2, and 13 (Table 4) [63].

Table 4. Results of in vitro antiproliferative study of derivatives of montanine-type AA and manthine [63].

Compound	GI ₅₀ In Vitro Values (μM)					
	Resistant to Apoptosis			Sensitive to Apoptosis		
	A549	SKMEL-28	U373	MCF7	Hs683	B16F10
1	6	26	51	17	6	7
2	5	8	31	13	4	8
Manthine	3	4	5	4	3	3
3	59	>100	>100	82	>100	40
4	10	14	20	20	7	7
5	23	28	42	28	24	10
6	59	65	72	44	67	10
7	18	9	9	23	24	4
8	86	67	>100	68	95	11
9	>100	>100	>100	>100	>100	>100
10	>100	>100	>100	>100	>100	>100
11	>100	>100	>100	>100	>100	>100
12	78	>100	>100	78	71	39
13	9	18	25	19	5	7
14	>100	>100	>100	>100	>100	72



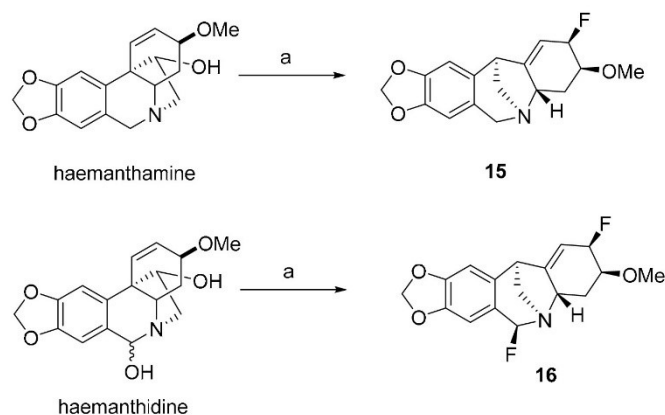
Scheme 1. Preparation of C2-derived montanine-type derivatives, in order to study antiproliferative potential. Reagents and conditions for synthesis: (a) MsCl, py, 0 °C, 8 h, then MeOH, NaH (yield 65%); (b) MsCl, Et₃N, CH₂Cl₂, rt, 48 h, (yield 55%) (c) MsCl, py, 0 °C, 8 h, then aq. NaHCO₃ (yield 74%); (d) MsCl, py, 0 °C, 8 h, then EtOH, NaH (yield 65%); (e) MsCl, py, 0 °C, 8 h, then CH₂=CH-CH₂-OH, NaH (yield 68%) (f) MsCl, py, 0 °C, 8 h, then CH≡C-CH₂-OH, NaH (yield 50%) (g) MsCl, py, 0 °C, 8 h, then BnNH₂, NaH (yield 67%); (h) MsCl, py, 0 °C, 8 h, then indole, NaH (yield 62%); (j) MsCl, py, 0 °C, 8 h, then pyrrole, NaH (yield 55%).



Scheme 2. Further modifications of montanine derivatives and rearrangement of haemanthidine. Reagents and conditions for synthesis: (a) m-CPBA, CH_2Cl_2 , rt, 30 min, (yield 70%); (b) MeCN, rt, $\text{CH}\equiv\text{C}-\text{CH}_2-\text{Br}$, 24 h, (yield 78%) (c) NIS (2.4 eq), $\text{In}(\text{OTf})_3$, MeCN, 45 °C, 12 h, (yield 55%); (d) NIS, $\text{In}(\text{OTf})_3$, MeCN, 45 °C, 12 h, (yield 72%); (e) CBr_4 , Ph_3P , CH_2Cl_2 , rt, 4 h, (yield 64%) (f) MsCl (4 eq), py, 0 °C, 8 h, then aq. NaHCO_3 (yield 46%).

Quaternization of the nitrogen produced inactive compounds like **9** and **10**, suggesting that charged derivatives cannot cross the cell membrane. Finally, the substitution pattern on ring B appears to be critical as derivatization at positions C7 and C10 in compounds **11** and **12** led to the loss of antiproliferative activity [63]. The rearrangement of haemanthidine to the corresponding montanine derivative **14** gave a completely inactive substance suggesting that C6 should be free to maintain antiproliferative activity (Scheme 2; Table 4) [47,63].

Derivatives of montanine-type alkaloids **1**, **15**, and **16** developed by the rearrangement of haemanthidine and haemanthidine by Cedrón et al. in 2009 (Scheme 3) and pancracine were screened for their antimalarial potential against the F-32 Tanzanian strains of *P. falciparum* [92]. All the derivatives displayed higher activity (Table 5) than the natural alkaloid pancracine. The results indicated that the presence of one or more halogens is able to increase antimalarial activity [92].



Scheme 3. Preparation of further derivatives of montanine-type AA by rearrangement from haemanthamine and haemanthidine. Reagents and conditions for synthesis: (a) DAST, DCM, -78°C , 24 h, (yield for **15** 60%; yield for **16** 49%).

Table 5. Results of in vitro assay of derivatives **1**, **15**, **16** and pancracine against *Plasmodium falciparum* F-32.

Compound	IC ₅₀ (μg/mL)
Pancracine	0.9 ± 0.04
1	0.4 ± 0.02
15	0.6 ± 0.04
16	0.7 ± 0.04
Chloroquine	0.013

6. Conclusions

This review summarizes the phytochemical and biological investigations of montanine-type AA. These alkaloids bear a characteristic 5,11-methanomorphanthridine structural core. To date, only 14 montanine-type AA have been isolated from nature, suggesting that they are quite rare. Some representatives of these alkaloids have been studied for different biological activities. Because of their unique architecture and promising antitumor activity, these alkaloids attracted synthetic effort for total synthesis, and also for the preparation of derivatives using several halogenating agents to study structure-activity relationships. Interestingly, montanine-type alkaloids can be easily obtained from alkaloids with a haemanthamine skeleton, which are more common and available from Amaryllidaceae plants. In the light of the presented overview of scientific data, the montanine-type AA can be recognized as an interesting source for the development of new drugs for the treatment of various diseases.

Author Contributions: Conceptualization, D.K., N.M., R.H., L.C., M.Ř., L.O., and G.B.; Methodology, L.C., R.H., Formal analysis, D.K., N.M., R.H. and L.O. Investigation, D.K., N.M., and R.H. Writing—original draft preparation, L.C., D.K., N.M., R.H. Writing—reviewing and editing, D.K., N.M., R.H., M.Ř., L.O., G.B., and L.C. All authors have read and agreed to the published version of the manuscript.

Funding: This research has been funded by projects of Charles University (No. SVV UK 260 548; Progres/UK Q40-01 and Q42), and pre-application research into innovative medicines and medical technologies project (Reg. No. CZ.02.1.01/0.0/0.0/18_069/0010046), co-funded by the European Union.

Conflicts of Interest: The authors declare no conflict of interest.

References

1. Dahlgren, R.M.T.; Clifford, H.T.; Yeo, P.F. *The Families of the Monocotyledons. Structure, Evolution and Taxonomy*, 1st ed.; Springer: New York, NY, USA, 1985; pp. 1–520.
2. Elgorashi, E.E.; van Staden, J. Bioactivity and bioactive compounds from African Amaryllidaceae. In *African Natural Plant Products: New Discoveries and Challenges in Chemistry and Quality*; ACS Symposium Series; Juliani, H.R., Simon, J.E., Ho, C.T., Eds.; American Chemical Society: Washington, DC, USA, 2009; Volume 1021, pp. 151–170.
3. Nair, J.J.; Bastida, J.; van Staden, J. In vivo cytotoxicity studies of Amaryllidaceae alkaloids. *Nat. Prod. Commun.* **2016**, *11*, 121–132. [[CrossRef](#)] [[PubMed](#)]
4. Dalecká, M.; Havelek, R.; Královec, K.; Brůčková, L.; Cahliková, L. Amaryllidaceae family alkaloids as potential drugs for cancer treatment. *Chem. Listy* **2013**, *107*, 701–708.
5. Jin, Z. Amaryllidaceae and Scelletium alkaloids. *Nat. Prod. Rep.* **2016**, *33*, 1318–1343. [[CrossRef](#)] [[PubMed](#)]
6. Havelek, R.; Muthna, D.; Tomsik, P.; Kralovec, K.; Seifrtova, M.; Cahlikova, L.; Hostalkova, A.; Safratova, M.; Perwein, M.; Cermakova, E.; et al. Anticancer potential of Amaryllidaceae alkaloids evaluated by screening with a panel of human cells, real-time cellular analysis and Ehrlich tumor-bearing mice. *Chem. Biol. Interact.* **2017**, *275*, 121–132. [[CrossRef](#)] [[PubMed](#)]
7. Fennell, C.W.; van Staden, J. *Crinum* species in traditional and modern medicine. *J. Ethnopharmacol.* **2001**, *78*, 15–26. [[CrossRef](#)]
8. Graham, J.G.; Quinn, M.L.; Fabricant, D.S.; Farnsworth, N.R. Plants used against cancer—An extension of the work of Jonathan Hartwell. *J. Ethnopharmacol.* **2000**, *73*, 347–377. [[CrossRef](#)]
9. Caamal-Fuentes, E.; Torres-Tapia, L.W.; Simá-Polanco, P.; Peraza-Sánchez, S.R.; Moo-Puc, R. Screening of plants used in Mayan traditional medicine to treat cancer-like symptoms. *J. Ethnopharmacol.* **2011**, *135*, 719–724. [[CrossRef](#)]
10. Herrera, M.R.; Machocho, A.K.; Brun, R.; Viladomat, F.; Codina, C.; Bastida, J. Crinine and lycorane type alkaloids from *Zephyranthes citrina*. *Planta Med.* **2001**, *67*, 191–193. [[CrossRef](#)]
11. Nair, J.J.; van Staden, J. Pharmacological and toxicological insights to the South African Amaryllidaceae. *Food Chem. Toxicol.* **2013**, *62*, 262–275. [[CrossRef](#)]
12. Ingrassia, L.; Lefranc, F.; Mathieu, V.; Darro, F.; Kiss, R. Amaryllidaceae isocarbostyryl alkaloids and their derivatives as promising antitumor agents. *Transl. Oncol.* **2008**, *1*, 1–13. [[CrossRef](#)]
13. Kornienko, A.; Evidente, A. Chemistry, biology, and medicinal potential of narciclasine and its congeners. *Chem. Rev.* **2008**, *108*, 1982–2014. [[CrossRef](#)] [[PubMed](#)]
14. Anand, R.; Gill, K.D.; Mahdi, A.A. Therapeutics of Alzheimer’s disease: Past, present and future. *Neuropharmacology* **2014**, *76*, 27–50. [[CrossRef](#)] [[PubMed](#)]
15. Kilgore, M.B.; Kutchan, T.M. The Amaryllidaceae alkaloids: Biosynthesis and methods for enzyme discovery. *Phytochem. Rev.* **2016**, *15*, 317–337. [[CrossRef](#)] [[PubMed](#)]
16. Reis, A.; Magne, K.; Massot, S.; Tallini, L.R.; Scopel, M.; Bastida, J.; Ratet, P.; Zuanazzi, J.A.S. Amaryllidaceae alkaloids: Identification and partial characterization of montanine production in *Rhodophiala bifida* plant. *Sci. Rep.* **2019**, *9*, 1–11. [[CrossRef](#)]
17. Singh, A.; Desgagné-Penix, I. Biosynthesis of the Amaryllidaceae alkaloids. *Plant Sci. Today* **2014**, *1*, 114–120. [[CrossRef](#)]
18. Wang, R.; Xu, S.; Wang, N.; Xia, B.; Jiang, Y.; Wang, R. Transcriptome analysis of secondary metabolism pathway, transcription factors, and transporters in response to methyl jasmonate in *Lycoris aurea*. *Front. Plant Sci.* **2017**, *7*, 1971. [[CrossRef](#)]
19. Ferdousi, A. A Metabolomics and Transcriptomics Comparison of *Narcissus pseudonarcissus* cv. Carlton Feld and In Vitro Tissues in Relation to Alkaloid Production. Ph.D. Thesis, University of Liverpool, Liverpool, UK, 2017.
20. Singh, A.; Desgagné-Penix, I. Transcriptome and metabolome profiling of *Narcissus pseudonarcissus* ‘King Alfred’ reveal components of Amaryllidaceae alkaloid metabolism. *Sci. Rep.* **2017**, *7*, 17356. [[CrossRef](#)]
21. Fuganti, C.; Ghiringhelli, D.; Grasselli, P. Stereochemistry of hydrogen removal β to nitrogen in the biological conversion of *O*-methylnorbelladine into the montanine-type alkaloids. *J. Chem. Soc. Chem. Commun.* **1973**, *13*, 430–431. [[CrossRef](#)]
22. Wildman, W.C.; Olesen, B. Biosynthesis of montanine. *J. Chem. Soc. Chem. Commun.* **1976**, *14*, 551. [[CrossRef](#)]

23. Feinstein, A.I.; Wildman, W.C. Biosynthetic oxidation and rearrangement of vittatine and its derivatives. *J. Org. Chem.* **1976**, *41*, 2447–2450. [[CrossRef](#)]
24. Laurain-Mattar, D.; Ptak, A. Amaryllidaceae alkaloid accumulation by plant in vitro system. In *Bioprocessing of Plant In Vitro Systems, Reference Series in Phytochemistry*; Pavlov, A., Bley, T., Eds.; Springer International Publishing: Cham, Switzerland, 2016; pp. 1–22.
25. Jin, Z. Amaryllidaceae and Scelletium alkaloids. *Nat. Prod. Rep.* **2007**, *24*, 886–905. [[CrossRef](#)] [[PubMed](#)]
26. Wildman, W.C.; Kaufman, C.J. Alkaloids of the Amaryllidaceae. III. Isolation of five new alkaloids from *Haemanthus* species1. *J. Am. Chem. Soc.* **1955**, *77*, 1248–1252. [[CrossRef](#)]
27. Cedrón, J.C.; Oberti, J.C.; Estévez-Braun, A.; Ravelo, A.G.; del Arco-Aguilar, M.; López, M. *Pancreatium canariense* as an important source of Amaryllidaceae alkaloids. *J. Nat. Prod.* **2009**, *72*, 112–116. [[CrossRef](#)] [[PubMed](#)]
28. Viladomat, F.; Bastida, J.; Codina, C.; Campbell, W.E.; Mathee, S. Alkaloids from *Boophane flava*. *Phytochemistry* **1995**, *40*, 307–311. [[CrossRef](#)]
29. Guan, Y.; Zhang, H.; Pan, C.; Wang, J.; Huang, R.; Li, Q. Flexible synthesis of montanine-like alkaloids: Revisiting the structure of montabuphine. *Org. Biomol. Chem.* **2012**, *10*, 3812–3814. [[CrossRef](#)] [[PubMed](#)]
30. Matveenko, M.; Banwell, M.G.; Willis, A.C. A chemoenzymatic total synthesis of the structure assigned to the alkaloid (+)-montabuphine. *Org. Lett.* **2008**, *10*, 4693–4696. [[CrossRef](#)]
31. Farinon, M.; Clarimundo, V.S.; Pedrazza, G.P.; Gulko, P.S.; Zuanazzi, J.A.; Xavier, R.M.; de Oliveira, P.G. Disease modifying anti-rheumatic activity of the alkaloid montanine on experimental arthritis and fibroblast-like synoviocytes. *Eur. J. Pharmacol.* **2017**, *799*, 180–187. [[CrossRef](#)]
32. Wildman, W.C.; Brown, C.L. Mass spectra of 5,11-methanomorphanthridine alkaloids. The structure of pancracine. *J. Am. Chem. Soc.* **1968**, *90*, 6439–6446. [[CrossRef](#)]
33. Masi, M.; Van Slambrouck, S.; Gunawardana, S.; van Rensburg, M.J.; James, P.C.; Mochel, J.G.; Heliso, P.S.; Albalawi, A.S.; Cimmino, A.; van Otterlo, W.A.L.; et al. Alkaloids isolated from *Haemanthus humilis* Jacq., an indigenous South African Amaryllidaceae: Anticancer activity of coccinine and montanine. *S. Afr. J. Bot.* **2019**, *126*, 277–281. [[CrossRef](#)]
34. Stafford, G.I.; Birer, C.; Brodin, B.; Christensen, S.B.; Eriksson, A.H.; Jäger, A.K.; Rønsted, N. Serotonin transporter protein (SERT) and P-glycoprotein (P-gp) binding activity of montanine and coccinine from three species of *Haemanthus* L. (Amaryllidaceae). *S. Afr. J. Bot.* **2013**, *88*, 101–106. [[CrossRef](#)]
35. Silva, A.F.S.; de Andrade, J.P.; Machado, K.R.B.; Rocha, A.B.; Apel, M.A.; Sobral, M.E.G.; Henriques, A.T.; Zuanazzi, J.A. Screening for cytotoxic activity of extracts and isolated alkaloids from bulbs of *Hippeastrum vittatum*. *Phytomedicine* **2008**, *15*, 882–885. [[CrossRef](#)] [[PubMed](#)]
36. Ortiz, J.E.; Pigni, N.B.; Andujar, S.A.; Roitman, G.; Suvire, F.D.; Enriz, R.D.; Tapia, A.; Bastida, J.; Feresin, G.E. Alkaloids from *Hippeastrum argentinum* and their cholinesterase-inhibitory activities: An in vitro and in silico study. *J. Nat. Prod.* **2016**, *79*, 1241–1248. [[CrossRef](#)] [[PubMed](#)]
37. Cahliková, L.; Benešová, N.; Macáková, K.; Urbanová, K.; Opletal, L. GC/MS analysis of three Amaryllidaceae species and their cholinesterase activity. *Nat. Prod. Commun.* **2011**, *6*, 1255–1258. [[CrossRef](#)] [[PubMed](#)]
38. Duffield, A.M.; Aplin, R.T.; Budzikiewicz, H.; Djerassi, C.; Murphy, C.F.; Wildman, W.C. Mass spectrometry in structural and stereochemical problems. LXXXII. 1 A study of the fragmentation of some Amaryllidaceae alkaloids2. *J. Am. Chem. Soc.* **1965**, *87*, 4902–4912. [[CrossRef](#)] [[PubMed](#)]
39. Ishizaki, M.; Hoshino, O.; Iitaka, Y. Total synthesis of montanine-type Amaryllidaceae alkaloids, which possess a 5, 11-methanomorphanthridine ring system, through cyclization with sodium bis (2-methoxyethoxy) aluminum hydride (SMEAH): The first stereoselective total syntheses of (±)-montanine, (±)-coccinine, (±)-O-acetylmontanine, (±)-pancracine, and (±)-brunsvigine. *J. Org. Chem.* **1992**, *57*, 7285–7295.
40. Bao, X.; Cao, Y.X.; Chu, W.D.; Qu, H.; Du, J.Y.; Zhao, X.H.; Ma, X.Y.; Wang, C.T.; Fan, C.A. Bioinspired total synthesis of montanine-type Amaryllidaceae alkaloids. *Angew. Chem. Int. Edit.* **2013**, *52*, 14167–14172. [[CrossRef](#)] [[PubMed](#)]
41. Crouch, N.R.; Pohl, T.L.; Mulholland, D.A.; Ndlovu, E.; Van staden, J. Alkaloids from three ethnomedicinal *Haemanthus* species: *H. albiflos*, *H. deformis* and *H. paucifolius* (Amaryllidaceae). *S. Afr. J. Bot.* **2005**, *71*, 49–52. [[CrossRef](#)]
42. da Silva, A.F.S.; de Andrade, J.P.; Bevilacqua, L.R.M.; de Souza, M.M.; Izquierdo, I.; Henriques, A.T.; Zuanazzi, J.A.S. Anxiolytic-, antidepressant- and anticonvulsant-like effects of the alkaloid montanine isolated from *Hippeastrum vittatum*. *Pharmacol. Biochem. Behav.* **2006**, *85*, 148–154. [[CrossRef](#)]

43. Al Shammari, L.; Al Mamun, A.; Koutová, D.; Majorošová, M.; Hulcová, D.; Šafratová, M.; Breiterová, K.; Maříková, J.; Havelek, R.; Cahlíková, L. Alkaloid profiling of *Hippeastrum* cultivars by GC-MS, isolation of Amaryllidaceae alkaloids and evaluation of their cytotoxicity. *Rec. Nat. Prod.* **2020**, *14*, 154–159. [[CrossRef](#)]
44. Berkov, S.; Evstatieva, L.; Popov, S. Alkaloids in Bulgarian *Pancreatum maritimum* L. *Zeitschrift für Naturforschung C* **2004**, *59*, 65–69. [[CrossRef](#)]
45. Bozkurt, B.; Kaya, G.I.; Somer, N.U. Chemical composition and enzyme inhibitory activities of Turkish *Pancreatum maritimum* bulbs. *Nat. Prod. Commun.* **2019**, *14*, 1–14. [[CrossRef](#)]
46. Labraña, J.; Machocho, A.K.; Kricsfalusy, V.; Brun, R.; Codina, C.; Viladomat, F.; Bastida, J. Alkaloids from *Narcissus angustifolius* subsp. *transcarpathicus*. *Phytochemistry* **2002**, *60*, 847–852. [[CrossRef](#)]
47. Cedrón, J.C.; Ravelo, A.G.; León, L.G.; Padrón, J.M.; Estévez-Braun, A. Antiproliferative and structure activity relationships of Amaryllidaceae alkaloids. *Molecules* **2015**, *20*, 13854–13863. [[CrossRef](#)]
48. Li, X.; Yu, H.Y.; Wang, Z.Y.; Pi, H.F.; Zhang, P.; Ruan, H.L. Neuroprotective compounds from the bulbs of *Lycoris radiata*. *Fitoterapia* **2013**, *88*, 82–90. [[CrossRef](#)] [[PubMed](#)]
49. Hong, A.W.; Cheng, T.H.; Raghukumar, V.; Sha, C.K. An expedient route to montanine-type Amaryllidaceae alkaloids: Total syntheses of (–)-brunsvigine and (–)-manthine. *J. Org. Chem.* **2008**, *73*, 7580–7585. [[CrossRef](#)] [[PubMed](#)]
50. Inubushi, Y.; Fales, H.M.; Warnhoff, E.W.; Wildman, W.C. Structures of montanine, coccinine, and manthine. *J. Org. Chem.* **1960**, *25*, 2153–2164. [[CrossRef](#)]
51. Clark, R.C.; Warren, F.L.; Pachler, K.G.R. Alkaloids of the Amaryllidaceae: Brunsvigine: NMR, ORD/CD and mass spectrometry, degradation and interconversion studies. *Tetrahedron* **1975**, *31*, 1855–1859. [[CrossRef](#)]
52. Dry, L.J.; Poynton, M.; Thompson, M.E.; Warren, F.L. The alkaloids of the Amaryllidaceae. Part IV. The alkaloids of *Brunsvigia cooperi* Baker. *J. Chem. Soc.* **1958**, 4701–4704. [[CrossRef](#)]
53. Wildman, W.C.; Brown, C.L.; Michel, K.H.; Bailey, D.T.; Heimer, N.E.; Shaffer, R.; Murphy, C.F. Alkaloids from *Rhodophiala bifida*, *Crinum erubescens* and *Sprekelia formisissima*. *Pharmazie* **1967**, *22*, 725.
54. Nair, J.J.; Bastida, J.; Viladomat, F.; van Staden, J. Cytotoxic agents of the crinane series of Amaryllidaceae alkaloids. *Nat. Prod. Comm.* **2012**, *7*, 1677–1688. [[CrossRef](#)]
55. He, M.; Qu, C.; Gao, O.; Hu, X.; Hong, X. Biological and pharmacological activities of Amaryllidaceae alkaloids. *RSC Adv.* **2015**, *5*, 16562–16574. [[CrossRef](#)]
56. Sener, B.; Orhan, I.; Satayavivad, J. Antimalarial activity screening of some alkaloids and the plant extracts from Amaryllidaceae. *Phytother. Res.* **2003**, *17*, 1220–1223. [[CrossRef](#)] [[PubMed](#)]
57. Osorio, E.J.; Berkov, S.; Brun, R.; Codina, C.; Viladomat, F.; Cabezas, F.; Bastida, J. In vitro antiprotozoal activity of alkaloids from *Phaedranassa dubia* (Amaryllidaceae). *Phytochem. Lett.* **2010**, *3*, 161–163. [[CrossRef](#)]
58. Kulhánková, A.; Cahlíková, L.; Novák, Z.; Macáková, K.; Kuneš, J.; Opletal, L. Alkaloids from *Zephyranthes robusta* Baker and their acetylcholinesterase and butyrylcholinesterase inhibition activity. *Chem. Biodivers.* **2013**, *10*, 1120–1127. [[CrossRef](#)]
59. Havelek, R.; Seifrtová, M.; Královec, K.; Bručková, L.; Cahlíková, L.; Dalecká, M.; Vávrová, J.; Řezáčová, M.; Opletal, L.; Bílková, Z. The effect of Amaryllidaceae alkaloids Haemanthamine and Haemanthidine on cell cycle progression and apoptosis in p53-negative human leukemic Jurkat cells. *Phytomedicine* **2014**, *21*, 479–490. [[CrossRef](#)]
60. Nair, J.J.; Van Staden, J.; Bastida, J. Cytotoxic alkaloids constituents of the Amaryllidaceae. In *Studies in Natural Products Chemistry*, 1st ed.; Rahman, A.U., Ed.; Elsevier: Amsterdam, The Netherlands, 2016; Volume 49, pp. 107–156.
61. Fuchs, S.; Hsieh, L.T.; Saarberg, W.; Erdelmeier, C.A.J.; Wichelhaus, T.A.; Schaefer, L.; Koch, E.; Fürst, R. *Haemanthus coccineus* extract and its main bioactive component narciclasine display profound anti-inflammatory activities in vitro and in vivo. *J. Cell Mol. Med.* **2015**, *19*, 1021–1032. [[CrossRef](#)]
62. Breiterová, K.; Koutová, D.; Maříková, J.; Havelek, R.; Kuneš, J.; Majorošová, M.; Opletal, L.; Hošťálková, A.; Jenčo, J.; Řezáčová, M.; et al. Amaryllidaceae alkaloids of different structural types from *Narcissus* L. cv. Professor Einstein and their cytotoxic activity. *Plants* **2020**, *9*, 137. [[CrossRef](#)]
63. Govindaraju, K.; Ingels, A.; Hasan, M.N.; Sun, D.; Mathieu, V.; Masi, M.; Evidente, A.; Kornienko, A. Synthetic analogues of the montanine-type alkaloids with activity against apoptosis-resistant cancer cells. *Bioorg. Med. Chem. Lett.* **2018**, *28*, 589–593. [[CrossRef](#)]

64. Pagliosa, L.B.; Monteiro, S.C.; Silva, K.B.; De Andrade, J.P.; Dutilh, J.; Bastida, J.; Cammarota, M.; Zuanazzi, J.A.S. Effect of isoquinoline alkaloids from two *Hippeastrum* species on in vitro acetylcholinesterase activity. *Phytomedicine* **2010**, *17*, 698–701. [CrossRef]
65. Evidente, A.; Andolfi, A.; Abou-Donia, A.H.; Touema, S.M.; Hammada, H.M.; Shawky, E.; Motta, A. (–)-Amarbellisine, a lycorine-type alkaloid from *Amaryllis belladonna* L. growing in Egypt. *Phytochemistry* **2004**, *65*, 2113–2118. [CrossRef]
66. Mathew, S.; Faheem, M.; Al-Malki, A.L.; Kumosani, T.A.; Qadri, I. In silico inhibition of GABARAP activity using antiepileptic medicinal derived compounds. *Bioinformation* **2015**, *11*, 189–195. [CrossRef] [PubMed]
67. Castilhos, T.S.; Giordani, R.B.; Henriques, A.T.; Menezes, F.S.; Zuanazzi, J.A.S. Avaliacao in vitro das atividades antiinflamatória, antioxidante e antimicrobiana do alcaloide montanina. *Rev. Bras. Pharmacogn.* **2007**, *17*, 209–214. [CrossRef]
68. De Oliveira, P.G.; Pedrazza, G.P.R.; Farinon, M.; Machado, X.R.; Zuanazzi, J.A.S.; Spies, F. Process for Extracting the Alkaloid Fraction of *Rhodophiala bifida* (Herb.) Traub and Uses Thereof. US Patent 2020/0000798 A1, 2 January 2020.
69. Kohelová, E.; Peřinová, R.; Maafi, N.; Korábečný, J.; Hulcová, D.; Mařiková, J.; Kučera, T.; Martínez González, L.; Hrabínova, M.; Vorčáková, K.; et al. Derivatives of the β -crinane Amaryllidaceae alkaloid haemanthamine as multi-target directed ligands for Alzheimer's Disease. *Molecules* **2019**, *24*, 1307. [CrossRef] [PubMed]
70. Tallini, L.R.; Bastida, J.; Cortes, N.; Osorio, E.H.; Theoduloz, C.; Schmeda-Hirschmann, G. Cholinesterase inhibition activity, alkaloid profiling and molecular docking of Chilean *Rhodophiala* (Amaryllidaceae). *Molecules* **2018**, *23*, 1532. [CrossRef] [PubMed]
71. Masondo, N.A.; Stafford, G.I.; Aremu, A.O.; Makunga, N.P. Acetylcholinesterase inhibitors from southern African plants: An overview of ethnobotanical, pharmacological potential and phytochemical research including and beyond Alzheimer's disease treatment. *S. Afr. J. Bot.* **2019**, *120*, 39–64. [CrossRef]
72. Cahlíková, L.; Pérez, D.I.; Štěpánková, S.; Chlebek, J.; Šafratová, M.; Hošťálková, A.; Opletal, L. In vitro inhibitory effects of 8-O-demethylmaritidine and undulatine on acetylcholinesterase and their predicted penetration across the blood–brain barrier. *J. Nat. Prod.* **2015**, *78*, 1189–1192. [CrossRef]
73. Hulcová, D.; Mařiková, J.; Korábečný, J.; Hošťálková, A.; Jun, D.; Kuneš, J.; Chlebek, J.; Opletal, L.; De Simone, A.; Nováková, L.; et al. Amaryllidaceae alkaloids from *Narcissus pseudonarcissus* L. cv. Dutch Master as potential drugs in treatment of Alzheimer's disease. *Phytochemistry* **2019**, *165*, 112055. [CrossRef]
74. Ishizaki, M.; Hoshino, O.; Iitaka, Y. A first total synthesis of montanine-type Amaryllidaceae alkaloids, (\pm)-coccinine, (\pm)-montanine, and (\pm)-pancracine. *Tetrahedron Lett.* **1991**, *32*, 7079–7082. [CrossRef]
75. Overman, L.E.; Shim, J. Synthesis applications of cationic aza-Cope rearrangements. 23. First total synthesis of Amaryllidaceae alkaloids of the 5,11-methano morphanthridine type. An efficient total synthesis of (\pm)-pancracine. *J. Org. Chem.* **1991**, *56*, 5005–5007. [CrossRef]
76. Ishizaki, M.; Kurihara, K.I.; Tanazawa, E.; Hoshino, O. Radical-mediated synthesis of the 5,11-methanomorphanthridine ring system: Formal total synthesis of montanine-type Amaryllidaceae alkaloids, (\pm)-montanine, (\pm)-coccinine and (\pm)-pancracine. *J. Chem. Soc. Perkin Trans. 1* **1993**, *1*, 101–110. [CrossRef]
77. Overman, L.E.; Shim, J. Total synthesis of Amaryllidaceae alkaloids of the 5,11-methanomorphanthridine type. Efficient total synthesis of (–)-pancracine and (\pm)-pancracine. *J. Org. Chem.* **1993**, *58*, 4662–4672. [CrossRef]
78. Jin, J.; Weinreb, S.M. Application of a stereospecific intramolecular allenylsilane imino ene reaction to enantioselective total synthesis of the 5,11-methanomorphanthridine class of Amaryllidaceae alkaloids. *J. Am. Chem. Soc.* **1997**, *119*, 5773–5784. [CrossRef]
79. Pearson, W.H.; Lian, B.W. Application of the 2-azaallyl anion cycloaddition method to an enantioselective total synthesis of (+)-coccinine. *Angew. Chem. Int. Ed. Engl.* **1998**, *37*, 1724–1726. [CrossRef]
80. Ikeda, M.; Hamada, M.; Yamashita, T.; Matsui, K.; Sato, T.; Ishibashi, H. Stereoselective synthesis of (3R*, 3aS*, 7aS*)-3-aryloctahydroindol-2-ones using radical cyclisation: A formal synthesis of (\pm)-pancracine. *J. Chem. Soc. Perkin Trans. 1* **1999**, *14*, 1949–1956. [CrossRef]
81. Banwell, M.G.; Edwards, A.J.; Jolliffe, K.A.; Kemmler, M. An operationally simple and fully regiocontrolled formal total synthesis of the montanine-type Amaryllidaceae alkaloid (\pm)-pancracine. *J. Chem. Soc. Perkin Trans. 1* **2001**, *12*, 1345–1348. [CrossRef]

82. Sha, C.K.; Hong, A.W.; Huang, C.M. Synthesis of aza bicyclic enones via anionic cyclization: Application to the total synthesis of (–)-Brunsvigine. *Org. Lett.* **2001**, *3*, 2177–2179. [[CrossRef](#)]
83. Pandey, G.; Banerjee, P.; Kumar, R.; Puranik, V.G. Stereospecific route to 5,11-methanomorphanthridine alkaloids via intramolecular 1,3-dipolar cycloaddition of nonstabilized azomethine ylide: Formal total synthesis of (±)-pancracine. *Org. Lett.* **2005**, *7*, 3713–3716. [[CrossRef](#)]
84. Banwell, M.G.; Kokas, O.J.; Willis, A.C. Chemoenzymatic approaches to the montanine alkaloids: A total synthesis of (+)-brunsvigine. *Org. Lett.* **2007**, *9*, 3503–3506. [[CrossRef](#)]
85. Kokas, O.J.; Banwell, M.G.; Willis, A.C. Chemoenzymatic approaches to the montanine alkaloids: A total synthesis of (+)-nangustine. *Tetrahedron* **2008**, *64*, 6444–6451. [[CrossRef](#)]
86. Anada, M.; Tanaka, M.; Shimada, N.; Nambu, H.; Yamawaki, M.; Hashimoto, S. Asymmetric formal synthesis of (–)-pancracine via catalytic enantioselective C–H amination process. *Tetrahedron* **2009**, *65*, 3069–3077. [[CrossRef](#)]
87. Pansare, S.V.; Lingampally, R.; Kirby, R.L. Stereoselective synthesis of 3-aryloctahydroindoles and application in a formal synthesis of (–)-pancracine. *Org. Lett.* **2010**, *12*, 556–559. [[CrossRef](#)] [[PubMed](#)]
88. Pandey, G.; Kumar, R.; Banerjee, P.; Puranik, V.G. One-step stereospecific strategy for the construction of the core structure of the 5,11-methanomorphanthridine alkaloids in racemic as well as in optically pure form: Synthesis of (±)-pancracine and (±)-brunsvigine. *Eur. J. Org. Chem.* **2011**, *2011*, 4571–4587. [[CrossRef](#)]
89. Pandey, G.; Gadre, S.R. Stereoselective construction of 5,11-methanomorphanthridine and 5,10b-phenanthridine structural frameworks: Total syntheses of (±)-pancracine, (±)-brunsvigine, (±)-maritidine, and (±)-crinine. *Pure Appl. Chem.* **2012**, *84*, 1597–1619. [[CrossRef](#)]
90. Yang, H.; Hou, S.; Tao, C.; Liu, Z.; Wang, C.; Cheng, B.; Li, Y.; Zhai, H. Rhodium-catalyzed denitrogenative [3 + 2] cycloaddition: Access to functionalized hydroindolones and the framework of montanine-type Amaryllidaceae alkaloids. *Chem. Eur. J.* **2017**, *23*, 12930–12936. [[CrossRef](#)]
91. Pandey, G.; Dey, D.; Tiwari, S.K. Synthesis of biologically active natural products by [3 + 2] cycloaddition of non-stabilized azomethine ylides (AMY): Concepts and realizations. *Tetrahedron Lett.* **2017**, *58*, 699–705. [[CrossRef](#)]
92. Cedrón, J.C.; Estévez-Braun, A.; Ravelo, A.; Gutiérrez, D.; Flores, N.; Bucio, M.A.; Pérez-Hernández, N.; Joseph-Nathan, P. Bioactive montanine derivatives from halide-induced rearrangements of haemanthamine-type alkaloids. Absolute configuration by VCD. *Org. Lett.* **2009**, *11*, 1491–1494. [[CrossRef](#)]



© 2020 by the authors. Licensee MDPI, Basel, Switzerland. This article is an open access article distributed under the terms and conditions of the Creative Commons Attribution (CC BY) license (<http://creativecommons.org/licenses/by/4.0/>).

4.2 Alkaloid profiling of *Hippeastrum* cultivars by GC-MS, isolation of Amaryllidaceae alkaloids and evaluation of their cytotoxicity

Al Shammari, L.; Al Mamun, A.; Koutová, D.; Majorošová, M.; Hulcová, D.; Šafratová, M.; Breiterová, K.; Maříková, J.; Havelek, R.; Cahlíková, L.

Rec. Nat. Prod. 2020, 14, 154–159.

IF2020 1,735, Q3 (Plant Sciences)

Důkladná fytochemická analýza rostlinných extraktů je předpokladem pro nalezení nových kandidátních léčiv. Tato studie měla za cíl experimentálně prozkoumat výskyt a stanovit kvantitativní profil jednotlivých typů alkaloidů izolovaných z šesti kultivarů rodu *Hippeastrum* (česky hvězdník). V cibulových extraktech šesti okrasných hybridních odrůd byly nalezeny molekuly, z nichž 18 z nich bylo identifikováno dle hmotnostních spekter, retenčních časů a retenčních indexů jako alkaloidy čeledi Amaryllidaceae, patřící do jednotlivých strukturních typů této čeledi (krininový, haemanthaminový, galanthaminový, homolykorinový, lykorinový, montaninový a tazettinový). První výsledky poukázaly na fakt, že tyto kultivary jsou bohatým zdrojem neuniformní skupiny alkaloidů několika strukturních typů sloučenin, které se v základních aspektech liší intramolekulárním oxidativním spojením, úrovní cyklizace, kondenzace a vazbou postranních molekul. Lykorin byl identifikován ve všech studovaných kultivarech. Galanthamin, velmi známý a klinicky používaný alkaloid v terapii Alzheimerovy choroby, byl identifikován pouze u některých kultivarů a ve stopovém množství. Rovněž bylo pomocí preparativní TLC izolováno pět alkaloidů čeledi Amaryllidaceae v čisté formě, které byly analyzovány pomocí hmotnostní spektrometrie, 1D a 2D NMR spektroskopie. Výsledky těchto analýz byly komparovány s literárními údaji, díky čemu se finálně povedlo identifikovat molekuly jako montanin, vittatin, 11-hydroxyvittatin, lykorin a hippeastrin.

Dalším krokem této studie bylo tedy posouzení cytotoxického účinku u těch sloučenin, které dosud nebyly systematicky popsány s využitím screeningu na minipanelu *in vitro*. Zhodnotili jsme tedy cytotoxický účinek montaninu, vittatinu a hippeastrinu. Cytotoxická aktivita těchto alkaloidů byla hodnocena pomocí testu WST-1 v panelu 9 buněčných linií, které představovaly modely různých typů nádorové patologie (Jurkat, MOLT-4, A549, HT-29, PANC-1, A2780, HeLa, MCF-7, SAOS-2). Současně byl použit také model nenádorových lidských plicních fibroblastů MRC-5. Koncentrační limit k porovnání účinku mezi jednotlivými alkaloidy byl stanoven na 10 $\mu\text{mol.l}^{-1}$ a bylo hodnoceno průměrné růstové procento GP. Z

naměřených dat byl jednoznačně nejúčinnější montanin, který inhiboval růst buněk pod 50 % při použité koncentraci $10 \mu\text{mol.l}^{-1}$ v celém panelu buněčných linií. Přírozeným dalším krokem bylo tedy stanovit hodnotu 50 % inhibiční koncentrace IC_{50} montaninu, hodnoty se pohybovaly v rozmezí od $1,04 \pm 0,14 \mu\text{mol.l}^{-1}$ do $2,30 \pm 0,45 \mu\text{mol.l}^{-1}$. Srovnáme-li tyto hodnoty s dosud publikovanými daty (Masi a kol. 2019, Silva a kol., 2008), ve kterých se hodnoty IC_{50} montaninu rovněž pohybovaly v nízkém mikromolárním koncentračním rozmezí, můžeme zhodnotit, že montanin je opravdu velmi účinným alkaloidem z hlediska inhibice růstu nádorových buněk. Publikace otevírá cestu pro bližší studium účinku montaninu na proliferační aktivitu, na viabilitu, na distribuci buněk v jednotlivých fázích buněčného cyklu, na indukci programované buněčné smrti, nebo na spřažené buněčné mechanismy a molekulární signalizaci.

Alkaloid Profiling of *Hippeastrum* Cultivars by GC-MS, Isolation of Amaryllidaceae Alkaloids and Evaluation of Their Cytotoxicity

Latifah Al Shammari ¹, Abdullah Al Mamun ¹, Darja Koutová ²,
Martina Majorošová ², Daniela Hulcová ^{1,3}, Marcela Šafratová ³,
Kateřina Breiterová ¹, Jana Maříková ⁴, Radim Havelek ² and
Lucie Cahlíková ^{1,*}

¹ADINACO Research Group, Department of Pharmaceutical Botany, Faculty of Pharmacy, Charles University, Heyrovského 1203, 500 05 Hradec Kralove, Czech Republic

²Department of Medical Biochemistry, Faculty of Medicine in Hradec Kralove, Charles University, Simkova 870, Hradec Kralove 500 03, Czech Republic

³Department of Pharmacognosy, Faculty of Pharmacy, Charles University, Heyrovského 1203, 500 05 Hradec Kralove, Czech Republic

⁴Department of Organic and Bioorganic Chemistry, Faculty of Pharmacy, Charles University, Heyrovského 1203, 500 05 Hradec Kralove, Czech Republic

(Received June 17, 2019; Revised August 28, 2019; Accepted August 29, 2019)

Abstract: Different species, hybrids and varieties of the genus *Hippeastrum* (Amaryllidaceae) are planted for ornamental purposes and at the same time they represent a rich source of interesting secondary metabolites called Amaryllidaceae alkaloids. These compounds display a wide spectrum of biological activities. In the current study, six *Hippeastrum* taxa were evaluated for their alkaloid profile by GC-MS. Using preparative TLC, five alkaloids were isolated in pure form, and three of them evaluated for cytotoxic and antiproliferative potencies on a panel of human cancer cells of different histotype (Jurkat, MOLT-4, A549, HT-29, PANC-1, A2780, HeLa, MCF-7 and SAOS-2). In parallel, normal MRC-5 human fibroblasts were employed to determine the compounds' overall toxicity against non-cancer cells. The most intriguing cytotoxic profile was demonstrated by montanine (**1**) with IC₅₀ values between 1.04 – 1.99 μM.

Keywords: Amaryllidaceae; *Hippeastrum*; alkaloids; montanine; cytotoxicity. © 2019 ACG Publications. All rights reserved.

1. Plant Source

In the course of phytochemical studies of Amaryllidaceae plants we analysed different *Hippeastrum* cultivars. The fresh bulbs of all *Hippeastrum* taxa (between 150 g - 250 g) were obtained from the herbal dealer Lukon Glads (Sadská, Czech Republic). The botanical identification was performed by Prof. L. Opletal, CSc. Voucher specimens are deposited in the herbarium of the Faculty of

* Corresponding author: E-Mail: cahlikova@faf.cuni.cz

The article was published by ACG Publications
<http://www.acgpubs.org/journal/records-of-natural-products> March-April 2020 EISSN:1307-6167
DOI: <http://doi.org/10.25135/rnp.147.19.06.1302>

Pharmacy in Hradec Králové under the following numbers: *Hippeastrum* cv. Pretty Nymph CUFPH-16130/AL-569, *H.* cv. Artic Nymph CUFPH-16130/AL-574, *H.* cv. Daphne CUFPH-16130/AL-563, *H.* cv. Double King CUFPH-16130/AL-567, *H.* cv. Ferrari CUFPH-16130/AL-562, and *H.* cv. Spartacus CUFPH-16130/AL-570.

2. Previous Studies

Plants of the genus *Hippeastrum*, commonly called amaryllis, and *Amaryllis belladonna*, commonly called belladonna lily or naked lady, are similar in appearance except that *A. belladonna* has a solid flower stem while *Hippeastrum* has a hollow one [1]. Plants known as “amaryllis”, “Dutch amaryllis”, and “giant amaryllis” belong to the genus *Hippeastrum*, and those grown today are mostly hybrids of several species from South America and South Africa. *Hippeastrum* species have been traditionally used to cure piles, tumors and various inflammatory disorders [2].

The antitumor properties of the Amaryllidaceae alkaloids, such as lycorine, haemanthamine, and pancratistatine, are well known [3]. Lycorine and haemanthamine are easily isolated from natural sources and displayed significant *in vitro* cytotoxic activity against several different types of cancer cell lines including MOLT-4, Hep-G2, HeLa, MCF-7, CEM, K562, A549, Caco-2, and HT-29 [4,5].

The Amaryllidaceous cultivars have advantages for commercial alkaloid production since they are available in large quantities. To our knowledge, no studies have been carried out until now on the alkaloidal profile of a collection of *Hippeastrum* cultivars. In the current study, six *Hippeastrum* horticultural cultivars were evaluated for their alkaloid profile by GC-MS. Furthermore, five alkaloids were isolated in pure form from alkaloidal extracts and three of them were tested for their cytotoxic activity. The cytotoxicity of the isolated compounds has been studied on a panel of ten cancerous and noncancerous cell lines.

3. Present Study

In the bulb extracts of the studied six ornamental varieties of *Hippeastrum* cultivars, 20 compounds with typical mass spectra of Amaryllidaceae alkaloids were detected. Eighteen of them were identified based on their mass spectra, retention times and retention indexes and belong to the crinine, haemanthamine, galanthamine, homolycorine, lycorine, montanine, and tazettine structural types of Amaryllidaceae alkaloids. The alkaloids marked as A1, A2 and A3 displayed mass spectra typical for Amaryllidaceae alkaloids, however left unidentified. Considering their low concentrations (< 5% of TIC), their isolation and structural elucidation could be problematic. From the mass spectrum of alkaloid A2, some structural aspects can be concluded. The fragmentation pattern, especially the presence of an intense peak at m/z 109 such as in masonine and homolycorine [6], indicates the homolycorine structural-type of Amaryllidaceae alkaloids. Other fragments of the mass spectrum displayed only weak intensities, and are not valuable for exact identification of detected alkaloid. The relative proportion of each alkaloid was determined as a percentage of the total ion current (TIC). The peak areas reflect the ability of each compound to be ionized and thus the data given in Table 1 are semiquantitative. Nevertheless, they can be used for comparison between samples. Furthermore, five Amaryllidaceae alkaloids from different *Hippeastrum* cultivars have been isolated by preparative TLC in pure form.

Based on the obtained GC-MS results it can be concluded that cultivars of *Hippeastrum* are a rich source of different biologically active Amaryllidaceae alkaloids (Table 1). Lycorine, the most abundant Amaryllidaceae alkaloid, has been identified in all the studied cultivars, with the highest concentration being detected in *Hippeastrum* cv. Daphne (56% of TIC). In fresh bulbs, galanthamine, the most well known Amaryllidaceae alkaloid, was detected, but only in some cultivars, and mostly in trace concentration. In the alkaloidal extract of *H.* cv. Pretty Nymph, two alkaloids of the homolycorine structural type have been identified as major components, namely homolycorine (40% of TIC) and hippeastrine (22 % of TIC).

Using preparative TLC, five Amaryllidaceae alkaloids (Figure 1) have been isolated in pure form from various *Hippeastrum* cultivars. The compounds were identified by MS, 1D and 2D NMR spectroscopic analyses and by comparison of the obtained data with the literature as montanine (1), vittatine (2), 11-hydroxyvittatine (3), lycorine (4) and hippeastrine (5).

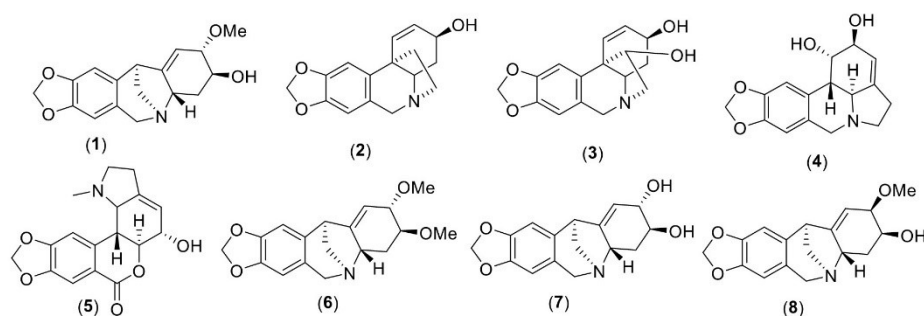


Figure 1. Structures of isolated Amaryllidaceae alkaloids from *Hippeastrum* cultivars, and structures of discussed Amaryllidaceae alkaloids of montanine-structural type

Table 1. Composition of the alkaloidal extracts of six *Hippeastrum* cultivars analyzed by GC-MS

Alkaloid	RI	Liter. values of RI	<i>Hippeastrum</i> cv. Ferrari	<i>Hippeastrum</i> cv. Double King	<i>Hippeastrum</i> cv. Daphne	<i>Hippeastrum</i> cv. Arctic Nymph	<i>Hippeastrum</i> cv. Pretty Nymph	<i>Hippeastrum</i> cv. Spartacus	Ref. for MS, RI data
Ismine	2278	2280	t			t			[7]
Trisphaeridine	2284	2282	t						[8]
Galanthamine	2408	2410			t	t		t	c,d [9]
Lycoramine	2442	2417		<1					c,d [10]
Vittatine/erinine*	2498	2472	9	9	<1	4		3	c,d [7]
A1	2518	n.a.			3				
9-O-Demethyllycosinine B	2575	2499	t	<1					[11]
11,12-Dehydroanhydrolycorine	2604	2606	<1		t				[7,9]
A2 Homolycorine type	2609	n.a.		3	<1				
Montanine	2615	2611	6	16			21	12	c,d [7]
Haemanthamine	2640	2641	3	4	3	4		8	c,d [7]
Tazettine/Pretazzenine*	2655	2653	5		t			43	c,d [7]
Pancracine	2719	2718	7	6			3		c,d [7]
11-Hydroxyvittatine	2736	2732	49	23		18		8	c, [9]
Lycorine	2749	2746	9	30	56	44	15	26	c,d [7]
Homolycorine	2769	2767	5	2			40		c, [8]
3-Epimacronine	2813	2811	t						c,d [7]
Pseudolycorine	2823	2831	4	2	3	15			[9,10]
Hippeastrine	2918	2917	1	3	34	5	22	t	c, [7]
A3	3012	n.a.				4	t		

*Cannot be distinguished by GC-MS; *For GC conditions see Experimental section; ^b Values are expressed as a percentage of the total ion current (TIC); ^c Standard; ^dNIST 11; t stands for trace, n.a. stands for not available

To study the anticancer effect of three of the isolated compounds, which have not been described by our laboratory previously {montanine (1), vittatine (2) and hippeastrine (5)}, cytotoxic and antiproliferative potencies were screened on a panel of human cancer cells of different histotype (Jurkat, MOLT-4, A549, HT-29, PANC-1, A2780, HeLa, MCF-7 and SAOS-2). In parallel, normal MRC-5 human fibroblasts were employed to determine the compounds' overall toxicity against non-cancer cells. The cytotoxic activity of these alkaloids was evaluated using the WST-1 metabolic activity assay. To find the best of them with very high cytotoxicity, the alkaloids were tested for growth-inhibitory activity in all 10 cell lines at a single dose of 10 μ M (Figure 2). For each alkaloid tested, the sensitivity in an individual cell line and the mean growth percent (GP) value was calculated as an average of 10 cell lines proliferation in percent (Table S1). The threshold GP value for this screen was < 50% (50% tumor growth inhibition), indicating good activity at 10 μ M. The most active alkaloid in the field of cytotoxicity and antiproliferative activity seemed to be montanine (1), which was found to inhibit Jurkat, MOLT-4, A549, HT-29, PANC-1, A2780, HeLa, MCF-7 and SAOS-2 cancer cell growth with a score \leq 50% at 10 μ M

concentration (Table S2). Thus, IC_{50} values of montanine (**1**) in the range below 10 μM were determined. As shown in Table 2, montanine (**1**) showed highest activity towards Jurkat, MOLT-4 and A549 cells. Jurkat cells were highly sensitive to montanine treatment (**1**), with an IC_{50} of 1.04 μM .

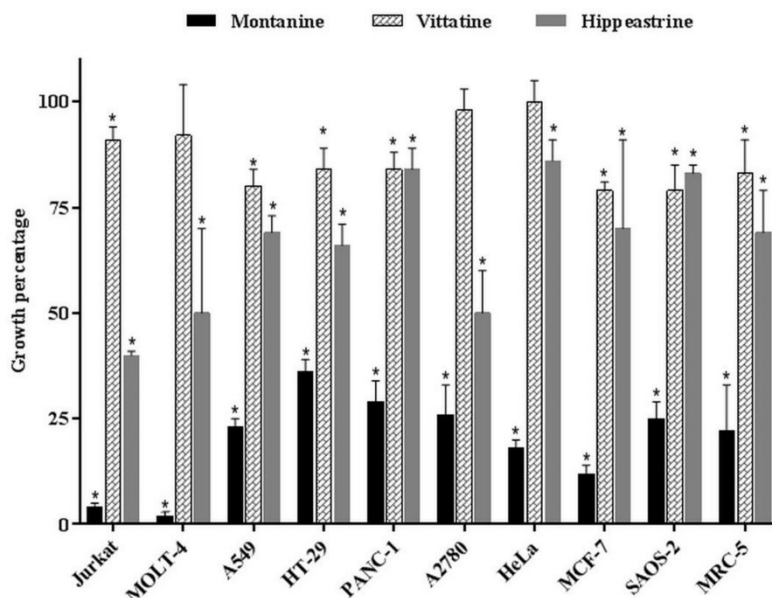


Figure 2. The growth inhibitory effect of montanine, vittatine and hippeastrine following a single-dose exposure at a concentration of 10 μM on 9 cancer cell lines (Jurkat, MOLT-4, A549, HT-29, PANC-1, A2780, HeLa, MCF-7, SAOS-2) and the non-cancer cell line MRC-5 using WST-1 cytotoxicity assay. Bars indicate mean \pm SD, $n = 3$. * - significantly different from 0.1% DMSO mock treated control ($p \leq 0.05$).

Alkaloids of montanine structural type such as montanine (**1**), pancracine (**7**), coccinine (**8**) and manthine (**6**) seem to be promising compounds in the search for new anticancer drugs. They are characterized by a 5,11-methanomorphanthridine ring system and differ only in the substitutions and configuration at C-2 and C-3 centers (Figure 1) [12]. Some of these compounds have been screened on different cancerous cells [13,14]. Montanine (**1**) and manthine (**6**) showed strong *in vitro* growth inhibitory effect on three cancer cell lines resistant to apoptosis (A549, SKMEL-29, U373) and three cancer cell lines sensitive to apoptosis (MCF7, Hs683, B16F10) with IC_{50} values between 5 and 31 μM [14], but for both of them the molecular mechanism of the anticancer activity is still waiting to be described. In another recent study, the C-2 α -/C-2 β -methoxy isomers montanine (**1**) and coccinine (**8**) were found to have a significant effect on the proliferation of human breast, colon, lung, and melanoma cancer cell lines during 48 h of treatment. The obtained results revealed that montanine (**1**) has a more promising cytotoxic activity (IC_{50} values were $1.9 \pm 0.4 \mu\text{M}$ for A549 cells, $6.8 \pm 0.5 \mu\text{M}$ for HCT-15 cells, $23.2 \pm 1.9 \mu\text{M}$ for SK-MEL-28 cells, $4.4 \pm 0.4 \mu\text{M}$ for MCF-7 cells, $3.4 \pm 0.9 \mu\text{M}$ for MDA-MB-231 cells, $3.6 \pm 1.7 \mu\text{M}$ for Hs578T cells) in comparison with coccinine (**8**) (IC_{50} values were $5.9 \pm 0.8 \mu\text{M}$ for A549 cells, $16.8 \pm 1.8 \mu\text{M}$ for HCT-15 cells, $>50 \mu\text{M}$ for SK-MEL-28 cells, $7.9 \pm 0.9 \mu\text{M}$ for MCF-7 cells, $13.8 \pm 0.8 \mu\text{M}$ for MDA-MB-231 cells, $5.3 \pm 0.4 \mu\text{M}$ for Hs578T cells) [15]. However, since previous studies demonstrated that montanine (**1**), manthine (**6**) and coccinine (**8**) could effectively suppress viability and proliferation of human cancer cells, the molecular mechanism of their cytotoxic activity has not yet been fully explored and is still waiting to be described.

Table 2. IC₅₀ values of montanine (**1**) for human cancer and non-cancer cells^{a, b}.

Cell type	IC ₅₀ (μM) ^{a, b}
Jurkat	1.04 ± 0.14
MOLT-4	1.26 ± 0.11
A549	1.09 ± 0.31
HT-29	1.35 ± 0.47
PANC-1	2.30 ± 0.45
A2780	1.67 ± 0.29
HeLa	1.99 ± 0.22
MCF-7	1.39 ± 0.21
SAOS-2	1.36 ± 0.49
MRC-5	1.79 ± 0.50

^aIC₅₀ value is the mean concentration required to reduce the proliferation of cells by 50% after a 48 h treatment relative to a control. ^bIC₅₀ values are expressed in μM ± standard deviations of at least three independent replications.

In conclusion, plants of the genus *Hippeastrum* are an interesting source of Amaryllidaceae alkaloids of different structural types. The *Hippeastrum* cultivar Pretty Nymph has been selected for detailed phytochemical study because of its high content of the alkaloid montanine (16 % of TIC), which showed promising cytotoxic activity on a panel of nine cancerous cell lines. After isolation of a sufficient amount of montanine from *H. cv* Pretty Nymph, the molecular mechanism of the compound's cytotoxic activity will be studied in more detail. To look at montanine's ability to decrease the proliferation of cancer cells, the real-time label free cell proliferation method xCELLigence RTCA will be used. The impact of montanine on the distribution of cell population in a specific phase of cell cycle and induction of apoptosis will be determined using a flow-cytometry method. If either the intrinsic or extrinsic pathway of apoptosis is involved in montanine-induced cytotoxicity, activity of caspases, especially of -3/7, -8, and 9 will be measured. The follow-up step to reveal the molecular mechanism underlying the cytotoxic effect of montanine will be the detection of proteins related to apoptosis induction or to activation of cell cycle check point controls.

Acknowledgments

The authors wish to thank Prof. Gerald Blunden for critical reading of the manuscript and corrections of English. This project has been supported by Charles University grants (GA UK Nr. 178518, SVV UK 260 412; 260 401; Progres/UK Q40 and Q42), and by the Pre-application research into innovative medicines and medical technologies project (Reg. No. CZ.02.1.01/0.0/0.0/18_069/0010046) co-funded by the European Union.

Supporting Information

Supporting information accompanies this paper on <http://www.acgpubs.org/journal/records-of-natural-products>

ORCID

Latifah Al Shammari: [0000-0002-9835-0695](https://orcid.org/0000-0002-9835-0695)

Abdullah Al Mamun: [0000-0002-3441-8814](https://orcid.org/0000-0002-3441-8814)

Darja Koutová: [0000-0002-7311-4119](https://orcid.org/0000-0002-7311-4119)

Martina Majorošová: [0000-0002-3595-2568](https://orcid.org/0000-0002-3595-2568)

Daniela Hulcová: [0000-0003-2414-3551](https://orcid.org/0000-0003-2414-3551)

Marcela Šafratová: [0000-0003-4690-5107](https://orcid.org/0000-0003-4690-5107)

Kateřina Breiterová: [0000-0003-4784-5601](https://orcid.org/0000-0003-4784-5601)

Jana Mařiková: [0000-0001-9758-2067](https://orcid.org/0000-0001-9758-2067)

Radim Havelek: [0000-0003-0528-1334](https://orcid.org/0000-0003-0528-1334)

Lucie Cahliková: [0000-0002-1555-8870](https://orcid.org/0000-0002-1555-8870)

References

- [1] K. Carter (2007). *Amaryllis: Amaryllis belladonna (Brunsvigia rosea) and Hippeastrum hybrids*. Center for Landscape and Urban Horticulture, Cooperative Extension/Botany Plant Sciences Department. University of California Riverside.
- [2] C.P. Deepa and B.B. Kuriakose (2014). Pharmacognostic and phytochemical evaluation of the bulbs of *Hippeastrum punicum* (Lam.) Voss, *Int. J. Pharmacog. Phytochem. Res.* **6**, 399-404.
- [3] K. Habartová, L. Cahliková, M. Řezáčová and R. Havelek (2016). The biological activity of alkaloids from the Amaryllidaceae: from cholinesterases inhibition to anticancer activity, *Nat. Prod. Commun.* **11**, 1587-1594.
- [4] R. Havelek, D. Muthná, P. Tomšík, K. Královec, M. Seifrtová, L. Cahliková, A. Hošťálková, M. Šafatová, M. Perwein, E. Čermáková and M. Řezáčová (2017). Anticancer potential of Amaryllidaceae alkaloids evaluated by screening with a panel of human cells, real-time cellular analysis and Ehrlich tumor-bearing mice, *Chem. Biol. Int.* **275**, 121-132.
- [5] I. Doskočil, A. Hošťálková, M. Šafatová, N. Benešová, J. Havlík, R. Havelek, J. Kuneš, K. Královec, J. Chlebek and L. Cahliková (2015). Cytotoxic activities of Amaryllidaceae alkaloids against gastrointestinal cancer cells. *Phytochem. Lett.* **13**, 394-398.
- [6] H.K. Schooes, D.T. Smith, A.L. Burlingame, P.W. Jeffs and W. Döpke (1968). Mass spectra of Amaryllidaceae alkaloids: The lycorenine series, *Tetrahedron* **24**, 2825-2837.
- [7] J.P. de Andrade, R.B. Giordani, L. Torras-Claveria, N.B. Pigni, S. Berkov, M. Font-Bardia, T. Calvet, E. Konrath, K. Bueno, L.G. Sachett, J.H. Dutilh, W. de Souza Borges, F. Viladomat, A.T. Henriques, J.J. Nair, J.A.S. Zuanazzi and J. Bastida (2016). The Brazilian Amaryllidaceae as a source of acetylcholinesterase inhibitory alkaloids, *Phytochem. Rev.* **15**, 147-160.
- [8] S. Berkov, J. Bastida, B. Sidjimova, F. Viladomat and C. Codina (2008). Phytochemical differentiation of *Galanthus nivalis* and *Galanthus elwesii* (Amaryllidaceae): A case study, *Biochem. System. Ecol.* **36**, 638-645.
- [9] R.L. Tallini, J. Bastida, N. Cortes, H.E. Osorio, C. Theoduloz and G. Schmeda-Hirschmann (2019). Cholinesterase inhibition activity, alkaloid profiling and molecular docking of Chilean *Rhodophiala* (Amaryllidaceae), *Molecules* **23**, 1532/1-1532/27.
- [10] L.M. Trujillo-Chacón, J. E. Alarcón-Enos, C. L. Céspedes-Acuna, L. Bustamante, M. Baeza, M. G. López, C. Fernández-Mendivil, F. Cabezas and E. R. Pastene-Navarete (2019). Neuroprotective activity of isoquinoline alkaloids from Chilean Amaryllidaceae against oxidative stress-induced toxicity on human neuroblastoma SH-SY5Y cells and mouse hippocampal slice culture, *Food Chem. Toxicol.* **132**, 11065.
- [11] Y. Guo, J.P. de Andrade, N.B. Pigni, L. Torras-Claveria, L. R. Tallini, W. de S. Borges, F. Viladomat, J.J. Nair, J.A.S. Zuanazzi and J. Bastida (2016). New alkaloids from *Hippeastrum papilo* (RAVENNA) VAN SCHEEPEN, *Helv. Chim. Acta* **99**, 143-147.
- [12] X. Bao, Y.-X. Cao, W.-D. Chu, H. Qu, J.-Y. Du, X.-H. Zhao, X.-Y. Ma, C.-T. Wang and C.-A. Fan (2013). Bioinspired total synthesis of montanine-type Amaryllidaceae alkaloids, *Angew. Chem.* **52**, 14167-14172.
- [13] M. Farinon, V.S. Clarimundo, G.P. Pedrazza, P.S. Gulko, J.A. Zuanazzi, R.M. Xavier and P.G. de Oliveira (2017). Disease modifying anti-rheumatic activity of the alkaloid montanine on experimental arthritis and fibroblast-like synoviocytes, *Eur. J. Pharmacol.* **15**, 180-187.
- [14] K. Govindaraju, A. Ingels, M.N. Hasan, D. Sun, V. Mathieu, V. Masi, A. Evidente and A. Kornienko (2018). Synthetic analogues of the montanine-type alkaloids with activity against apoptosis-resistant cancer cells, *Bioorg. Med. Chem. Lett.* **28**, 589-593.
- [15] M. Masi, S. van Slambrouck, S. Gunawardana, M.J. van Rensburg, P.C. James, J.G. Mochel, P.S. Heliso, A.S. Albalawi, A. Cimmino, W.A.L. van Otterlo, A. Kornienko, I.R. Green and A. Evidente (2019). Alkaloids isolated from *Haemanthus humilis* Jacq., an indigenous South African Amaryllidaceae: Anticancer activity of coccinine and montanine, *S. Afr. J. Bot.*, (<https://doi.org/10.1016/j.sajb.2019.01.036>).

ACG
publications

© 2019 ACG Publications

4.3 Amaryllidaceae alkaloids of different structural types from *Narcissus* L. cv. Professor Einstein and their cytotoxic activity

Breiterová, K.; Koutová, D.; Maříková, J.; Havelek, R.; Kuneš, J.; Majorošová, M.; Opletal, L.; Hošťálková, A.; Jenčo, J.; Řezáčová, M.

Plants 2020, 9, 137.

IF2020 3,935, Q1 (Plant Sciences)

Tato publikace byla zaměřena na izolaci a identifikaci alkaloidů čeledi Amaryllidaceae z rostliny *Narcissus* L. cv. Professor Einstein a stanovení jejich cytotoxického účinku. K objasnění chemických struktur byla použita celá řada spektroskopických metod a získaná data byla porovnána s dosud publikovanými v odborné literatuře. Přínosem této podrobné fytochemické analýzy byla izolace a identifikace 23 alkaloidů 6 strukturních typů patřící do čeledi Amaryllidaceae a jednoho dosud nepopsaného alkaloidu. Tato bílá amorfnní pevná látka, strukturně odpovídající lykorinovému typu čeledi Amaryllidaceae, byla označena jako 7-oxonorpluviin. Ostatní alkaloidy bychom zařadili do skupin, jejichž reprezentativní molekulou je homolykorin, galantamin, haemanthamin, lykorin, montanin a tazettin. I v této studii jsme zvolili jednotnou strategii výběru panelu buněčných linií představující odlišný nádorový histotyp a rovněž nenádorovou buněčnou linii lidských plicních fibroblastů. V experimentech, ve kterých byl detekován cytotoxický účinek jednotlivých dosud netestovaných izolovaných alkaloidů pomocí metabolického testu buněčné proliferace WST-1 s použitím jednotné racionální koncentrace $10 \mu\text{mol.l}^{-1}$ v časovém intervalu 48 h, byl efekt pozorován u buněk Jurkat, MOLT-4, A549, HT-29, PANC-1, HeLa, MCF-7, A2780, SAOS-2 a MRC-5. Výsledné hodnoty byly uvedeny jako růstové procento GP a hodnota IC_{50} byla následně měřena u těch alkaloidů, u kterých hodnota GP klesla pod 50 %. Ze získaných výsledků bylo patrné, že pouze pankracin, alkaloid montaninového typu, inhiboval ve výše zmíněné koncentraci růst všech buněčných linií pod 50 %, vyjma buněčné linie PANC-1, u které byla hodnota GP lehce nad 50 %. Test buněčné proliferace WST-1 byl použit rovněž ke stanovení hodnot IC_{50} , opět v intervalu 48 h v koncentračním rozmezí od $0,1 \mu\text{mol.l}^{-1}$ do $100 \mu\text{mol.l}^{-1}$. Nejnižší hodnota IC_{50} pankracinu byla $2,20 \pm 0,25 \mu\text{mol.l}^{-1}$ (SAOS-2) a nejvyšší $5,15 \pm 0,34 \mu\text{mol.l}^{-1}$ (MRC-5). Srovnáme-li tyto hodnoty s výsledky jediné studie hodnotící cytotoxický účinek pankracinu, popisující hodnoty IC_{50} u čtyř buněčných linií v rozmezí od $4,3 \pm 0,7 \mu\text{mol.l}^{-1}$ do $9,1 \pm 1,0 \mu\text{mol.l}^{-1}$ v intervalu 48 h, a dále s naměřenými hodnotami IC_{50} pro strukturně velmi podobný montanin (viz výše), lze odvodit, že pankracin je velmi účinný a slibný alkaloid s významným inhibičním dopadem na růst nádorových buněk.

Jelikož byl pankracin izolován v dostatečném množství pro získání dalších cenných dat v oblasti biologicky účinných látek, v následující studii byl prozkoumán jeho efekt na viabilitu a proliferaci buněčné linie adenokarcinomu plic A549 a leukemické linie MOLT-4 s cílem poodhalit molekulární mechanismy vedoucí k tomuto účinku, viz kapitola 4.4.

Article

Amaryllidaceae Alkaloids of Different Structural Types from *Narcissus* L. cv. Professor Einstein and Their Cytotoxic Activity

Kateřina Breiterov¹, Darja Koutov², Jana Mařikov³, Radim Havelek², Jiř Kuneř³,
Martina Majorořov², Lubomr Opletal¹, Anna Hořalkov¹, Jaroslav Jeno¹,
Martina Řezcov² and Lucie Cahlkov^{1,*}

¹ ADINACO Research Group, Department of Pharmaceutical Botany, Faculty of Pharmacy, Charles University, Heyrovskho 1203, 500 05 Hradec Krlov, Czech Republic; breiterk@faf.cuni.cz (K.B.); opletal@faf.cuni.cz (L.O.); HOSTA4AA@faf.cuni.cz (A.H.); jencoj@faf.cuni.cz (J.J.)

² Department of Medical Biochemistry, Faculty of Medicine in Hradec Krlov, Charles University, řimkova 870, 500 03 Hradec Krlov, Czech Republic; koutova.darja@lfhk.cuni.cz (D.K.); havelekr@lfhk.cuni.cz (R.H.); SeifrtovaM@lfhk.cuni.cz (M.M.); rezacovaM@lfhk.cuni.cz (M.R.)

³ Department of Organic and Bioorganic Chemistry, Faculty of Pharmacy, Charles University, Heyrovskho 1203, 500 05 Hradec Krlov, Czech Republic; marikoj2@faf.cuni.cz (J.M.); kunes@faf.cuni.cz (J.K.)

* Correspondence: cahlkova@faf.cuni.cz; Tel.: +420-495067311; Fax: +420-495067162

Received: 27 December 2019; Accepted: 19 January 2020; Published: 22 January 2020



Abstract: In this detailed phytochemical study of *Narcissus* cv. Professor Einstein, we isolated 23 previously known Amaryllidaceae alkaloids (1–23) of several structural types and one previously undescribed alkaloid, 7-oxonorpluviine. The chemical structures were identified by various spectroscopic methods (GC-MS, LC-MS, 1D, and 2D NMR spectroscopy) and were compared with literature data. Alkaloids which had not previously been isolated and studied for cytotoxicity before and which were obtained in sufficient amounts were assayed for their cytotoxic activity on a panel of human cancer cell lines of different histotype. Above that, MRC-5 human fibroblasts were used as a control noncancerous cell line to determine the general toxicity of the tested compounds. The cytotoxicity of the tested alkaloids was evaluated using the WST-1 metabolic activity assay. The growth of all studied cancer cell lines was inhibited by pancracine (montanine-type alkaloid), with IC₅₀ values which were in the range of 2.20 to 5.15 μ M.

Keywords: *Narcissus* cv. Professor Einstein; Amaryllidaceae; cytotoxicity; 7-oxonorpluviine; pancracine

1. Introduction

Plants from the Amaryllidaceae family have been used for centuries in folk medicine due to their therapeutic properties [1]. Plants from this family contain a distinct and still not fully explored group of alkaloids called Amaryllidaceae alkaloids (AA). They are most well known for their broad spectrum of biological properties such as antitumor [2,3], antimalarial [4], anti-inflammatory [5], antimicrobial [6], and AChE-inhibiting activities [7,8]. The AA are classified into 9 main structural types (crinine, galanthamine, haemanthamine, homolycorine, lycorine, montanine, narciclasine, norbelladine, and tazettine) alongside more than 10 others (plicamine, galanthindole, augustamine, graciline, etc.). These minor structure types are usually found in trace amounts and are most often represented by single alkaloids [9,10]. Galanthamine, a selective, competitive acetylcholinesterase inhibitor with antioxidant properties is the most important AA identified so far. It was isolated for the first time from *Galanthus woronowii* in the 1950s. Since 2000, when it was approved, it has been used to treat mild

and moderate stages of Alzheimer's disease [11]. The ability of AA to reduce proliferative activity and viability of cancer cells is equally important. Numerous products of natural origin are known for their cytotoxic activity. These products are also a source of substances capable of affecting apoptosis resistance [12]. Simultaneously, the anti-invasive and anti-metastatic effects of some plant alkaloids have been described [13,14]. For this reason, substances of natural origin represent a valuable source of potential anticancer drugs; many AAs are very promising anticancer compounds, for example, the widely studied haemanthamine [15] and lycorine [16]. A well thought-out basic study of natural compounds can serve as a springboard for clinical therapy.

The genus *Narcissus* L. belongs to the monocotyledonous family Amaryllidaceae. Various species of this genus are commonly known as daffodil, narcissus, jonquil, etc. Genus *Narcissus* comprises about 100 wildlife species native mainly to the Mediterranean area [17]. *Narcissus* spp. have been long-established in traditional treatment of several cancer illnesses throughout the world. Hippocrates of Kos (460–370 B.C.), the famous Ancient Greek physician, recommended a pessary impregnated with narcissus oil to treat uterine tumors [18]. The application of narcissus oil in cancer treatment was also recorded in the Middle Ages in China, North Africa, Central America, and Arabian countries [19].

Due to the ease of natural hybridization, spreading, and naturalization, as well as extensive cultivation, the taxonomy of *Narcissus* spp. is quite complicated. A broad spectrum of cultivars has been bred mainly for ornamental purposes, and the International Daffodil Register contains over 27,000 names of these cultivars [20]. For commercial production of AAs, the cultivars are preferred over native species because of their availability. Some *Narcissus* cultivars have been already studied in detail, and a number of AAs have been isolated throughout the years [7,10,21]. From previous phytochemical studies of 40 differing *Narcissus* cultivars, 14 AAs were identified in the alkaloid extract of *Narcissus* cv. Professor Einstein [17] (see Supplementary Materials). The alkaloid extract also showed promising cytotoxic activity against different cancer cell types in a preliminary study (see section Results). The interesting bioactivities and lack of detailed phytochemical studies of *N. cv. Professor Einstein* led us to explore the properties and alkaloid content of this cultivar.

2. Results

2.1. Isolation and Identification of Amaryllidaceae Alkaloids from *N. cv. Professor Einstein*

Extensive phytochemical study of fresh bulbs of *N. cv. Professor Einstein* resulted in the isolation of 23 known AA (1–23), and a new alkaloid (24). The compounds were analyzed by various spectroscopic methods (GC-MS, LC-MS, and 1D and 2D NMR spectroscopy) and identified by comparison with literature data as masonine (1) [22], homolycorine (2) [23], ismine (3) [24], caranine (4) [25], galanthamine (5) [26], narwedine (6) [27], lycoraminone (7) [28], pluviine (8) [25], incartine (9) [29], galanthine (10) [30], lycoramine (11) [26], epinorgalanthamine (12) [31], norlycoramine (13) [32], haemanthamine (14) [32], hippeastrine (15) [33], epimaritidine (16) [34], lycorine (17) [35], tazettine (18) [36], eugenie (19) [37], norpluviine (20) [38], 9-*O*-demethylmaritidine (21) [39], pancracine (22) [40], and 9-*O*-demethylhomolycorine (23) [23] (Figure 1). The alkaloids that were isolated were representatives of the homolycorine (1, 2, 15, 19, 23), galanthamine (5, 6, 7, 11, 12, 13), haemanthamine (14, 16, 21), lycorine (4, 8, 9, 10, 17, 20), montanine (22), tazettine (18), and miscellaneous (3) structure types.

The structure of compound 21 is already known, but confirmation of it was not possible due to the absence of its NMR data in the available literature. This led us to publish the complete ^1H and ^{13}C NMR spectra for this alkaloid. The structural constitution was elucidated utilizing 2D experiments such as gCOSY, gHSQC, and gHMBCAD (see Figure 2).

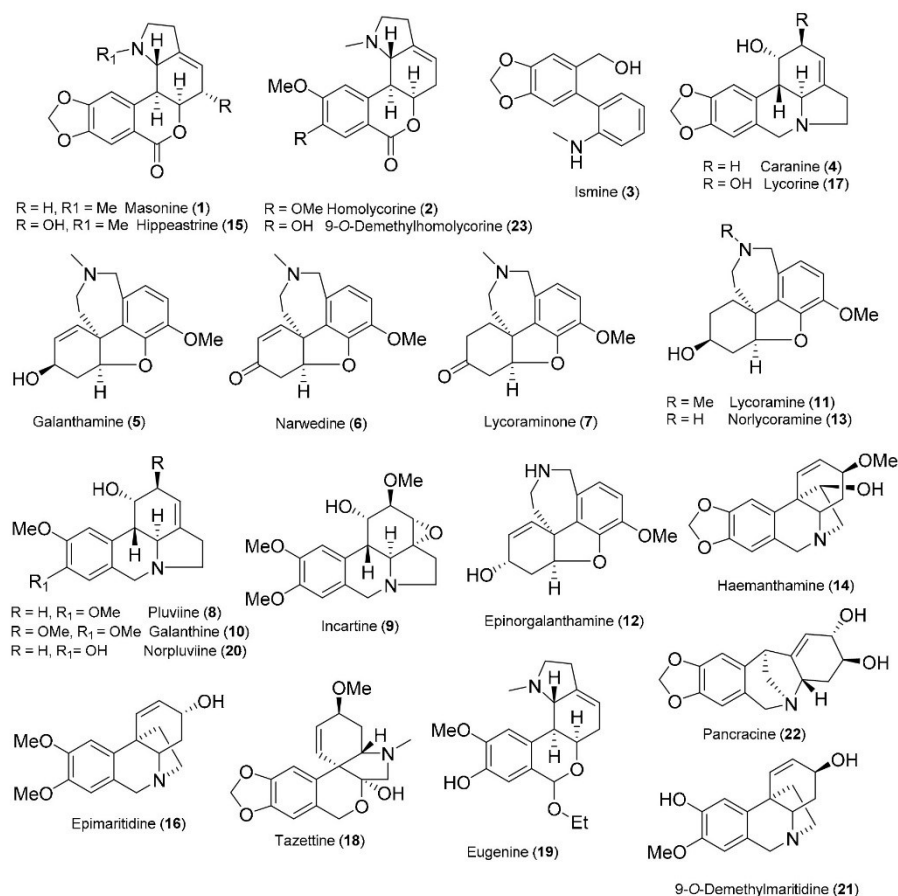


Figure 1. Structures of isolated alkaloids.

The new lycorine-type Amaryllidaceae alkaloid **24**, named 7-oxonorpluviine, was isolated as a white amorphous solid. Its HR-MS data showed a molecular ion $[M + H]^+$ at m/z 288.1242, corresponding to the formula $C_{16}H_{17}NO_4$. The 1H NMR data of **24** exhibited the presence of two aromatic protons (δ_H 7.45, H-8; 6.99, H-11), one olefinic proton (δ_H 5.71–5.67, H-3), one deshielded hydroxymethine proton (δ_H 4.95–4.91, H-1), one methoxy group (δ_H 3.98, C-10-OCH₃), one nitrogenated methine (δ_H 3.53–3.47, H-11c), one deshielded methylene group with diastereotopic protons (δ_H 3.35–3.25 and 3.06–2.98, H-5), one methine proton (δ_H 2.84, H-11b), and two methylene groups (δ_H 2.79–2.62 and 2.61–2.54, H-2 and H-4) (Table 1). While two protons were not detected by NMR in methanol-*d*₄, they should have been bound to the heteroatoms. The ^{13}C NMR spectrum exhibited 16 carbons. A 1,2,4,5-tetrasubstituted benzene ring was determined by gHMBCAD experiment. The identification was based on correlations from H-11 to C-7a (δ_C 117.4) and C-9 (δ_C 148.1), and from H-8 to C-10 (δ_C 154.5) and C-11a (δ_C 136.5), respectively. The deshielded aromatic carbons were substituted by a hydroxyl group (C-9) and a methoxy group (C-10). The carbonyl group C-7 (δ_C 167.6) was identified in the ^{13}C NMR spectrum; this signal was shown to be correlated with H-8 in gHMBCAD (Figure 2). The tertiary carbon C-11b (δ_C 41.9), which was correlated to H-11, was determined as a junction point between the aromatic substructural fragment and the rest of the molecule. The gCOSY experiment of

24 revealed cross-peaks of H-11b with H-11c and H-1, H-2 with H-1, H-3 with H-2 and H-11c, and H-5 with H-4. These correlations determined the hexahydroindole fragment in the structure (Figure 2). In addition, the gHMBCAD experiment supported this assumption by correlations from H-1 to C-3 (δ_C 118.3), from H-1 to C-11c (δ_C 60.9), from H-1 to C-11a (δ_C 137.7), and from H-5 to C-11c. The absolute configuration could not be determined due to insufficient amount of sample. The relative configuration was established and the result was supported by NOESY experiment (see Figure 2). This suggested configuration of either 1R, 11bS, 11cS or 1S, 11bR, 11cR is supported by the cross-peaks of H-11b and H-1. Moreover, no correlation of these protons with H-11c was detected.

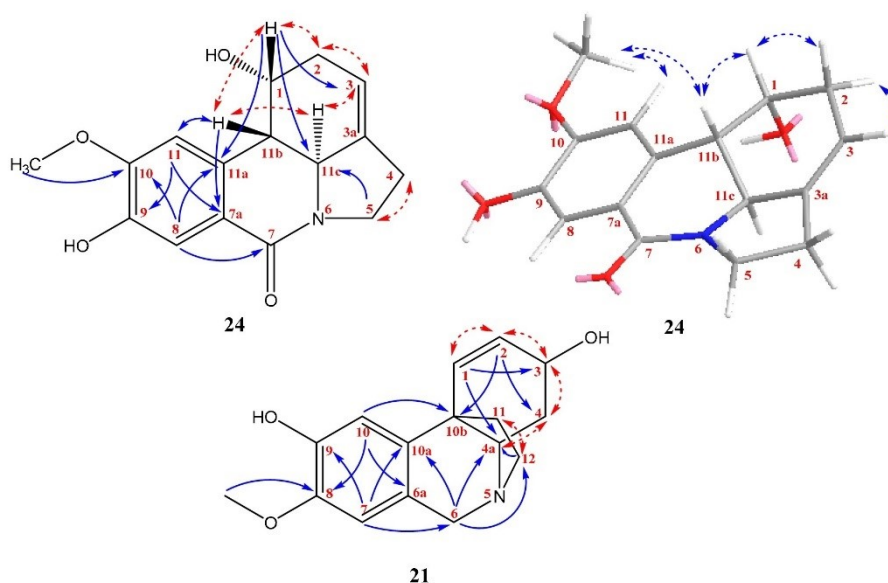


Figure 2. The constitution of **21**; the constitution of **24** and its relative configuration. The key gCOSY (red dashed arrows), gHMBCAD (blue arrows), and NOESY (blue dashed arrows) correlations are marked.

Table 1. 9-O-demethylmaritidine (**21**) and 7-oxonorpluviine (**24**) ^1H and ^{13}C NMR data.

Position	9-O-Demethylmaritidine (21) ^a		7-Oxonorpluviine (24) ^b	
	δ_C	δ_H (J in Hz)	δ_C	δ_H (J in Hz)
1	129.0	6.51 dd (10.2, 2.2)	77.3	4.95–4.91 m
2	131.1	5.79–5.74 m	32.2	2.79–2.62 m 2.61–2.54 m
3	67.8	4.48–4.41 m	118.3	5.71–5.67 m
3a	-	-	137.7	-
4	34.9	2.25–2.05 m 1.66–1.53 m	29.5	2.79–2.62 m
4a	66.7	3.26 dd (13.3, 3.6)	-	-
5	-	-	44.9	3.35–3.25 m 3.06–2.98 m
6	61.8	4.48–4.41 m 3.81 d (16.9)	-	-

Table 1. Cont.

Position	9-O-Demethylmaritidine (21) ^a		7-Oxonorpluviine (24) ^b	
	δ_C	δ_H (f in Hz)	δ_C	δ_H (f in Hz)
6a	123.9		-	-
7	109.2	6.51 s	167.6	
7a	-	-	117.4	
8	145.0		117.3	7.45 s
9	144.0		148.1	
10	108.5	6.88 s	154.5	
10a	138.2		-	-
10b	44.0		-	-
11	44.9	2.25–2.05 m	111.1	6.99 s
11a	-	-	136.5	
11b	53.2	3.50–3.42 m 2.98–2.90 m	41.9	2.84 dd (10.3, 2.2)
11c	-	-	60.9	3.53–3.47 m
C8-OCH ₃	55.9	3.84 s	-	-
C10-OCH ₃	-	-	56.7	3.98 s

^a measured in CDCl₃; ^b measured in CD₃OD; 500 MHz for ¹H and 125.7 MHz for ¹³C; δ in ppm.

2.2. Cytotoxic Study of Isolated Amaryllidaceae Alkaloids

A set of cell lines derived from various human tumor histotypes (leukemia—Jurkat, MOLT-4; adenocarcinomas of lung—A549, colon—HT-29, pancreas—PANC-1, cervix—HeLa, breast—MCF-7; ovarian carcinoma—A2780, and osteogenic sarcoma—SAOS-2) was used to screen the cytotoxic activity of all isolated compounds which had not been previously studied and were obtained in sufficient quantities. Normal human fetal lung fibroblasts (MRC-5) were used to study effect on non-tumorigenic cells. Growth-inhibitory activity of tested alkaloids was determined at a dose of 10 μ M (Table 2) using the WST-1 mitochondrial dehydrogenase activity assay.

Table 2. Cytotoxic activity of alkaloidal extract of *N. cv. Professor Einstein* (concentration 50 μ g·mL⁻¹), and isolated Amaryllidaceae alkaloids **1**, **2**, **7**, **13**, **16**, **20**, **21**, **22**, and **23** using a single dose (concentration of 10 μ M). WST-1 metabolic activity assay was used to analyze cell growth 48 h after treatment. The results are expressed as the mean values \pm SD of at least three independent experiments ($n = 3$). Cells treated with 1 μ M doxorubicin served as a positive control.

Cell Type	Extract	1	2	7	13	16	20	21	22	23	Dox.
Jurkat	3 \pm 1	76 \pm 5	78 \pm 7	102 \pm 9	102 \pm 2	102 \pm 4	96 \pm 12	97 \pm 6	17 \pm 5	100 \pm 10	2 \pm 0
MOLT-4	3 \pm 2	105 \pm 8	110 \pm 5	99 \pm 2	106 \pm 1	106 \pm 4	107 \pm 8	95 \pm 9	1 \pm 0	100 \pm 3	0 \pm 0
A549	25 \pm 2	109 \pm 22	114 \pm 21	107 \pm 8	93 \pm 7	110 \pm 10	111 \pm 2	104 \pm 7	29 \pm 3	109 \pm 9	11 \pm 5
HT-29	41 \pm 6	110 \pm 17	199 \pm 11	98 \pm 7	94 \pm 1	103 \pm 5	92 \pm 5	89 \pm 10	39 \pm 3	106 \pm 8	47 \pm 4
PANC-1	34 \pm 3	94 \pm 7	100 \pm 5	97 \pm 5	100 \pm 3	91 \pm 2	84 \pm 1	80 \pm 2	52 \pm 13	92 \pm 1	78 \pm 3
A2780	30 \pm 3	102 \pm 12	96 \pm 14	100 \pm 3	106 \pm 1	98 \pm 2	101 \pm 4	98 \pm 0	40 \pm 2	94 \pm 5	5 \pm 1
HeLa	35 \pm 3	117 \pm 14	108 \pm 10	98 \pm 9	93 \pm 5	97 \pm 8	91 \pm 12	93 \pm 9	28 \pm 6	96 \pm 10	11 \pm 6
MCF-7	11 \pm 1	98 \pm 9	102 \pm 6	95 \pm 7	99 \pm 5	96 \pm 7	100 \pm 3	91 \pm 3	18 \pm 2	102 \pm 8	37 \pm 3
SAOS-2	30 \pm 8	98 \pm 4	97 \pm 7	102 \pm 4	102 \pm 5	103 \pm 4	96 \pm 7	95 \pm 4	26 \pm 3	103 \pm 4	17 \pm 5
MRC-5	29 \pm 6	99 \pm 12	97 \pm 4	96 \pm 9	108 \pm 4	98 \pm 4	92 \pm 4	92 \pm 6	39 \pm 3	93 \pm 4	29 \pm 3

The efficacy of each alkaloid in decreasing the growth of individual cell line, referred as the mean growth percentage (GP), was calculated as an average of all cell lines proliferation in percent. The

threshold GP value for this screen was <50% (50% tumor growth inhibition), meaning good activity at 10 μM , as can be seen in the result for pancracine (22) in Table 2. Pancracine was able to inhibit all cancer cells used in the study, with the exception of PANC-1, where IC_{50} values ranged from 2.20 to 5.15 μM (Table 3).

Table 3. IC_{50} values of pancracine and doxorubicin in human cancer and non-cancer cells ^{a,b}.

Cell Type	Pancracine	Doxorubicin
Jurkat	5.07 \pm 0.31	0.05 \pm 0.02
MOLT-4	2.71 \pm 0.25	<0.01
A549	2.29 \pm 0.43	0.43 \pm 0.06
HT-29	2.60 \pm 0.51	0.77 \pm 0.24
A2780	5.08 \pm 0.43	<0.01
HeLa	5.03 \pm 0.36	0.55 \pm 0.05
MCF-7	2.68 \pm 0.37	0.44 \pm 0.10
SAOS-2	2.20 \pm 0.25	0.1 \pm 0.17
MRC-5	5.15 \pm 0.34	0.72 \pm 0.23

^a Results are expressed in μM . ^b Results are the mean values \pm standard deviations of at least three independent replications.

Pancracine (22) is a montanine type of AA, in the same group as montanine, coccinine, and manthine. This structural type of AA seems to be a promising source of compounds in the search for new anticancer drugs. They are characterized by a 5,11-methanomorphanthridine ring system, the only differences being the substitutions and configuration at C-2 and C-3 centers (Figure 3) [40]. Some of these compounds have been screened against different cancerous cells [12,41].

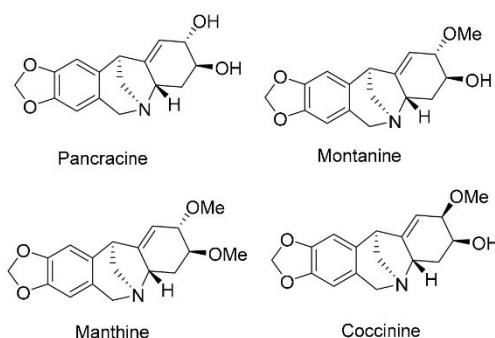


Figure 3. Structures of selected montanine-type Amariyllidaceae alkaloids.

Montanine and manthine showed strong *in vitro* growth inhibitory effect on three apoptosis-resistant cancer cell lines (A549, SKMEL-29, and U373) and three apoptosis-sensitive cancer cell lines (MCF7, Hs683, and B16F10) with IC_{50} values between 5 and 31 μM [12]. In another recent study, C-2 α -/C-2 β -methoxy isomers montanine and coccinine were found to significantly affect the proliferation of human breast, colon, lung, and melanoma cancer cell lines over 48 h of treatment. The obtained results revealed that montanine has a more promising cytotoxic activity (IC_{50} values were 1.9 \pm 0.4 μM for A549 cells, 6.8 \pm 0.5 μM for HCT-15 cells, 23.2 \pm 1.9 μM for SK-MEL-28 cells, 4.4 \pm 0.4 μM for MCF-7 cells, and 3.4 \pm 0.9 μM for MDA-MB-231 cells, 3.6 \pm 1.7 μM for Hs578T cells) when compared with coccinine (IC_{50} values were 5.9 \pm 0.8 μM for A549 cells, 16.8 \pm 1.8 μM for HCT-15 cells, >50 μM for SK-MEL-28 cells, 7.9 \pm 0.9 μM for MCF-7 cells, 13.8 \pm 0.8 μM for MDA-MB-231 cells, and 5.3 \pm 0.4 μM for Hs578T cells) [42]. Although previous studies, as well as our work, have demonstrated that AA of the montanine type can effectively suppress viability and proliferation of

human cancer cells, the molecular mechanism of this cytotoxic activity has not yet been fully explored and is still waiting to be described.

3. Experimental

3.1. General Experimental Procedures

All solvents were treated using standard techniques before use. All reagents were purchased from commercial sources (Sigma Aldrich, Prague, Czech Republic) and used without purification. The NMR spectra were obtained in CDCl₃ and CD₃OD at ambient temperature on a VNMR S500 (Varian, Palo Alto, CA, USA) spectrometer operating at 500 MHz for ¹H and 125.7 MHz for ¹³C. Chemical shifts were recorded as δ values in parts per million (ppm) and were indirectly referenced to tetramethylsilane (TMS) via the solvent signal (CDCl₃—7.26 ppm for ¹H and 77.0 ppm for ¹³C; CD₃OD—3.30 ppm for ¹H and 49.0 ppm for ¹³C). Coupling constants (*J*) are given in Hz. For unambiguous assignment of ¹H and ¹³C signals, 2D NMR experiments, namely gCOSY, gHSQC, gHMBC, and NOESY were measured using standard parameter settings and standard pulse programs provided by the producer of the spectrometer. HRMS were obtained with a Waters Synapt G2-Si hybrid mass analyzer of a quadrupole-time-of-flight (Q-TOF) type, coupled to a Waters Acquity I-Class UHPLC system. The EI-MS were obtained on an Agilent 7890A GC 5975 inert MSD operating in EI mode at 70 eV (Agilent Technologies, Santa Clara, CA, USA). A DB-5 column (30 m × 0.25 mm × 0.25 μ m, Agilent Technologies, USA) was used. The temperature program was: 100–180 °C at 15 °C/min, 1 min hold at 180 °C, 180–300 °C at 5 °C/min, and 5 min hold at 300 °C; detection range *m/z* 40–600. The injector temperature was 280 °C. The flow-rate of the carrier gas (helium) was 0.8 mL/min. A split ratio of 1:15 was used. TLC was carried out on Merck precoated silica gel 60 F254 plates. Compounds on the plate were observed under UV light (254 and 366 nm) and visualized by spraying with Dragendorff's reagent.

3.2. Plant Material

Fresh bulbs of *Narcissus* cv. Professor Einstein were obtained from the herbal dealer Lukon Glads (Sadská, Czech Republic). The botanical identification was performed by Professor L. Opletal, CSc. A voucher specimen is deposited in the Herbarium of the Faculty of Pharmacy in Hradec Králové under number CUFPH-16130/AL-447.

3.3. Extraction and Isolation of Alkaloids

Fresh bulbs (34 kg) were cut, minced, and underwent comprehensive extraction with ethanol (EtOH) (96%, *v/v*, 2 \times). Each portion (approximately 1.2 kg) was boiled twice for 30 min under reflux. The combined extracts were filtered and evaporated under reduced pressure. The crude extract (638 g) was dissolved in 1.5 L of 5% hydrochloric acid (HCl), filtered twice, and diluted with distilled water to 4.5 L at pH 1. The water solution was defatted with diethyl ether (Et₂O; 2 \times 4 L), alkalized with 10% Na₂CO₃ to pH 10, and exhaustively extracted with chloroform (CHCl₃; 4 \times 4 L). The organic phase was evaporated to give 58 g of dark brown residue. The purification process was repeated to give 32 g of concentrated alkaloidal residue (brown syrup). The obtained extract, which was Dragendorff positive, was fractionated by column chromatography on neutral Al₂O₃ (ACROSS, 2100 g) deactivated with 6 % of distilled water. The extract was eluted with light petrol enriched with CHCl₃ (gradually from 30:70 to 80:20), then with CHCl₃ gradually enriched with EtOH (from 1:99 to 50:50), and finally with pure EtOH. Fractions of 250 mL were collected and monitored by TLC, yielding 495 fractions, which were combined into 15 final fractions and analyzed by TLC and GC-MS.

Combined fractions I–III (60 mg) were separated by preparative TLC (toluene:EtOAc: Et₂NH 8:1:1, 1 \times) and gave three sub-fractions. Sub-fraction I–III/2 was recrystallized from an ethanol and chloroform mixture (1:1) to give masonine (1, 5 mg). Sub-fraction I–III/3 was further chromatographed by preparative TLC (toluene:Et₂NH 95:5, 1 \times) to give homolycorine (2, 6 mg). Fractions IV (35 mg) and VI (25 mg), based on TLC, contained no alkaloidal compound, and were not used for isolation of

alkaloids. Preparative TLC of fraction V (50 mg; toluene:EtOAc:Et₂NH 8:1:1, 1×) gave sub-fractions V/1–V/4. Sub-fraction V/3 was further chromatographed by preparative TLC (cyclohexane:Et₂NH 9:1, 2×) to give ismine (3, 4 mg). Fraction VII (1.69 g) was chromatographed by preparative TLC (toluene:Et₂NH 95:5, 2×) to give sub-fractions VII/1–VII/4. Caranine (4, 7 mg) was obtained by subsequent TLC of sub-fraction VII/2 (201 mg). Sub-fraction VII/3 (350 mg) was subjected to repeated preparative TLC (cyclohexane: toluene:Et₂NH 50:45:5, 2×) to give galanthamine (5, 35 mg), narwedine (6, 15 mg), and lycoraminone (7, 30 mg). Pluviine (8, 25 mg) was obtained from sub-fraction VII/4 (150 mg) by crystallization from hot ethanol (10 mL). Fraction VIII (30 mg) was subjected to preparative TLC (cyclohexane:isopropanol:Et₂NH 77.5:15:7.5, 1×) to give sub-fractions VIII/1–VIII/4. Sub-fraction VIII/2 (203 mg) was further chromatographed by preparative TLC (cyclohexane:Et₂NH 95:5, 2×) to give incartine (9, 5 mg), galanthine (10, 6 mg), and lycoramine (11, 80 mg). Epinorgalanthamine (12, 10 mg) was obtained from VIII/4 by preparative TLC (cyclohexane:EtOAc:isopropanol:Et₂NH 45:45:5:5, 2×). Fraction IX (138 mg) was chromatographed by preparative TLC (toluene:EtOAc:Et₂NH 7:2.5:0.5, 1×) to give norlycoramine (13, 35 mg). Haemanthamine (14, 320 mg) was obtained from fraction X (1.02 g) by crystallization from an ethanol and chloroform mixture (1:1). Hippeastrine (15, 166 mg) was obtained from fraction XI (616 mg) by crystallization from an ethanol and chloroform mixture (1:1). Mother liquor of fraction XI was subjected to preparative TLC (toluene:EtOAc:Et₂NH 15:75:10, 1×) to give epimaritidine (16, 127 mg). Fraction XII (1.43 g) was dissolved in hot ethanol and lycorine (17, 752 mg) crystallized from the mixture. Tazzetine (18, 1.85 g) crystallized (EtOH:CHCl₃ 7:3, 100 mL) from fraction XIII (3.11 g). The mother liquor (890 mg) was chromatographed by preparative TLC (cyclohexane:acetone:NH₃ 50:50:1, 3×) to give sub-fractions XIII/1–XIII/3. Subfraction XIII/1 (89 mg) was dissolved in hot ethanol and eugenie (19, 20 mg) crystallized from the solution. Fraction XIV (6.5 g), by column chromatography on Al₂O₃ (800 g), yielded seven sub-fractions XIV/1–XIV/7. Subfraction XIV/6 was subjected to preparative TLC (cyclohexane:acetone:NH₃ 10:80:1) to give norpluviine (20, 62 mg) and 9-O-demethylmaritidine (21, 15 mg). Subfraction XIV/7 (2.5 g) was subjected to preparative TLC (toluene:acetone:EtOH:NH₃ 40:40:6:4, 2×) to obtain pancracine (22, 247 mg) and subfraction XIV/7-B (1.95 g). 9-O-Demethylhomolycorine (23, 1.42 g) was obtained from sub-fraction XIV/7-B by preparative TLC (toluene:Et₂NH, 95:5, 3×). Fraction XV (672 mg) was separated by preparative TLC (EtOAc:MeOH:Et₂NH 8:1:1, 1×) into four sub-fractions, XV/1–XV/4. Sub-fraction XV/3 was further chromatographed by preparative TLC to give 7-oxonorpluviine (24, 6 mg).

3.4. In Vitro Cytotoxicity Study

3.4.1. Cell Culture and Culture Conditions

Selected human tumor and non-tumor cell lines Jurkat (acute T cell leukemia), MOLT-4 (acute lymphoblastic leukemia), A549 (lung carcinoma), HT-29 (colorectal adenocarcinoma), PANC-1 (pancreas epithelioid carcinoma), A2780 (ovarian carcinoma), HeLa (cervix adenocarcinoma), MCF-7 (breast adenocarcinoma), SAOS-2 (osteosarcoma), and MRC-5 (normal lung fibroblasts) were purchased from either ATCC (Manassas, VA, USA) or Sigma-Aldrich (St. Louis, MO, USA) and cultured according to the providers' culture method guidelines. All cell lines were maintained at 37 °C in a humidified 5% carbon dioxide and 95% air incubator. Cells in the maximum range of either 10 passages for a primary cell line (MRC-5), or in the maximum range of 20 passages for cancer cell lines (Jurkat, MOLT-4, A549, HT-29, PANC-1, A2780, HeLa, MCF-7, and SAOS-2) and in an exponential growth phase were used for this study.

3.4.2. Cell Treatment

All the alkaloids evaluated and doxorubicin, used as positive control, were dissolved in dimethyl sulfoxide (DMSO) (Sigma-Aldrich, St. Louis, MO, USA) to prepare stock solutions with a concentration of 10–50 mM based on their solubility. Stock solutions were freshly prepared before use in the experiments. For the experiments, the stock solutions were diluted with the appropriate culture

medium to create final concentrations (10 μM for a single-dose alkaloid cytotoxicity screen and 1 μM for doxorubicin, used as a reference compound) making sure that the concentration of DMSO was <0.1% to avoid toxic effects on the cells. Control cells were sham-treated with a DMSO vehicle only (0.1%; control).

3.4.3. WST-1 Cytotoxicity Assay

The WST-1 (Roche, Mannheim, Germany) reagent was used to determine the cytostatic effect of the test compounds. WST-1 is designed for the spectrophotometric quantification of cell proliferation, growth, viability, and chemosensitivity in cell populations using a 96 well plate format (Sigma, St. Louis, MO, USA). The principle of WST-1 is based on photometric detection of the reduction of tetrazolium salt to a colored formazan product. The cells were seeded at a previously established optimal density (30,000 Jurkat, 25,000 MOLT-4, 500 A549, 1500 HT-29, 2000 PANC-1, 5000 A2780, 500 HeLa, 1500 MCF-7, 2000 SAOS-2, and 2000 MRC-5 cells/well) in 100 μL of culture medium, and adherent cells were allowed to reattach overnight. Thereafter, the cells were treated with 100 μL of either corresponding alkaloids or doxorubicin stock solutions to obtain the desired concentrations and incubated in 5% CO_2 at 37 $^\circ\text{C}$. WST-1 reagent diluted 4-fold with PBS (50 μL) was added 48 h after treatment. Absorbance was measured after 3 h incubation with WST-1 at 440 nm. The measurements were performed in a Tecan Infinite M200 spectrometer (Tecan Group, Männedorf, Switzerland). All experiments were performed at least three times with triplicate measurements at each drug concentration per experiment. The viability was quantified as described in Havelek et al. according to the following formula: (%) viability = $(A_{\text{sample}} - A_{\text{blank}}) / (A_{\text{control}} - A_{\text{blank}}) \times 100$, where A is the absorbance of the employed WST-1 formazan measured at 440 nm [43]. The viability of the treated cells was normalized to the viability of cells treated with 0.1% DMSO (Sigma-Aldrich, St. Louis, MO, USA) as a vehicle control.

3.5. Statistical Analysis

The descriptive statistics of the results were calculated and the charts made in either Microsoft Office Excel 2010 (Microsoft, Redmond, WA, USA) or GraphPad Prism 5 biostatistics (GraphPad Software, La Jolla, CA, USA). In this paper, all of the values have been expressed as arithmetic means with SD of triplicates ($n = 3$), unless otherwise noted. The significant differences between the groups were analyzed using Student's *t*-test and a *p* value ≤ 0.05 was considered statistically significant. IC_{50} curves of pancracine and standard cytostatic treatment doxorubicin were generated and values of IC_{50} were deducted with GraphPad Prism 5 Biostatistics.

4. Conclusions

In conclusion, 24 Amaryllidaceae alkaloids of various structural types were isolated from fresh bulbs of *Narcissus* cv. Professor Einstein. The constitution of a newly isolated alkaloid, 7-oxopliviine, was structurally determined. The complete NMR data for 9-*O*-demethylmaritidine are reported. Isolated compounds not previously studied for cytotoxicity were assayed for their cytotoxicity on a set of nine human cancer cells of different histotypes. This study revealed promising cytotoxic activity of pancracine, a montanine-type alkaloid, which was isolated in an amount that will allow more detailed cytotoxic studies in the future, and also the preparation of semisynthetic derivatives. Taken together, the plant cultivar *Narcissus* cv. Professor Einstein is as a rich source of diverse alkaloids, some of which show interesting activities for further pharmaceutical research.

Supplementary Materials: The following are available online at <http://www.mdpi.com/2223-7747/9/2/137/s1>: Figure S1 GS/MS analysis of alkaloidal extract of *Narcissus* cv. Professor Einstein, Table S1 Alkaloids identified by GC/MS in fresh bulbs of *Narcissus* cv. Professor Einstein, Figure S2-1 ^1H NMR spectra of 9-*O*-demethylmaritidine (**21**) in CDCl_3 , Figure S2-2 ^{13}C NMR spectra of 9-*O*-demethylmaritidine (**21**) in CDCl_3 , Figure S3-1 ESI-HRMS spectra of new alkaloid 7-oxonorpluviine (**24**), Figure S3-2 ^1H NMR spectra of new alkaloid 7-oxonorpluviine (**24**) in CD_3OD , Figure S3-3 ^{13}C NMR spectra of new alkaloid 7-oxonorpluviine (**24**) in CD_3OD , Figure S3-4 gCOSY spectra of new alkaloid 7-oxonorpluviine (**24**) in CD_3OD , Figure S3-5 gHSQC spectra of new alkaloid

7-oxonorpluviine (**24**) in CD₃OD, Figure S3-6 gHMBC spectra of new alkaloid 7-oxonorpluviine (**24**) in CD₃OD, Figure S3-7 NOESY spectra of new alkaloid 7-oxonorpluviine (**24**) in CD₃OD.

Author Contributions: K.B., A.H., L.O. contributed to the isolation of Amaryllidaceae alkaloids. K.B., J.M., J.K., A.H., and J.J. assisted with the identification of the isolated alkaloids (MS, NMR, etc.). D.K., R.H., M.M., and M.Ř. were involved with the cytotoxicity assays. L.C. and M.Ř. designed the study, supervised the laboratory work and contributed to the critical reading of the manuscript. All of the authors read the final manuscript and approved the submission. All authors have read and agreed to the published version of the manuscript.

Funding: Research reported in this publication was supported by projects of Charles University (No. SVV UK 260 412; 260 401; Progres/UK Q40-01 and Q42), by MH CZ—DRO (University Hospital Hradec Kralove, No. 00179906), by Long-term development plan (Faculty of Military Health Sciences), and by the Pre-application research into innovative medicines and medical technologies project (Reg. No. CZ.02.1.01/0.0/0.0/18_069/0010046) co-funded by the European Union.

Acknowledgments: The authors wish to thank Gerald Blunden for critical reading of the manuscript and corrections of English, and to Lucie Nováková for measurement of the HRMS spectra of the new compound.

Conflicts of Interest: The authors declare no conflict of interest.

References

- Ingrassia, L.; Lefranc, F.; Mathieu, V.; Darro, F.; Kiss, R. Amaryllidaceae isocarboxystiril alkaloids and their derivatives as promising antitumor agents. *Transl. Oncol.* **2008**, *1*, 1–13. [[CrossRef](#)] [[PubMed](#)]
- Havelek, R.; Muthna, D.; Tomsik, P.; Kralovec, K.; Seifrtova, M.; Cahlikova, L.; Hostalkova, A.; Safratova, M.; Perwein, M.; Cermakova, E.; et al. Anticancer potential of Amaryllidaceae alkaloids evaluated by screening with a panel of human cells, real-time cellular analysis and Ehrlich tumor-bearing mice. *Chem. Biol. Interact.* **2017**, *275*, 121–132. [[CrossRef](#)] [[PubMed](#)]
- Nair, J.J.; van Standen, J. Cytotoxicity studies of lycorine alkaloids of the Amaryllidaceae. *Nat. Prod. Commun.* **2014**, *9*, 1193–1210. [[CrossRef](#)] [[PubMed](#)]
- Cho, N.; Du, Y.; Valenciano, A.L.; Fernandez-Murga, M.L.; Goetz, M.; Clement, J.; Cassera, M.B.; Kingston, D.G.I. Antiplasmodial alkaloids from bulbs of *Amaryllis belladonna* Steud. *Bioorg. Med. Chem. Lett.* **2018**, *28*, 40–42. [[CrossRef](#)] [[PubMed](#)]
- Zhan, G.; Zhou, J.; Liu, R.; Liu, T.; Guo, G.; Wang, J.; Xiang, M.; Xue, Y.; Luo, Z.; Zhang, Y.; et al. Galanthamine, plicamine, and secoplicamine alkaloids from *Zephyranthes candida* and their anti-acetylcholinesterase and antiinflammatory activities. *J. Nat. Prod.* **2016**, *79*, 760–766. [[CrossRef](#)]
- Locarek, M.; Novakova, J.; Kloucek, P.; Hostalkova, A.; Kokoska, L.; Gabrlova, L.; Safratova, M.; Opletal, L.; Cahlikova, L. Antifungal and antibacterial activity of extracts and alkaloids of selected Amaryllidaceae plant species. *Nat. Prod. Commun.* **2015**, *10*, 1537–1540.
- Hulcova, D.; Mařikova, J.; Korabecny, J.; Hostalkova, A.; Jun, D.; Kunes, J.; Chlebek, J.; Opletal, L.; De Simone, A.; Novakova, L.; et al. Amaryllidaceae alkaloids from *Narcissus pseudonarcissus* L. cv. Dutch Master as potential drugs in treatment of Alzheimer's disease. *Phytochemistry* **2019**, *165*, 112055. [[CrossRef](#)]
- Castillo-Ordonez, W.O.; Tamarozzi, E.R.; da Silva, G.M.; Aristizabal-Pachon, A.F.; Sakamoto-Hojo, E.T.; Takahashi, C.S.; Giuliatti, S. Exploration of the acetylcholinesterase inhibitory activity of some alkaloids from Amaryllidaceae family by molecular docking in silico. *Neurochem. Res.* **2017**, *42*, 2826–2830. [[CrossRef](#)]
- Jin, Z. Amaryllidaceae and Scelotium alkaloids. *Nat. Prod. Rep.* **2007**, *24*, 886–905. [[CrossRef](#)]
- Safratova, M.; Hostalkova, A.; Hulcova, D.; Breiterova, K.; Hrabcova, V.; Machado, M.; Fontinha, D.; Prudencio, M.; Kunes, J.; Chlebek, J.; et al. Alkaloids from *Narcissus poeticus* cv. Pink Parasol of various structural types and their biological activity. *Arch. Pharm. Res.* **2018**, *41*, 208–218. [[CrossRef](#)]
- Maelicke, A.; Samochocki, M.; Jostock, R.; Fehrenbacher, A.; Ludwig, J.; Albuquerque, E.X.; Zerlin, M. Allosteric sensitization of nicotinic receptors by galanthamine, a new treatment strategy for Alzheimer's disease. *Biol. Psychiatry* **2001**, *49*, 279–288. [[CrossRef](#)]
- Govindaraju, K.; Ingels, A.; Hasan, M.N.; Sun, D.; Mathieu, V.; Masi, M.; Evidente, A.; Kornienko, A. Synthetic analogues of the montanine-type alkaloids with activity against apoptosis-resistant cancer cells. *Bioorg. Med. Chem. Lett.* **2018**, *28*, 589–593. [[CrossRef](#)] [[PubMed](#)]
- Evidente, A.; Kireev, A.S.; Jenkins, A.R.; Romero, A.E.; Steelant, W.F.; Van Slambrouck, S.; Kornienko, A. Biological evaluation of structurally diverse Amaryllidaceae alkaloids and their synthetic derivatives: Discovery of novel leads for anticancer drug design. *Planta Med.* **2009**, *75*, 501–507. [[CrossRef](#)] [[PubMed](#)]

14. Ingrassia, L.; Lefranc, F.; Dewelle, J.; Pottier, L.; Mathieu, V.; Spiegl-Kreinecker, S.; Sauvage, S.; El Yazidi, M.; Dehoux, M.; Berger, W.; et al. Structure-activity relationship analysis of novel derivatives of narciclasine (an Amaryllidaceae isocarbostryl derivative) as potential anticancer agents. *J. Med. Chem.* **2009**, *52*, 1100–1114. [[CrossRef](#)] [[PubMed](#)]
15. Havelek, R.; Seifrtova, M.; Kralovec, K.; Bruckova, L.; Cahlikova, L.; Dalecka, M.; Vavrova, J.; Rezacova, M.; Opletal, L.; Bilkova, Z. The effect of Amaryllidaceae alkaloids haemanthamine and haemanthidine on cell cycle progression and apoptosis in p53-negative human leukemic Jurkat cells. *Phytomedicine* **2014**, *21*, 479–490. [[CrossRef](#)] [[PubMed](#)]
16. Li, L.; Zhang, Z.; Yang, Q.; Ning, M. Lycorine inhibited the cell growth of non-small cell lung cancer by modulating the miR-186/CDK1 axis. *Life Sci.* **2019**, *231*, 116528. [[CrossRef](#)] [[PubMed](#)]
17. Breiterova, K.; Locarek, M.; Kohelova, E.; Talackova, M.; Hulcova, D.; Opletal, L.; Cahlikova, L. Daffodils as potential crops of biologically-active compounds: Assessment of 40 ornamental taxa for their alkaloid profile and cholinesterases inhibition activity. *Nat. Prod. Commun.* **2018**, *13*, 419–422. [[CrossRef](#)]
18. Kornienko, A.; Evidente, A. Chemistry, biology, and medicinal potential of narciclasine and its congeners. *Chem. Rev.* **2008**, *108*, 1982–2014. [[CrossRef](#)]
19. Hartwell, J.L. Plants used against cancer. A survey. *Lloydia* **1967**, *30*, 379–436.
20. Kington, S. *The International Daffodil Register and Classified List*; Royal Horticultural Society: London, UK, 2008.
21. Pettit, G.R.; Tan, R.; Bao, G.-H.; Melody, N.; Doubek, D.L.; Gao, S.; Chapuis, J.-C.; Williams, L. Antineoplastic agents. 587. Isolation and structure of 3-epipancreatistatin from *Narcissus* cv. Ice Follies. *J. Nat. Prod.* **2012**, *75*, 771–773. [[CrossRef](#)]
22. Pigni, N.B.; Ríos-Ruiz, S.; Martínez-Francés, V.; Nair, J.J.; Viladomat, F.; Codina, C.; Bastida, J. Alkaloids from *Narcissus serotinus*. *J. Nat. Prod.* **2012**, *75*, 1643–1647. [[CrossRef](#)] [[PubMed](#)]
23. Huang, S.; Zhang, Y.; He, H.; Li, S.; Tang, G.; Chen, D.; Cao, M.; Di, Y.; Hao, X.J. A new Amaryllidaceae alkaloid from bulbs of *Lycoris radiata*. *Chin. J. Nat. Med.* **2013**, *11*, 406–410. [[CrossRef](#)] [[PubMed](#)]
24. Cowden, C.J.; Banwell, M.G.; Ho, I.C.S. Synthesis of putative structure of 5,6-dihydrobicolorin. *J. Nat. Prod.* **1994**, *57*, 1746–1750. [[CrossRef](#)]
25. Lamoral-Theys, D.; Andolfi, A.; Van Goietsenoven, G.; Cimmino, A.; Le Calvé, B.; Wauthoz, N.; Mégalizzi, V.; Gras, T.; Bruyere, C.; Dubois, J.; et al. Lycorine, the main phenanthridine Amaryllidaceae alkaloid, exhibits significant antitumor activity in cancer cells that display resistance to proapoptotic stimuli: An investigation of structure-activity relationship and mechanistic insight. *J. Med. Chem.* **2009**, *52*, 6244–6625. [[CrossRef](#)] [[PubMed](#)]
26. Chen, J.-Q.; Xie, J.-H.; Bao, D.-H.; Liu, S.; Zhou, Q.-L. Total synthesis of (–)-galanthamine and (–)-lycoramine via catalytic asymmetric hydrogenation and intramolecular reductive Heck cyclization. *Org. Lett.* **2012**, *14*, 2714–2717. [[CrossRef](#)] [[PubMed](#)]
27. Jegorov, A.; Buchta, M.; Sedmera, P.; Kuzma, M.; Havlicek, V. Accurate product ion mass spectra of galanthamine derivatives. *J. Mass. Spectrom.* **2006**, *41*, 544–548. [[CrossRef](#)] [[PubMed](#)]
28. Lee, T.B.K.; Goehring, K.E.; Ma, Z. One-Step conversion of galanthamine to lycoramine: A novel hydride-transfer reaction. *J. Org. Chem.* **1998**, *63*, 4535–4538. [[CrossRef](#)]
29. Berkov, S.; Reyes-Chilpa, R.; Codina, C.; Viladomat, F.; Bastida, J. Revised NMR data for incartine: An alkaloid from *Galanthus elwesii*. *Molecules* **2007**, *12*, 1430–1435. [[CrossRef](#)]
30. Berkov, S.; Bastida, J.; Sidjimova, B.; Viladomat, F.; Codina, C. Phytochemical differentiation of *Galanthus nivalis* and *Galanthus elwesii* (Amaryllidaceae): A case study. *Biochem. Syst. Ecol.* **2008**, *36*, 638–645. [[CrossRef](#)]
31. Bastida, J.; Viladomat, F.; Bergonon, S.; Fernandez, J.M.; Codina, C.; Rubiralta, M.; Quirion, J.-C. Alkaloids from *Narcissus leonensis*. *Phytochemistry* **1993**, *34*, 1656–1658. [[CrossRef](#)]
32. Bastida, J.; Lavilla, R.; Viladomat, F. The Alkaloids: Chemical and biological aspects of *Narcissus* alkaloids. In *The Alkaloids: Chemistry and Biology*; Cordell, G.A., Ed.; Elsevier: Amsterdam, The Netherlands, 1998; Volume 63, pp. 87–179.
33. Jeffs, P.W.; Abou-Donia, A.; Campau, D. Structures of 9-O-demethylhomolycorine and 5 α -hydroxyhomolycorine. alkaloids of *Crinum defixum*, *C. scabrum*, and *C. latifolium*. Assignment of aromatic substitution patterns from 1H-coupled 13C spectra. *J. Org. Chem.* **1985**, *50*, 1732–1737. [[CrossRef](#)]
34. Ghosal, S.; Ashutosh Razdan, S. (+)-Epimaritidine, an alkaloid from *Zephyranthes rosea*. *Phytochemistry* **1985**, *24*, 635–637. [[CrossRef](#)]

35. Berkov, S.; Sidjimove, B.; Evstatieva, L.; Popov, S. Intraspecific variability in the alkaloid metabolism of *Galanthus elwesii*. *Phytochemistry* **2004**, *65*, 579–586. [[CrossRef](#)] [[PubMed](#)]
36. Pham, L.H.; Gründemann, E.; Wagner, J.; Bartoszek, M.; Döpke, W. Two novel Amaryllidaceae alkaloids from *Hippeastrum equestre* Herb.: 3-O-demethyltazettine and egonine. *Phytochemistry* **1999**, *51*, 327–332. [[CrossRef](#)]
37. Via, J.; Arriortura, M.I.; Ochando, L.E.; Reventos, M.M.; Amigo, J.M.; Bastida, J. Structure of eugenine, an alkaloid from *Narcissus eugeniae*. *Acta Cryst. C* **1989**, *45*, 2020–2022. [[CrossRef](#)]
38. Berkov, S.; Romani, S.; Herrera, M.; Viladomat, F.; Codina, C.; Momekov, G.; Ionkova, I.; Bastida, J. Antiproliferative alkaloids from *Crinum zeylanicum*. *Phytother. Res.* **2011**, *25*, 1686–1692. [[CrossRef](#)]
39. Bastida, J.; Llabrés, J.M.; Viladomat, F.; Codina, C.; Rubiralta, M.; Feliz, M. 9-O-Demethylmaritidine: A new alkaloid from *Narcissus radinganorum*. *Planta Med.* **1988**, *54*, 524–526. [[CrossRef](#)]
40. Bao, X.; Cao, Y.-X.; Chu, W.-D.; Qu, H.; Du, J.-Y.; Zhao, X.-H.; Ma, X.-Y.; Wang, C.-T.; Fan, C.-A. Bioinspired total synthesis of montanine-type Amaryllidaceae alkaloids. *Angew. Chem. Int. Edit.* **2013**, *52*, 14167–14172. [[CrossRef](#)]
41. Farinon, M.; Clarimundo, V.S.; Pedrazza, G.P.; Gulko, P.S.; Zuanazzi, J.A.; Xavier, R.M.; de Oliveira, P.G. Disease modifying anti-rheumatic activity of the alkaloid montanine on experimental arthritis and fibroblast-like synoviocytes. *Eur. J. Pharmacol.* **2017**, *15*, 180–187. [[CrossRef](#)]
42. Masi, M.; van Slambrouck, S.; Gunawardana, S.; van Rensburg, M.J.; James, P.C.; Mochel, J.G.; Heliso, P.S.; Albalawi, A.S.; Cimmino, A.; van Otterlo, W.A.L.; et al. Alkaloids isolated from *Haemanthus humilis* Jacq., an indigenous South African Amaryllidaceae: Anticancer activity of coccinine and montanine. *S. Afr. J. Bot.* **2019**, *126*, 277–281. [[CrossRef](#)]
43. Havelek, R.; Siman, P.; Cmielova, J.; Stoklasova, A.; Vavrova, J.; Vinklerek, J.; Knizek, J.; Rezacova, M. Differences in vanadocene dichloride and cisplatin effect on MOLT-4 leukemia and human peripheral blood mononuclear cells. *Med. Chem.* **2012**, *8*, 615–621. [[CrossRef](#)] [[PubMed](#)]



© 2020 by the authors. Licensee MDPI, Basel, Switzerland. This article is an open access article distributed under the terms and conditions of the Creative Commons Attribution (CC BY) license (<http://creativecommons.org/licenses/by/4.0/>).

4.4 Pancracine, a Montanine-Type Amaryllidaceae Alkaloid, Inhibits Proliferation of A549 Lung Adenocarcinoma Cells and Induces Apoptotic Cell Death in MOLT-4 Leukemic Cells

Koutová, D.; Havelek, R.; Peterová, E.; Muthná, D.; Královec, K.; Breiterová, K.; Cahlíková, L.; Řezáčová M.

Int. J. Mol. Sci. 2021, 22(13):7014.

IF2020 5,923, Q1 (Biochemistry and Molecular Biology)

Snahou kolektivu autorů bylo navázat na předchozí publikovanou studii, ve které byl izolován pankracin, montaninový typ alkaloidu patřící do čeledi Amaryllidaceae, a jehož cytotoxicita byla charakterizována nízkými hodnotami IC_{50} pro různé typy nádorových buněčných linií.

Dle hodnot IC_{50} byly vybrány dvě buněčné linie představující odlišný nádorový histotyp, suspenzní leukemická linie hematopoetického původu MOLT-4 a adherentní buněčná linie adenokarcinomu plic A549.

Leukemická linie MOLT-4 se vyznačuje zvýšenou citlivostí vůči cytotoxickým agens a reaguje v mnohem větší míře apoptotickou odpovědí buněk. Zajímalo nás, zda a jak bude tato buněčná linie reagovat vzhledem k buněčnému přežívání či buněčné smrti na různé dávky pankracinu v různých časových intervalech. Co se týče vlivu na proliferaci a viabilitu buněk, z výsledků je patrné, že hodnota IC_{50} $2,71 \pm 0,25 \mu\text{mol.l}^{-1}$ stanovená pro buněčnou linii MOLT-4 koresponduje se zjištěním, že účinek na tyto buňky je jednak cytostatistický, ale rovněž cytotoxický. Životaschopnost buněk MOLT-4 se významně snížila při hodnotě koncentrace pankracinu $5 \mu\text{mol.l}^{-1}$ a růst buněk byl inhibován již při použití nejmenší koncentrace $2,5 \mu\text{mol.l}^{-1}$ v kratším časovém intervalu 24 h. Vystala tedy otázka, jak účinek pankracinu ovlivňuje distribuci buněčné populace v jednotlivých fázích buněčného cyklu. Správné měření vyžadovalo užití pouze nejnižších koncentrací, ve vyšších koncentracích a v pozdějším intervalu už nebylo možné detekovat procento buněk v jednotlivých fázích vzhledem ke zvýšené míře buněčné smrti. Data poukázala na redistribuci buněk v buněčném cyklu, kdy bylo pozorováno zvýšené procento buněk v sub-G1 fázi oproti negativní kontrole. To, zda byla buněčná smrt navozená pankracinem apoptotická, dokázal experiment, při kterém byla sledována aktivita kaspáz spojených s indukcí apoptózy. Pankracin v koncentraci $10 \mu\text{mol.l}^{-1}$ a vyšší způsobil zvýšenou aktivitu efektorové kaspázy -3,-7, kaspázy -9 odpovědnou za aktivaci vnitřní apoptotické dráhy a kaspázy -8, odpovědnou za aktivaci vnější apoptotické dráhy. Následující experiment metody značení Annexinem V a propidiumjodidem (PI) potvrdil, že

pankracin statisticky významně zvýšil procento apoptotických buněk v časně i pozdní fázi apoptózy. S tím rovněž souvisí i detekce proteinů účastnících se molekulárních dějů v pozadí účinku pankracinu. Účinek pankracinu v koncentraci $5 \mu\text{mol.l}^{-1}$ indukující apoptózu byl doprovázen statisticky významně vyšší hladinou tumor supresorového proteinu p53 fosforylovaného na serinu 392. Jelikož je známo, že p53 fosforylovaný na serinu 392 se účastní přenosu signálů vedoucí k buněčné smrti, pozorované zvýšení množství proteinu Bax s tím velice dobře koreluje. K zastavení buněčného cyklu při přechodu G1/S-fáze dochází aktivací inhibitorů Cdk p21 a p27, jejichž hladiny byly rovněž za stejných podmínek zvýšeny. Proapoptický efekt p38 MAPK fosforylovaný na Thr 180 a Tyr 182 byl pozorován v souladu s detekovanou indukcí apoptózy.

Buněčná odpověď adenokarcinomu plic A549 po ovlivnění rostoucí koncentrací pankracinu je statisticky významně cytostatická. Je obecně známo, že buněčná linie A549 je velmi rezistentní vůči standardní chemoterapeutické léčbě (Ashinuma et al. 2012), tato rezistence je patrná i z našich výsledků, neboť doxorubicin v koncentraci $0,25 \mu\text{mol.l}^{-1}$ významně snížil viabilitu těchto buněk až po 72 h. U těchto a dalších adherentních linií (HepG2, MCF-7, A2780) byla pozorována dávkově závislá dlouhodobá inhibice růstu měřením buněčné proliferace systémem xCELLigence. Statisticky významně byl tento efekt patrný i metodou počítání buněk barvením Trypanovou modří, kdy byl signifikantní pokles proliferace pozorovatelný s použitím koncentrace $2,5 \mu\text{mol.l}^{-1}$ za 48 h a s rostoucí koncentrací pankracinu efekt významně rostl. Efekt na viabilitu pozorován nebyl. Naše pozornost se opět zaměřila na procentuální změny distribuce buněk v jednotlivých fázích buněčného cyklu. Z našich dat vyplývá, že inhibice růstu buněk A549 způsobená pankracinem je spojená s akumulací buněk v G1/S fázi buněčného cyklu a detekcí proteinů účastnících se této zástavy bylo potvrzeno, že antiproliferativní účinek byl spojen s významně změněnými hladinami různých regulačních proteinů buněčného cyklu a jejich aktivovaných forem. Pankracin v dávce $20 \mu\text{mol.l}^{-1}$ a za 24 h způsobil signifikantní ($p \leq 0,05$) aktivaci p38 MAPK prostřednictvím fosforylace na Thr180 a Tyr182 a hypofosforylaci ERK na Thr202 a Tyr204. Další změny v hladinách proteinů byly patrné po 72 h, kdy pankracin v dávce $10 \mu\text{mol.l}^{-1}$ a vyšší snížil hladinu kinázy Akt prostřednictvím fosforylace na Thr308, zároveň statisticky významně ($p \leq 0,05$) zvýšil hladinu proteinu p27 a aktivoval protein Rb prostřednictvím hypofosforylace na Ser807 a Ser811. V delším časovém intervalu (72h) byla MAP kinasová aktivita ERK fosforylovaného na Thr202 a Tyr204 významně snížena ($p \leq 0,05$) pankracinem v koncentraci $10 \mu\text{mol.l}^{-1}$ a $20 \mu\text{mol.l}^{-1}$. Zatímco hyperfosforylace p38 MAPK na Thr180 a Tyr182 nastala při použití nižší

koncentrace $10 \mu\text{mol.l}^{-1}$. Pankracin neměl žádný vliv na změnu hladiny proteinů p53 a p21, což odpovídá předchozím výsledkům, kdy nebyl pozorován efekt na viabilitu buněk A549 a rovněž nebyla detekována zvýšená aktivita kaspáz u těchto buněk.

Tato publikace je první studií přispívající k pochopení cytostatického, cytotoxického, proapoptického a molekulárního mechanismu v pozadí účinku pankracinu, montaninového typu alkaloidu.



Article

Panracine, a Montanine-Type Amaryllidaceae Alkaloid, Inhibits Proliferation of A549 Lung Adenocarcinoma Cells and Induces Apoptotic Cell Death in MOLT-4 Leukemic Cells

Darja Koutová¹, Radim Havelek^{1,*}, Eva Peterová¹, Darina Muthná¹, Karel Královec², Kateřina Breiterová³, Lucie Cahlíková³ and Martina Řezáčová¹

¹ Department of Medical Biochemistry, Faculty of Medicine in Hradec Kralove, Charles University, Simkova 870, 500 03 Hradec Kralove, Czech Republic; koutova.darja@lfhk.cuni.cz (D.K.); PETEROVE@lfhk.cuni.cz (E.P.); MuthnaD@lfhk.cuni.cz (D.M.); rezacovam@lfhk.cuni.cz (M.Ř.)

² Department of Biological and Biochemical Sciences, Faculty of Chemical Technology, University of Pardubice, Studentska 573, 532 10 Pardubice, Czech Republic; karel.kralovec@upce.cz

³ ADINACO Research Group, Department of Pharmaceutical Botany, Faculty of Pharmacy, Charles University, Heyrovského 1203, 500 05 Hradec Kralove, Czech Republic; breiterk@faf.cuni.cz (K.B.); cahlikova@faf.cuni.cz (L.C.)

* Correspondence: havelekr@lfhk.cuni.cz; Tel.: +420-495-816-293



Citation: Koutová, D.; Havelek, R.; Peterová, E.; Muthná, D.; Královec, K.; Breiterová, K.; Cahlíková, L.; Řezáčová, M. Panracine, a Montanine-Type Amaryllidaceae Alkaloid, Inhibits Proliferation of A549 Lung Adenocarcinoma Cells and Induces Apoptotic Cell Death in MOLT-4 Leukemic Cells. *Int. J. Mol. Sci.* **2021**, *22*, 7014. <https://doi.org/10.3390/ijms22137014>

Academic Editor: Jamal Mahajna

Received: 19 May 2021

Accepted: 25 June 2021

Published: 29 June 2021

Publisher's Note: MDPI stays neutral with regard to jurisdictional claims in published maps and institutional affiliations.



Copyright: © 2021 by the authors. Licensee MDPI, Basel, Switzerland. This article is an open access article distributed under the terms and conditions of the Creative Commons Attribution (CC BY) license (<https://creativecommons.org/licenses/by/4.0/>).

Abstract: Panracine, a montanine-type Amaryllidaceae alkaloid (AA), is one of the most potent compounds among natural isoquinolines. In previous studies, panracine exhibited cytotoxic activity against diverse human cancer cell lines in vitro. However, further insight into the molecular mechanisms that underlie the cytotoxic effect of panracine have not been reported and remain unknown. To fill this void, the cell proliferation and viability of cancer cells was explored using the Trypan Blue assay or by using the xCELLigence system. The impact on the cell cycle was determined by flow cytometry. Apoptosis was evaluated by Annexin V/PI and by quantifying the activity of caspases (-3/7, -8, and -9). Proteins triggering growth arrest or apoptosis were detected by Western blotting. Panracine has strong antiproliferative activity on A549 cells, lasting up to 96 h, and antiproliferative and cytotoxic effects on MOLT-4 cells. The apoptosis-inducing activity of panracine in MOLT-4 cells was evidenced by the significantly higher activity of caspases. This was transmitted through the upregulation of p53 phosphorylated on Ser392, p38 MAPK phosphorylated on Thr180/Tyr182, and upregulation of p27. The panracine treatment negatively altered the proliferation of A549 cells as a consequence of an increase in G1-phase accumulation, associated with the downregulation of Rb phosphorylated on Ser807/811 and with the concomitant upregulation of p27 and downregulation of Akt phosphorylated on Thr308. This was the first study to glean a deeper mechanistic understanding of panracine activity in vitro. Perturbation of the cell cycle and induction of apoptotic cell death were considered key mechanisms of panracine action.

Keywords: Amaryllidaceae alkaloids; panracine; cytotoxicity; antiproliferative activity; cell cycle arrest; apoptosis

1. Introduction

Alkaloids are a large group of important natural compounds, and, thanks to their prophylactic or therapeutic values, they are undoubtedly a stable player in the field of medical treatment for many diseases. Approximately 50–60% of the new drugs approved between 1981 and 2010 either originated from plants or were prepared by variations of the chemical structures of the compounds previously described in plants [1]. Alkaloids isolated from Amaryllidaceae plants comprise a large group of approximately 600 naturally occurring isoquinoline alkaloids with a vast structural diversity [2]. Therefore, the large number of Amaryllidaceae alkaloids (AA) have been divided into several structurally

divergent skeleton types according to their biosynthetic origin, and ring structure and named after a representative alkaloid from the class [2,3].

Panpracine (Figure 1) belongs to the montanine types of AA, which possess a unique pentacyclic 5,11-methanomorphanthridine skeleton ring. At present, fourteen known AA share the 5,11-methanomorphanthridine scaffold, which is believed to be a significant carrier of the biological effects of montanine-type alkaloids [4,5]. Panpracine is distinct from other alkaloids of montanine types because of the presence of a double bond between C1 and C11a and two hydroxyls on stereocenters at C2 and C3 in the E ring of the 5,11-methanomorphanthridine framework [6]. Among the montanine skeleton type, montanine, coccinine, manthidine, and manthine were the first alkaloid members isolated from the *Haemanthus* species of the Amaryllidaceae plant family by Wildman et al. [7]. Thirteen years later, in 1968, Wildman and coworkers described another AA of a montanine type, panpracine, which they isolated from *Panpratium maritimum*, *Narcissus poeticus*, and *Rhodophiala bifida* [4]. Since then, attention has turned to investigations performed to gain a deeper understanding of montanine-type alkaloids, including either the possibility of isolation from other plants of the Amaryllidaceae family [6], preparing them by chemical de novo synthesis [5], or exploring their biological activity [6,8–10].

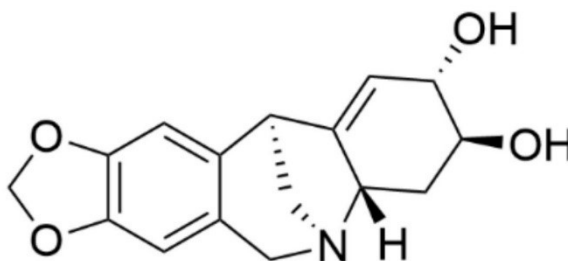


Figure 1. Chemical structure of panpracine.

In our previous work, we screened the cytotoxicity of AA of various structural types isolated from bulbs of *Narcissus* cv. Professor Einstein against a panel of eight cancer cell lines [6]. Among them, panpracine has shown the ability to reduce the proliferation of cancer cells of different histotypes with IC_{50} values reaching into the micromolar range after 48 h of treatment. MOLT-4, A549, HT-29, MCF-7, and SAOS-2 are sensitive cell lines with IC_{50} values below $3 \mu\text{M}$, whereas Jurkat A2780 and HeLa are more resistant, with IC_{50} values between 3 and $6 \mu\text{M}$ [9]. Consistently, other structure–activity studies investigating the antiproliferative effect of panpracine isolated from *Panpratium canariense* described its strong inhibitory effect from $4.3 \pm 0.7 \mu\text{M}$ to $9.1 \pm 1.0 \mu\text{M}$ on the growth of four cancer cell lines derived from ovarian (A2780), lung (SW1573), breast (T47-D), and colon (WiDr) carcinoma [9]. Moreover, a recent study reported the preparation of semisynthetic montanine-type alkaloid derivatives, which were screened in vitro for their antiproliferative activities against a panel of six cancer cell lines. Although the parent alkaloid of the montanine-type, manthine, was the most effective, the C2-OH and C2-indole-substituted 5,11-methanomorphanthridine derivatives also showed good antiproliferative activity [5]. In what concerns the other bioactivities, there were two studies reporting the antibiotic, antifungal, and antiparasitic effects of panpracine [11,12]. Antimicrobial activity testing using an agar diffusion technique and bacteria species *Staphylococcus aureus*, *Escherichia coli*, and *Pseudomonas aeruginosa* and the yeast *Candida albicans* displayed good inhibitory activity of panpracine against *Staphylococcus aureus* and *Pseudomonas aeruginosa* and moderate activity against *Candida albicans* [11]. The interesting biological activity was complemented by a study describing the antiprotozoal activities of panpracine isolated

from *Narcissus angustifolius* subsp. *transcarpathicus* against *Trypanosoma brucei rhodesiense*, *Trypanosoma cruzi*, and *Plasmodium falciparum* [12].

The AA and its derivatives exhibited various pharmacological activities. Most notably, the cytotoxic activity of the several AA were noteworthy [3,13,14]. Since recent studies have begun to uncover the mechanisms sustaining the cytotoxicity of AA, deeper investigations on some AA are still fragmentary. The initial pilot studies have suggested that the micro-mole cytotoxic potency of pancracine towards cancer cell lines deserves further in-depth investigation. Moreover, there is fundamental lack of reports on the mode of action of pancracine in vitro, greatly hindering further investigation on the montanine type of AA. The aim of this study was to reveal the mechanisms underlying the proliferative inhibition after pancracine treatment by evaluating its effect on cell cycle progression, apoptosis, and related signal transduction pathways.

2. Results

2.1. Pancracine Inhibits Proliferation of A549 Lung Cancer Cells and Reduces Both Proliferation and Viability of MOLT-4 Leukemic Cells

The cytotoxicity of pancracine against a panel of cancer cell lines having different histotypes was previously described by our group in the study of Breiterová et al. [6], where the cytotoxicity of pancracine expressed as 50% inhibitory concentration (IC_{50}) values was $2.29 \pm 0.43 \mu\text{M}$ for A549 cells and $2.71 \pm 0.25 \mu\text{M}$ for MOLT-4 cells. Following this study, which determined the cytotoxicity using the reduction of tetrazolium salt WST-1 as an end-point method, we decided to use the real-time label-free cell proliferation system xCELLigence RTCA. The xCELLigence system measures cell adhesion, viability, morphology, and the number of cells based on impedance, which are displayed as normalized cell index (CI) values. This system affords the continuous monitoring of cellular responses throughout an experiment, without the use of exogenous labels. Growth was observed in human A549 lung adenocarcinoma, MCF-7 breast adenocarcinoma, HepG2 hepatocellular carcinoma, and A2780 ovarian carcinoma treated with a range from 1 to $50 \mu\text{M}$ of pancracine, usually from 24 h after seeding, when the cells were in logarithmic growth and were treated, up to 96 h of incubation. Cells treated with 0.1% DMSO were used as a vehicle control and 5% DMSO-treated cells as a positive control. It is clear from the graph (Figure 2) that, with increasing the concentration of pancracine, there was a reduction in proliferation in all the tested cell lines. In the case of the A549 cell line, the treatment with $20 \mu\text{M}$ of pancracine stopped proliferation over the entire assay interval up to 96 h. The proliferation ability of A549 cells was also significantly reduced by 5 and $10 \mu\text{M}$ of pancracine. The numbers of proliferating cells unstained by Trypan blue were counted 24, 48, and 72 h after cell treatment with pancracine at 2.5-, 5-, 10-, and $20\text{-}\mu\text{M}$ concentrations. A ($p \leq 0.05$) significant antiproliferative effect occurred even at the lowest tested concentration of pancracine ($2.5 \mu\text{M}$) after 48 h and 72 h of treatment for A549 and 24 h and 48 h for the MOLT-4 cell line (Figure 3A). Regarding the effect of pancracine on cell viability, a considerable difference was seen between the overall resistant adherent cell line A549 and the suspension leukemic cell line MOLT-4 of hematopoietic origin (Figure 3B). A slight decrease in viable cells occurred only at the highest concentrations tested (10 and $20 \mu\text{M}$ of pancracine) in the A549 cell line. In the case of the MOLT-4 leukemic cell line, which is particularly more sensitive to anticancer chemotherapeutic treatments, there was a significant ($p \leq 0.05$) effect on the cell viability, beginning with the $5\text{-}\mu\text{M}$ concentration of pancracine, after a longer interval of 48 h of treatment and $10\text{-}\mu\text{M}$ pancracine after 24 h of treatment. The susceptibility of MOLT-4 and resistance of A549 cells to pancracine-induced cell death showed good correlation with the higher percentages of surviving A549 cells after the $0.25\text{-}\mu\text{M}$ doxorubicin treatment (24 and 48 h) compared to MOLT-4 cells.

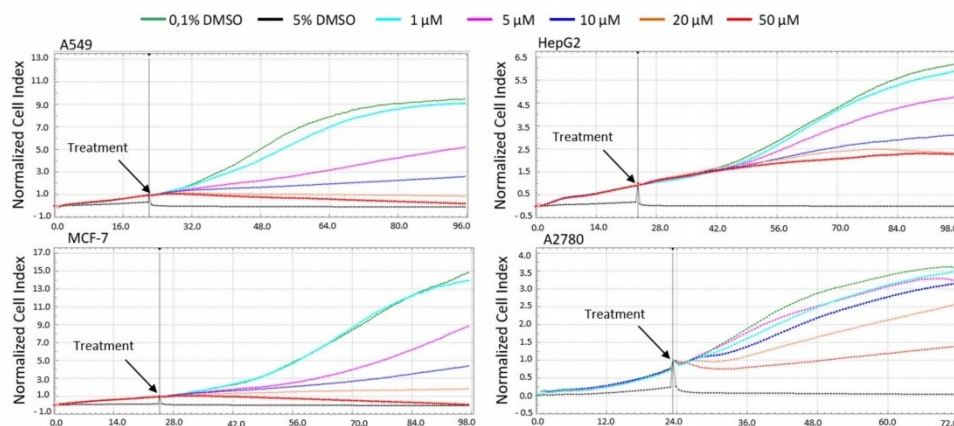


Figure 2. Dynamic real-time monitoring of proliferation and cytotoxicity using the xCELLigence system dedicated to adherent cancer cell lines. Growth kinetics are shown of human A549 lung adenocarcinoma, MCF-7 breast adenocarcinoma, HepG2 hepatocellular carcinoma, and A2780 ovarian carcinoma treated with pancracine. Cells treated with 0.1% DMSO were used as the vehicle control and 5% DMSO-treated cells as a positive control. The normalized cell index was measured over 72 h. Plots shown are representative of at least three replicate experiments in each case.

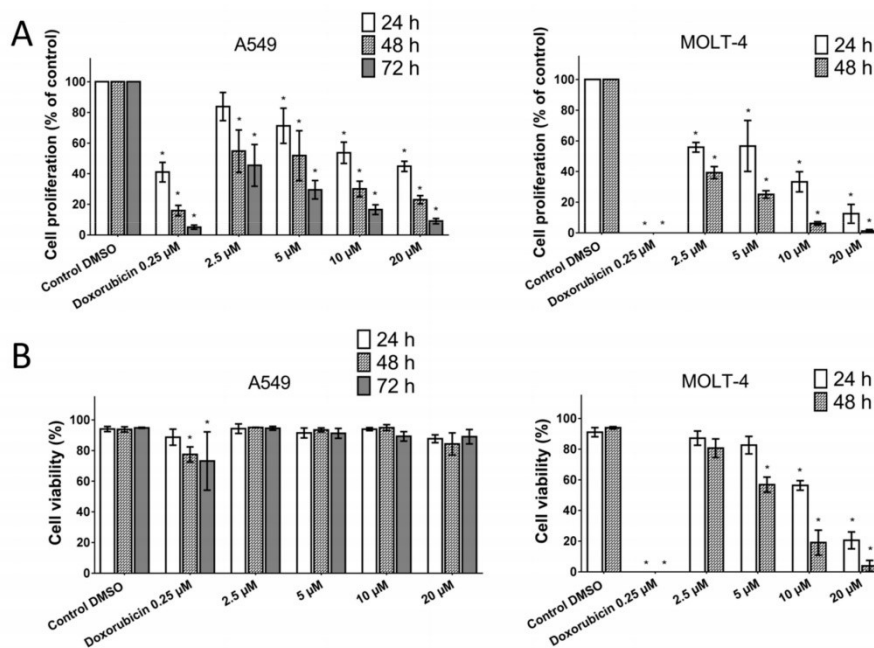


Figure 3. The effect of pancracine on the proliferation (A) and viability (B) of MOLT-4 and A549 cells. Changes in the proliferation and viability following pancracine treatment were monitored by the Trypan blue exclusion test at 24 and 48 h in MOLT-4 cells and at 24, 48, and 72 h in A549 cells. Results are shown as the mean \pm SD from three experiments. * Significantly different to the control ($p \leq 0.05$). Cells treated with 0.25- μ M doxorubicin were used as a positive control.

2.2. Reduced Proliferation of A549 and MOLT-4 Cells Is Associated with Cell Cycle Redistribution

To determine the effect of pancracine on the cell populations at different stages of the cell cycle, a flow cytometry method was used. A significant ($p \leq 0.05$) increase in the cell population, preferentially in the G1 phase, occurred with the use of 5- μM pancracine in A549 cells after 24 h. In addition, an increased ($p \leq 0.05$) percentage of cells accumulated in G1, with a decrease ($p \leq 0.05$) in S-phase cells, and a concurrent increase ($p \leq 0.05$) in G2-phase cells occurred following the use of the highest concentration of pancracine (20 μM) and a 24-h interval of treatment (Figure 4A). A significant ($p \leq 0.05$) increase of A549 cells in the G2 phase with a concomitant reduction of cells in the G1 and S phases was observed after 48 h treatment with 20 μM (Figure 4B).

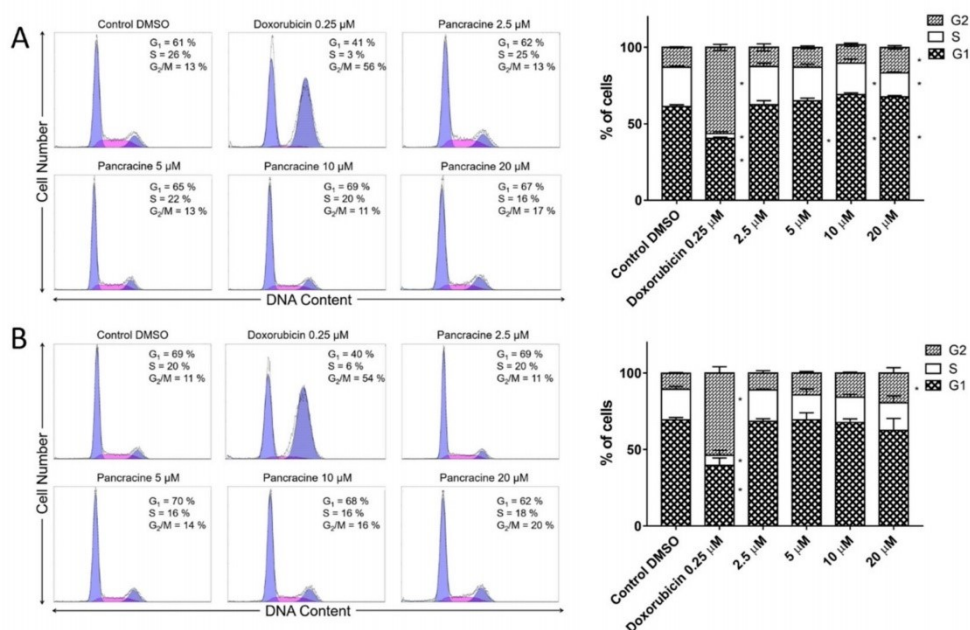


Figure 4. Cell cycle analysis of A549 cells after pancracine treatment. The figure shows representative histograms at 24 (A) and 48 (B) hours after treatment with 2.5- μM , 5- μM , 10- μM , and 20- μM pancracine, with a mean percentage of cells cycling through phases G1, S, and G2 from the flow cytometry measurements of three individual treatments. The bar graph summarizes the cumulative data on the percentage of cells in each phase of the cell cycle. Data are presented as the mean values \pm SD, $n = 3$. * Significantly different to the control ($p \leq 0.05$).

The situation with the MOLT-4 cell line was different. Due to its increased sensitivity leading to excessive cell death at higher doses, only lower concentrations of pancracine were used at 48 h for the cell cycle analysis of MOLT-4 cells. As shown in Figure 5A,B, a statistically significant ($p \leq 0.05$) increase in the cell population in G1 and a decrease in the S-phase population occurred when using a 2.5- μM concentration and a 24-h treatment interval. A statistically significant ($p \leq 0.05$) increase in the cell population in G1 and a statistically significant ($p \leq 0.05$) decrease in the S-phase population occurred when using a 5- μM concentration and 48-h treatment. Pancracine treatment reduced the rate of cycling cells, which was accompanied by an increased fraction of sub-G1-phase cells in the DNA fluorescence histogram. In MOLT-4 cells, the application of pancracine induced an increase in the percentage of sub-G1 after 24 h (2.5 μM —5.7% \pm 0.4%, 5 μM —10.2% \pm 2%, and 10 μM —19.6% \pm 0.7%) compared with the negative control (3.9% \pm 1.9%) and an increase

in the percentage of sub-G1 after 48 h (2.5 μM —5.6% \pm 1.2% and 5 μM —15% \pm 0.8%) compared with the negative control (4.3% \pm 0.8%)—data not shown.

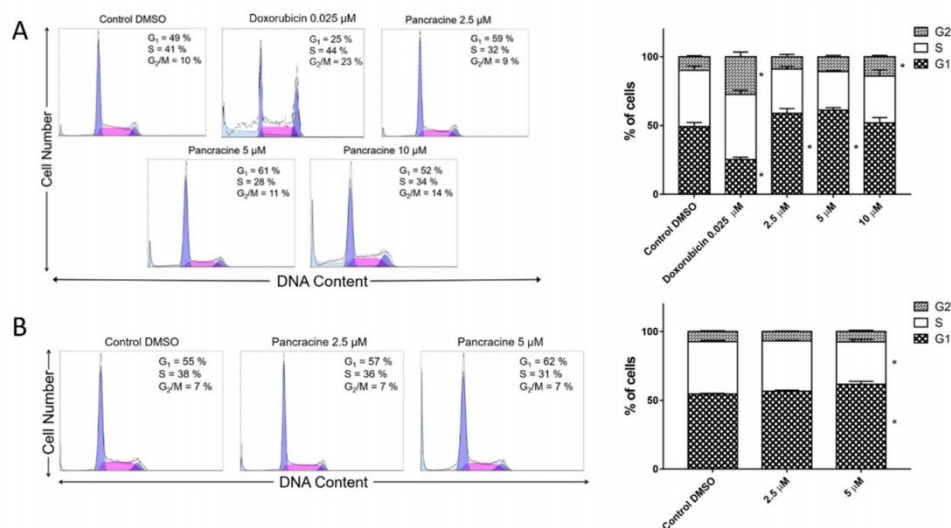


Figure 5. Cell cycle analysis of MOLT-4 cells after pancracine treatment. The figure shows representative histograms after (A) 24 h of treatment with 2.5- μM , 5- μM , and 10- μM pancracine and (B) 48 h of treatment with 2.5- μM and 5- μM pancracine, with a mean percentage of cells cycling through phases G1, S, and G2 from a flow cytometry measurement of three individual treatments. The bar graph summarizes the cumulative data on the percentage of cells in each phase of the cell cycle. Data are presented as the mean values \pm SD, $n = 3$. * Significantly different to the control ($p \leq 0.05$).

2.3. Pancracine Induced Apoptosis in MOLT-4 Cells

In order to determine whether the tumor cell death is associated with apoptosis, we used the detection of caspase-3, -7, -8, and -9 activity after 24 h of pancracine treatment in A549 and MOLT-4 cells. Each type of caspase is responsible for a specific cellular response; effector caspase-3 and -7 respond to the activation of caspase-8 for the extrinsic apoptosis pathway and to the activation of caspase-9 for activation of the intrinsic mitochondrial pathway of apoptosis. In the case of the effect of pancracine on the induction of apoptosis, no caspase activity was observed in A549 cells (Figure 6A). A clearly different situation was found after the application of 10- and 20- μM concentrations of pancracine to the MOLT-4 cell line, when there was a significant ($p \leq 0.05$) increase in the activity of all types of caspases tested compared to the negative control (Figure 6B). Hence, to confirm further the observations that pancracine can induce apoptosis in MOLT-4, the surface exposure of phosphatidylserine and a loss in the membrane integrity was determined using Annexin and PI staining 24 h following the treatment. The combination of these fluorescent probes allowed us to separate living cells (Annexin V/PI-negative), apoptotic cells (Annexin V-positive and PI-negative), and a cell population in the late phase of apoptotic cell death (Annexin V- and PI-positive). As shown in Figure 7, 24 h after the administration of 2.5-, 5-, 10-, and 20- μM pancracine, the early apoptotic rates were 3%, 4%, 10%, and 14% and late apoptotic rates 2%, 3%, 14%, and 34%, respectively.

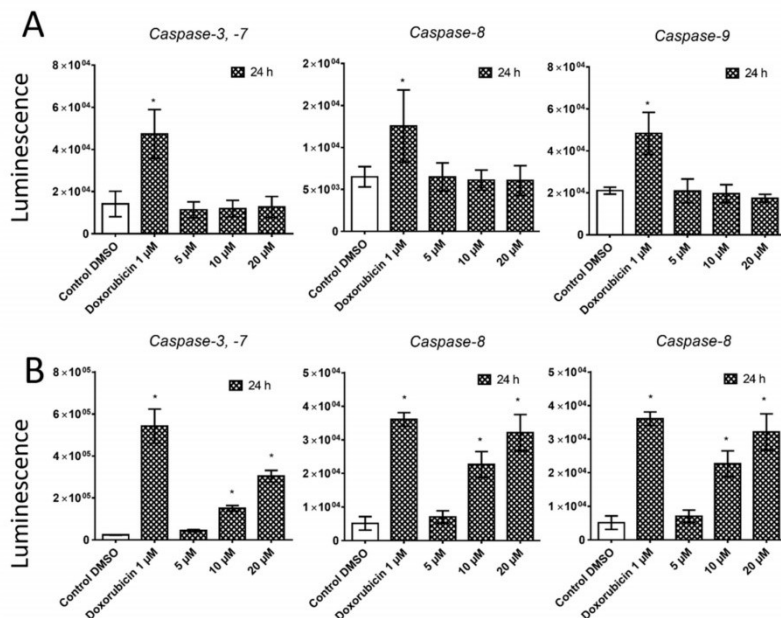


Figure 6. The effect of pancratine on the activity of caspase-3, caspase-7, caspase-8, and caspase-9 in A549 (A) and MOLT-4 (B) cells. Results are shown as the mean ± SD from three independent experiments. * Significantly different to the control ($p \leq 0.05$). Cells treated with 1- μ M doxorubicin were used as a positive control.

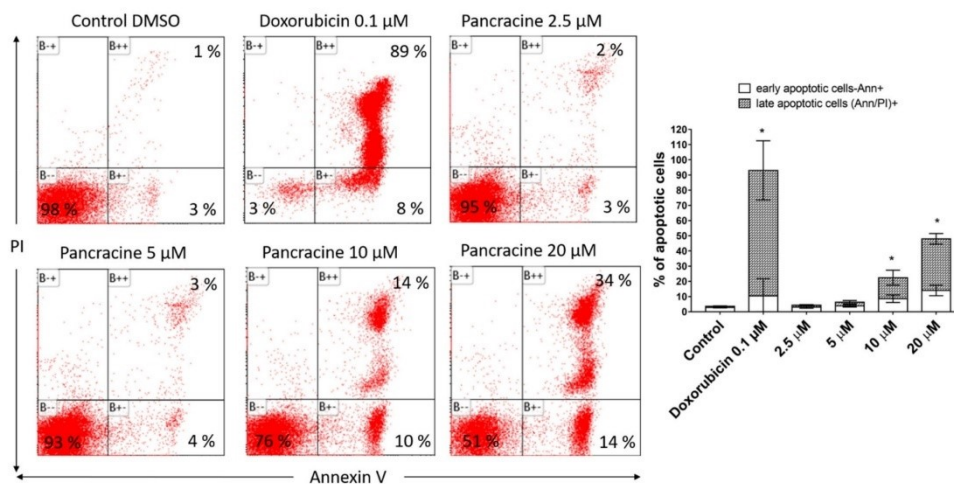


Figure 7. Induction of apoptosis in MOLT-4 leukemic cells after pancratine treatment. Apoptosis was determined by Annexin V and PI staining 24 h after treatment. Representative histograms of one of three independent measurements are shown. Doxorubicin at a 0.1- μ M dose was used as a positive control. The bar graph represents the percentage of early and late apoptotic cells detected by flow cytometry (mean ± SD, $n = 3$). * Significantly different to the control for early and late apoptotic cells ($p \leq 0.05$).

2.4. G1/S Arrest in A549 Is Associated with the Akt/p27/pRb Signaling Pathway and the Proapoptotic Activity in MOLT-4 Is Associated with Upregulation of p53 Phosphorylated at Serine 392

Based on previous results, we were interested in the detection of proteins that orchestrate cell cycle redistribution and apoptosis. To investigate the expression levels of prime upstream signaling factors and their activation—namely, cell cycle checkpoint kinase 1 (Chk1), extracellular regulated kinase 1/2 (ERK1/2), p38 mitogen-activated protein kinase (MAPK), Akt protein kinase, retinoblastoma tumor suppressor protein (pRb), p53 protein, cyclin-dependent kinase inhibitor p21 and p27, and proapoptotic protein Bax, we performed electrophoresis and Western blotting.

Concerning the molecular alterations in A549 cells following pancracine application (Figure 8), the antiproliferative activity was associated with significantly altered levels of various cell cycle regulatory proteins and their activated forms. The treatment with 20- μ M pancracine for 24 h caused a significant ($p \leq 0.05$) activation of p38 MAPK through phosphorylation at Thr180 and Tyr182 and decreased phosphorylation of ERK at Thr202 and Tyr204. There was neither a considerable downregulation of Akt kinase nor p27 and pRb after 24 h of treatment, whereas greater changes in the protein levels occurred after 72 h. After 72 h of exposure, pancracine dosed at 10 μ M and higher decreased Akt kinase through phosphorylation on Thr308, significantly ($p \leq 0.05$) increased the level of p27 protein, and activated the Rb protein through hypophosphorylation at Ser807/811. Furthermore, at a prolonged exposure time of 72 h, the protein levels of ERK phosphorylated on Thr202 and Tyr204 were decreased significantly ($p \leq 0.05$) after treatment with both 10- and 20- μ M pancracine, while increased the phosphorylation of p38 MAPK at Thr180 and Tyr182 shifts towards a lower 10- μ M dose of pancracine. In contrast, pancracine had no effect on the levels of p53 and p21 during the entire treatment period (Supplementary Figure S1).

To clarify the mechanism of pancracine-induced apoptosis, the expression of apoptosis-related proteins in MOLT-4 cells was determined at 4 h post-treatment using 5- and 10- μ M concentrations. As shown in Figure 9, the apoptosis-inducing effect of pancracine at 5 μ M was accompanied by a statistically significant ($p \leq 0.05$) upregulation of p53 phosphorylated at Ser392. Since Ser392 phosphorylated p53 is known to be involved in the transduction of death signals, the observed increase in the amount of Bax protein correlates well. Cell cycle arrest at G1/S-phase transition occurs by the activation of inhibitors of cyclin-dependent kinases p21 and p27, which were upregulated in MOLT-4 under the same treatment (5 μ M) conditions. In line with the revealed apoptosis induction, proapoptotic p38 MAPK was phosphorylated at Thr180 and Tyr182 in a dose-dependent manner, reaching significant ($p \leq 0.05$) values with 10- μ M pancracine. Reduced levels of proteins p21, p27, and p53 phosphorylated on Ser392 after 10 μ M of treatment are probably due to the increased cell death of leukemic cells.

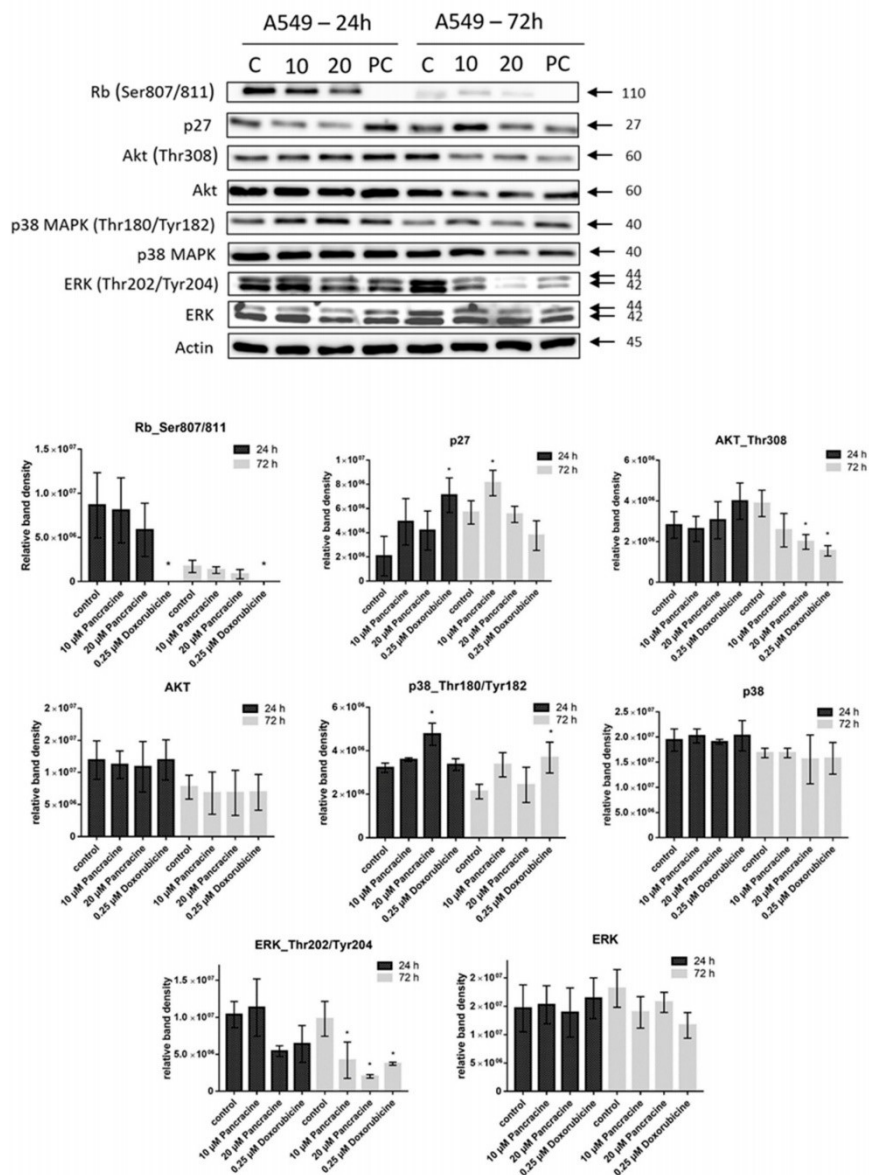


Figure 8. Western blot analysis of the proteins that regulate cell cycle progression, cell death, or cell survival in non-small cell lung adenocarcinoma A549 cells upon a treatment with either 10 μM or 20 μM of pancratine for 24 and 72 h. Control cells were mock-treated with 0.1% DMSO, indicated as C, and 0.25- μM doxorubicin-treated cells were used as a positive control, indicated as PC. Arrows indicate the molecular weights of proteins. The amount of selected proteins in bands was determined by densitometry. The quantitative data are shown as the relative intensity of each protein band in arbitrary units. These experiments were performed at least three times with similar results, and a cropped blot is shown from one representative experiment. Data are presented as the mean values \pm SD, $n = 3$. * Significantly different to the control ($p \leq 0.05$).

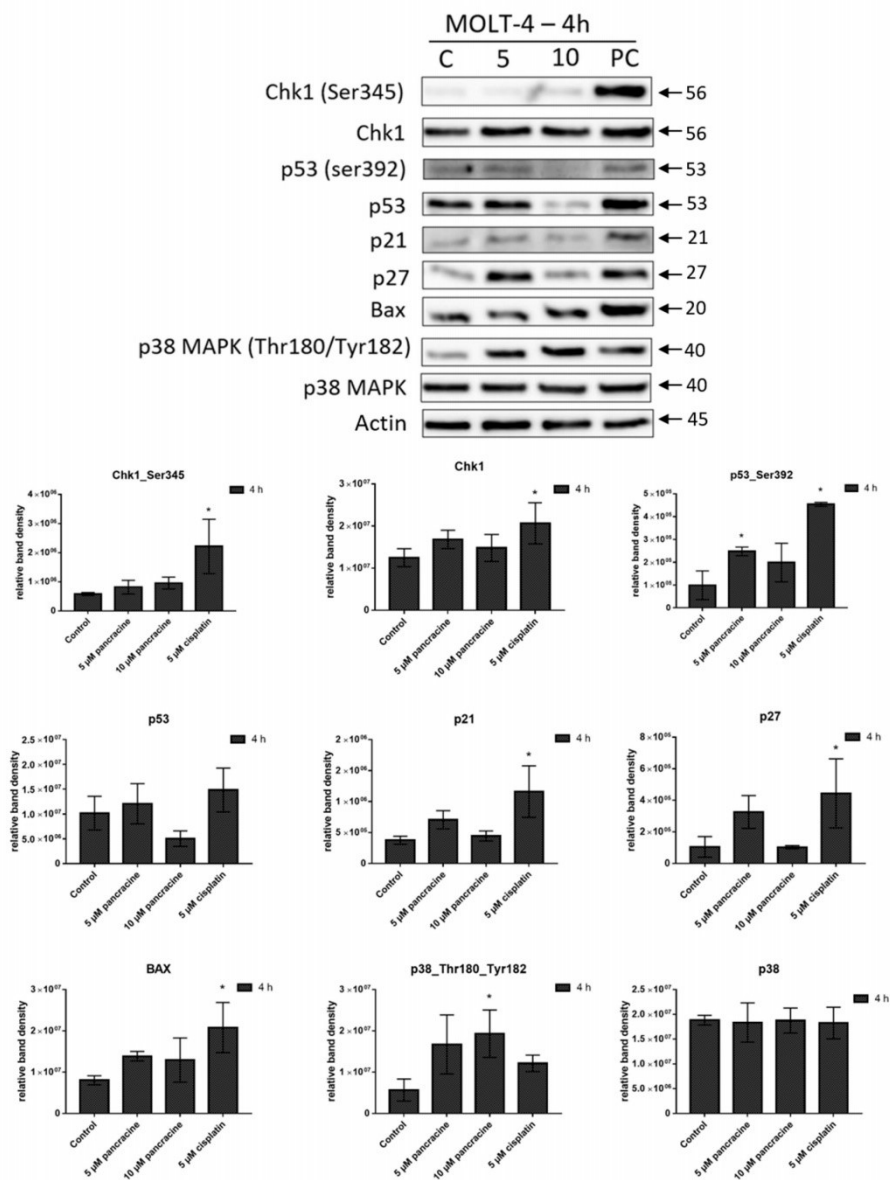


Figure 9. Western blot analysis of the proteins that regulate cell cycle progression, cell death, or cell survival in leukemic MOLT-4 cells upon treatment with either 5 μM or 10 μM of pancratine for 4 h. Control cells were mock-treated with 0.1% DMSO, indicated as C, and 5- μM cisplatin-treated cells were used as a positive control, indicated as PC. Arrows indicate the molecular weights of proteins. The amount of proteins in bands was determined by densitometry. The quantitative data are shown as the relative intensity of each protein band in arbitrary units. These experiments were performed at least three times with similar results, and a cropped blot is shown from one representative experiment. Data are presented as the mean values \pm SD, $n = 3$. * Significantly different to the control ($p \leq 0.05$).

3. Discussion

The unique chemical structure of montanine alkaloids, with their significant biological activity, together with their rarity in nature, has led to a synthetic effort to produce ample amounts for biological studies and subsequent use in clinical therapy [15–21]. This also includes the preparation of montanine-type alkaloids by rearrangement of the haemantamine-type ring system [21,22]. Unfortunately, without understanding the molecular mechanisms of their actions, it is not possible to take advantage of their promising biological activity over other AAs. If we focus on the anticancer potential of montanine alkaloids, only the IC₅₀ values have been available so far, with pancracine having values from 2.29 ± 0.43 μM to 5.15 ± 0.34 μM, using tumor cells derived from A549 (lung adenocarcinoma), HT-29 (colon adenocarcinoma), A2780 (ovarian carcinoma), HeLa (cervix carcinoma), MCF-7 (breast carcinoma), SAOS-2 (osteosarcoma), Jurkat (acute T-cell leukemia), and MOLT-4 (acute lymphoblastic leukemia) [6]. The IC₅₀ values in the low-micromolar range were found to correspond closely to those found in an earlier study published by Cedrón et al. [9], which described the cytotoxic effect of pancracine on tumor cells with IC₅₀ values ranging from 4.3 ± 0.7 μM to 9.1 ± 1.0 μM. Montanine, which is the main representative of this group of substances, seems to be more active than pancracine, because its IC₅₀ values ranged from 1.04 ± 0.14 μM to 2.30 ± 0.45 μM in the study of Al Shammari et al. [23]. Since pancracine differs from montanine by only one substituent on the E ring of the 5,11-methanomorphanthridine structure, it can be hypothesized that the molecular mechanism of action of these substances may be similar.

By selecting one apoptosis-resistant cancer cell line and one apoptosis-sensitive leukemia cell line as an experimental model counterpart, the aim of this study was to approximate the effect of pancracine on these cells, including events that lead to either cell cycle perturbation or apoptosis.

The A549 cancer cell line represents non-small cell lung cancer (NSCLC) with very poor prognosis and with high chemoresistance to the standard cytotoxic drug treatments. Considering the IC₅₀ values of pancracine for A549 cells (2.29 ± 0.43 μM) [6], the strong antiproliferative effect of this compound on the A549 cancer cell line determined in this study by a real-time cell monitoring method is fully consistent with the previous findings. This growth inhibitory effect persists for 96 h. We extended this real-time cell proliferation measuring with the end-point Trypan blue exclusion test. A statistically significant antiproliferative effect on A549 cells was already demonstrated using a concentration of 2.5 mM at all time intervals (24, 48, and 72 h). The impact on cell viability of the A549 cells was negligible, as concentrations up to 20 μM failed to reduce the A549 viability below 80%. According to the real-time cell monitoring method, a 50-μM concentration of pancracine seemed to be lethal for A549 cancer cells. Cell cycle arrest at the G1/S transition occurs by the activation of several signaling pathways. One of these acts through the activation of MAPK systems by the phosphorylation of p38 MAPK, which phosphorylates several nuclear factors, such as tumor suppressor p53, activating transcription factor ATF-2, myocyte enhancer factor MEF-2, and transcription factor Myc [24]. Another possibility is signaling through the Akt kinase. The phosphorylated pAkt kinase inhibits the p27 protein [25]. p27 is a tumor suppressor that inhibits the phosphorylation of Rb by inhibition of the cyclin-dependent kinase (CDK) complex and, as a result, prevents the separation of transcription factor E2F from Rb, which, in total, prevents the transcription of genes required for G1/S transition [25]. Our results show that the proliferation of A549 cells is inhibited by cell cycle arrest in the G1 phase through the upregulation of phosphorylated p38 MAPK after 24 h and either a 10- or 20-μM pancracine treatment. Cell cycle arrest initiated through the downregulation of phosphorylated pRb protein, upregulation of p27 concomitantly with the downregulation of Akt kinase phosphorylated on Thr308, and downregulation of ERK was observed after a longer time interval (72 h) using the same experimental conditions. Besides, apoptosis is not induced at the cellular level, as proved by the activity of caspase-3/7, -8, and -9 in A549 cells. For a better overview, Figure 10 shows the schematic representation

of proposed AKT/p27/pRb upstream signaling events involved in the antiproliferative activity of pancracine against A549 lung adenocarcinoma cells.

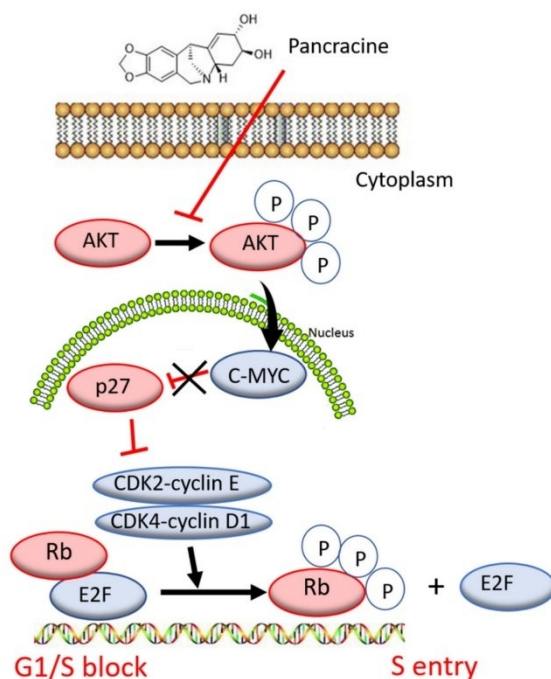


Figure 10. Proposed signaling pathway involved in the action of pancracine in A549 cells.

MOLT-4 is a T-lymphoblastic cell line originally derived from the peripheral blood of a 19-year-old patient with acute lymphoblastic leukemia in relapse. These cells responded to pancracine treatment with a half-maximal inhibitory concentration (IC_{50}) of $2.71 \pm 0.25 \mu\text{M}$ [6]. A similar strong antiproliferative effect as that seen on A549 cells was observed after the pancracine treatment of MOLT-4 cells. However, unlike in the A549 cell line, a significant strong activity in decreasing the viability of leukemic cells was observed. The viability of MOLT-4 cells decreased, even after treatment with $2.5\text{-}\mu\text{M}$ pancracine, and treatment with the higher dose of $20 \mu\text{M}$ led to a decrease of viable cells down to 20%. Due to the greater potency of pancracine with decreasing viability rates at higher concentrations, only the lower concentrations of 2.5, 5, and $10 \mu\text{M}$ after 24 h and 2.5 and $5 \mu\text{M}$ after 48 h of treatment could be used to detect the percentage of leukemic MOLT-4 cells in the cell cycle. Several publications showed that leukemic cells undergo apoptotic cell death [26–28]. MOLT-4 cells die due to ionizing radiation and other DNA damage-inducing agents by the apoptotic process of the activation of caspase-8 and -9 and release of cytochrome c [27]. In this study, the leukemic MOLT-4 cells died due to apoptosis activation at $5 \mu\text{M}$, increasing the activity of effector caspase-3/7 and the activation of caspase-9 responsible for the mitochondrial apoptosis pathway and caspase-8 responsible for the pathway through death receptors. The apoptosis of MOLT-4 cells significantly increased 24 h after the exposure to a $10\text{-}\mu\text{M}$ dose of pancracine, as detected using Annexin V and PI staining. Using a concentration of $20 \mu\text{M}$, 50% of the cells were either in the early or late phase of apoptosis. Activation of the ATM/Chk2/p53 signaling pathway was described in MOLT-4 cells after ionizing radiation exposure [29]. Additionally, the cytotoxic effect of valproic acid is accompanied by the activation of p21 and upregulation

of p53 phosphorylated on Ser392 [28]. In our study, the significant apoptosis-inducing effect of pancracine was accompanied by the signaling pathway, including an increase of p27 protein, Bax, and activation of p38 MAPK through phosphorylation at Thr180 and Tyr182, and seemed to be activated by the upregulation of p53 phosphorylated at Ser392.

As far as we know, a study of the molecular mechanism of action of montanine-type AA has not yet been published, but when considering the biosynthesis of this group of alkaloids, one can consider other AA with similar structures. Haemantamine, with its α -crinane structure, also belongs to the isoquinoline group of Amaryllidaceae alkaloids, and its activity has been recently reviewed [3]. Haemantamine, even at a dose of 5 μ M, also induced apoptosis in p53-deficient acute T-cell leukemia Jurkat cells [14]. In addition, alkaloids based on the montanine skeleton can be prepared by a rearrangement of the haemantamine (α -crinane)-type ring system [21,22]. The mechanism of action of haemantamine lies in the targeting of the A-site cleft on the large ribosomal subunit and rearranging rRNA to halt the elongation phase of translation, which leads to repressing cancer cell growth [30].

In conclusion, the later stages of preclinical testing of new chemotherapeutics have always preceded a deeper knowledge of the molecular mechanisms of their cytostatic and cytotoxic activity. Pancracine, with its strong inhibitory effect on tumor cell proliferation and viability, may be one of the potential pharmacophore scaffolds in cancer therapy. Additionally, this initial pilot study presented here attempts to open a more detailed study of the mechanisms of action of montanine-type AA.

4. Materials and Methods

4.1. Cell Culture and Culture Conditions

Experiments were performed with selected human tumor cell lines MOLT-4 (acute lymphoblastic leukemia), A549 (lung adenocarcinoma), A2780 (ovarian carcinoma), MCF-7 (breast adenocarcinoma), and HepG2 (hepatocellular carcinoma), which were purchased from the European Collection of Cell Cultures (ECACC, Salisbury, UK) and cultured in accordance with the provider's culture method guidelines. All cell lines were maintained under standard cell culture conditions at 37 °C in a humidified incubator in an atmosphere of 5% CO₂ and 95% air. Cells were passaged every 2 to 3 days to obtain exponential growth. Cells in the maximum range of 20 passages were used for this study.

4.2. Cell Treatment

Pancracine (purity > 95%) was provided by the ADINACO Research Group from the Department of Pharmaceutical Botany, Faculty of Pharmacy in Hradec Kralove, Charles University, Hradec Kralove, Czech Republic. Results of the ¹H-NMR, HPLC/UV, and GC/MS analyses are shown in Supplementary Figures S2–S4. The compound was isolated from fresh bulbs of *Narcissus* L. cv. Professor Einstein (Amaryllidaceae) within a detailed phytochemical study [5]. Fresh stock solutions of pancracine in concentrations of 50 mM were dissolved in dimethyl sulfoxide (DMSO) (Sigma-Aldrich, St. Louis, MO, USA). Stock solutions were freshly prepared before use. For the experiments, the stock solutions were diluted with the complete culture medium to create final concentrations of 1–50 μ M (50 μ M is the highest concentration used in xCELLigence measurements), making sure that the concentration of DMSO was <0.1% to avoid toxic effects on the cells. Negative control cells were sham-treated with a DMSO vehicle only (0.1%; control). Cells treated with 5% DMSO; cisplatin (Sigma-Aldrich, St. Louis, MO, USA) at 5 μ M; or doxorubicin (Sigma-Aldrich, St. Louis, MO, USA) at 0.25 nM, 0.25 μ M, and 1 μ M were used as a positive control.

4.3. Screening for Antiproliferative Activity Using the xCELLigence System

The xCELLigence system (Roche, Basel, Switzerland and ACEA Biosciences, San Diego, CA, USA) was used to monitor cell adhesion, proliferation, and cytotoxicity. It was connected and tested by a resistor plate before the RTCA single-plate station was placed inside the incubator at 37 °C with an atmosphere containing 5% CO₂. First, the

seeding concentration for the experiments was optimized for each cell line. After seeding, the respective number of cells in 190 μ L of medium per well of the E-plate 96 and the proliferation, attachment, and spreading of the cells were monitored every 30 min by the xCELLigence system. Approximately 24 h after seeding, when the cells were in the log growth phase, they were exposed in triplicates to 10 μ L of sterile deionized water containing pancracine to obtain final concentrations of 1–50 μ M. Controls received sterile deionized water + DMSO with a final concentration of 0.1%. Cells treated with 5% DMSO were used as a positive control. Growth curves were normalized to the time point of treatment. Evaluations were performed using xCELLigence 1.2.1 software (Roche, Basel, Switzerland and ACEA Biosciences, San Diego, CA, USA).

4.4. Proliferation and Viability Measurement Using Trypan Blue Exclusion Test

Cell proliferation and viability of MOLT-4 and A549 cells were monitored 24, 48, and 72 h after treatment with 2.5, 5, 10, and 20 μ M of pancracine in the case of A549 cells (1.5×10^5 cell in 5 mL placed in 25-cm² Falcon flasks) and 24 and 48 h in the case of MOLT-4 cells (1×10^6 cell in 5 mL placed in 25-cm² Falcon flasks) with the same concentration range of pancracine. Cells treated with 0.25- μ M doxorubicin were used as a positive control. Cell membrane integrity was determined using the Trypan blue exclusion technique—mixing 10 μ L of 0.4% Trypan blue and 10 μ L of cell suspension. The Trypan blue dye exclusion test is used to determine the percentage of viable cells and number of viable cells present in a cell suspension. It is based on the principle that live cells possess intact cell membranes that exclude certain dyes, such as Trypan Blue, whereas dead cells do not. The assay is easy to perform; a cell suspension is mixed with dye and then visually examined by microscope to determine whether cells take up or exclude the dye. Then, the individual cells are observed using a bright-field Nikon Eclipse E200 light microscope (Nikon, Tokyo, Japan); a viable cell will have a clear cytoplasm, whereas a nonviable cell will have a blue cytoplasm. In this assay, a hemocytometer (Bürker counting chamber) was used to determine exactly the number of cells in a suspension. We counted 25 squares (=1 horizontal line + 1 vertical line + 1 square). We counted only cells that were within the 0.2 mm \times 0.2 mm squares. We did not count cells that overlapped over the border. The surface of each square was 0.2 mm \times 0.2 mm = 0.04 mm². With a height of 0.1 mm, the volume was 0.004 mm³. Therefore, 25 squares corresponded to a volume of 0.1 mm³ (=0.1 μ L). Multiplication by 10,000 gave 1 mL. The calculation of proliferation in % followed this formula: (number of viable cells after treatment/number of viable cells in control DMSO) multiplied by 100. The calculation of viability in % followed this formula: (number of viable cells after treatment/number of total cells) multiplied by 100.

4.5. Cell Cycle Distribution and Internucleosomal DNA Fragmentation Analysis

The cells were washed with ice-cold PBS and fixed with 70% ethanol. In order to detect low molecular weight fragments of DNA, the cells were incubated for 5 min at room temperature in a buffer (192 mL of 0.2-M Na₂HPO₄ + 8 mL of 0.1-M citric acid, pH 7.8) and then labeled with propidium iodide in Vindelov's solution for 1 h at 37 °C. The DNA content was determined using a CyAn flow cytometer (Beckman Coulter, Miami, FL, USA) with an excitation wavelength of 488 nm. The data were analyzed using Multicycle AV software (Phoenix Flow Systems, San Diego, CA, USA).

4.6. Activity of Caspases

The induction of programmed cell death was determined by monitoring the activities of caspases-3/7, caspase-8, and caspase-9 by Caspase-Glo Assays (Promega, Madison, WI, USA) 24 h after treatment with 5, 10, and 20 μ M of pancracine. Cells treated with 1 μ M of doxorubicin were used as a positive control. The assay provides a proluminescent substrate in an optimized buffer system. The addition of a Caspase-Glo Reagent results in cell lysis, followed by caspase cleavage of the substrate and the generation of a luminescent signal. A total of 1×10^4 cells were seeded per well using a 96-well plate format (Sigma-Aldrich,

St. Louis, MO, USA). After treatment, the Caspase-Glo Assay Reagent was added to each well (50 μ L/well) and incubated for 30 min before luminescence was measured using a Tecan Infinite M200 microplate reader (Tecan Group, Männedorf, Switzerland).

4.7. Analysis of Apoptosis

Apoptosis was determined by flow cytometry using an Alexa Fluor[®]488 Annexin V/Dead Cell Apoptosis kit (Life Technologies, Grand Island, NY, USA) in accordance with the manufacturer's instructions. The Alexa Fluor[®]488 Annexin V/Dead Cell Apoptosis kit employs the property of Alexa Fluor[®]488 conjugated to Annexin V to bind to phosphatidylserine in the presence of Ca^{2+} , and the ability of propidium iodide (PI) to enter cells with damaged cell membranes and bind to DNA. Measurements were performed immediately using a CytoFLEX LX flow cytometer (Beckman Coulter, Miami, FL, USA). List mode data were analyzed using Kaluza Analysis 2.1 software (Beckman Coulter, Miami, FL, USA).

4.8. Western Blot Analysis

Whole-cell lysates (Cell Lysis Buffer; Cell Signaling Technology, Danvers, MA, USA) were prepared 24 and 72 h following the treatment of A549 with 10 μ M and 20 μ M of pancracine and 4 h following the treatment of MOLT-4 cells with 5 μ M and 10 μ M of pancracine. Cells treated with 0.1% DMSO were used as a negative control. Cells treated with either 5 μ M of cisplatin or 0.25 μ M of doxorubicin were used as a positive control. Quantification of the protein content was performed using the BCA assay (Sigma-Aldrich, St. Louis, MO, USA). The lysates (20 μ g of purified protein) were loaded into lanes of polyacrylamide gel. After electrophoresis separation, the proteins were transferred to a PVDF membrane (Bio-Rad, Hercules, CA, USA). Any nonspecific bindings of the membranes were blocked for 1 h in a Tris-buffered saline (TBS) containing 0.05% Tween 20 and 5%, *w/v*, nonfat dry milk. The membranes were washed in TBS. Incubation with a primary antibody against specific antigens and at the appropriate dilutions (1:1000 Chk1, 1:1000 Chk1_serine 345—Cell Signalling, Danvers, MA, USA; 1:1000 Rb, 1:1000 Rb_serine 807/811—Cell Signalling, Danvers, MA, USA; 1:10,000 β -actin—Sigma-Aldrich, St. Louis, MO, USA; 1:1000 ERK, 1:1000 ERK $\frac{1}{2}$ _threonine 202 and tyrosine 204—Cell Signalling, Danvers, MA, USA; 1:1000 p53 and 1:1000 p53_serine 392—Exbio, Prague, Czech Republic; 1:1000 p53_serine 15—Cell Signalling, Danvers, MA, USA; 1:1000 p21—Cell Signalling, Danvers, MA, USA; 1:1000 p27—Cell Signalling, Danvers, MA, USA; 1:1000 Akt and 1:1000 Akt_threonine 308—Cell Signalling, Danvers, MA, USA; 1:1000 p38, 1:1000 p38_threonine 180, and tyrosine 182—Cell Signalling, Danvers, MA, USA; and 1:1000 Bax—Cell Signalling, Danvers, MA, USA) was performed at 4 °C overnight. The following day, the membranes were washed 5 times with TBS, each time for 5 min, and once with TBS for 10 min and then incubated with an appropriate secondary antibody (DakoCytomation, Glostrup, Denmark, or Cell Signalling, Danvers, MA, USA) in a dilution of 1:1000 for 1 h at room temperature. Band detection was performed using a chemiluminescence detection kit (Roche, Basel, Switzerland). To ensure equal protein loading, each membrane was reprobed, and β -actin was detected. The densities of the proteins of interest were analyzed using the GeneTools image analysis system (Syngene, Cambridge, UK).

4.9. Statistical Analysis

The descriptive statistics of the results were calculated and the charts made using either Microsoft Office 365 Excel (Microsoft, Redmond, WA, USA) or GraphPad Prism 7 biostatistics (GraphPad Software, La Jolla, CA, USA) software. In this study, all the values were expressed as arithmetic means with SD of triplicates unless otherwise noted. For quantitative data, normality testing was performed to assess whether parametric or nonparametric tests should be used. For experiments with parametric variables, one-way analysis of variance (ANOVA) followed by post-hoc Dunnett's test was used to compare

the mean values among different groups, with a *p*-value less than 0.05 considered as statistically significant.

Supplementary Materials: The following are available online at <https://www.mdpi.com/article/10.3390/ijms22137014/s1>.

Author Contributions: R.H., M.Ř. and L.C.: conceptualization, funding acquisition, investigation, editing, and supervision. K.B., D.M., E.P., K.K., D.K. and R.H.: performing experiments. D.K. and R.H.: data analysis and manuscript writing. All authors have read and agreed to the published version of the manuscript.

Funding: This project reg. No. CZ.02.1.01/0.0/0.0/18_069/0010046: the Pre-application research into innovative medicines and medical technologies project, was co-funded by the European Union. This study was also supported in part by the Grant Agency of Charles University Progress/UK Q40/01 and SVV-260543/2020 of the Charles University.

Data Availability Statement: The descriptive statistics of the results were calculated and the charts made using either Microsoft Office 365 Excel (Microsoft, Redmond, WA, USA) or GraphPad Prism 7 biostatistics (GraphPad Software, La Jolla, CA, USA) software. In this study, all the values were expressed as arithmetic means with SD of triplicates, unless otherwise noted. For quantitative data, normality testing was performed to assess whether parametric or nonparametric tests should be used. For experiments with parametric variables, one-way analysis of variance (ANOVA), followed by post-hoc Dunnett's test was used to compare the mean values among different groups, with a *p*-value less than 0.05 considered as statistically significant.

Acknowledgments: The skillful technical assistance of Nadezda Mazankova and Bozena Janska is greatly acknowledged. The authors thank Gerald Blunden for proofreading the manuscript.

Conflicts of Interest: The authors declare that there are no conflict of interest.

Abbreviations

AA	Amaryllidaceae alkaloid
BCA	bicinchoninic acid
Chk1	Checkpoint kinase 1
DMSO	dimethyl sulfoxide
ECACC	European Collection of Cell Cultures
ERK	extracellular signal-regulated kinase
IC ₅₀	half maximal inhibitory concentration
p53	tumor suppressor protein p53
p21	inhibitor of cyclin dependent kinase
p27	inhibitor of cyclin dependent kinase
PI	propidium iodide
PVDF	polyvinylidene difluoride
Akt	protein kinase B
RTCA	real-time cell analysis
SD	standard deviation
TBS	Tris-buffered saline

References

- Newman, D.J.; Cragg, G.M. Natural products as sources of new drugs over the 30 years from 1981 to 2010. *J. Nat. Prod.* **2012**, *75*, 311–335. [[CrossRef](#)]
- Desgagné-Penix, I. Biosynthesis of alkaloids in Amaryllidaceae plants: A review. *Phytochem. Rev.* **2021**, *20*, 409–431. [[CrossRef](#)]
- Cahlíková, L.; Kawano, I.; Řezáčová, M.; Blunden, G.; Hulcová, D.; Havelek, R. The Amaryllidaceae alkaloids haemanthamine, haemanthidine and their semisynthetic derivatives as potential drugs. *Phytochem. Rev.* **2021**, *20*, 303–323. [[CrossRef](#)]
- Wildman, W.C.; Brown, C.L. Mass spectra of 5,11-methanomorphanthridine alkaloids. The structure of pancracine. *J. Am. Chem. Soc.* **1968**, *90*, 6439–6446. [[CrossRef](#)]

5. Govindaraju, K.; Ingels, A.; Hasan, M.N.; Sun, D.; Mathieu, V.; Masi, M.; Evidente, A.; Kornienko, A. Synthetic analogues of the montanine-type alkaloids with activity against apoptosis-resistant cancer cells. *Bioorg. Med. Chem. Lett.* **2018**, *28*, 589–593. [[CrossRef](#)] [[PubMed](#)]
6. Breiterová, K.; Koutová, D.; Maříková, J.; Havelek, R.; Kuneš, J.; Majorošová, M.; Opletal, L.; Hošťálková, A.; Jenco, J.; Rezáčová, M.; et al. Amaryllidaceae alkaloids of different structural types from *Narcissus* L. cv. Professor Einstein and their cytotoxic activity. *Plants* **2020**, *9*, 137. [[CrossRef](#)] [[PubMed](#)]
7. Wildman, W.C.; Kaufman, C.J. Alkaloids of the Amaryllidaceae. III. Isolation of five new alkaloids from *Haemanthus* species1. *J. Am. Chem. Soc.* **1955**, *77*, 1248–1252. [[CrossRef](#)]
8. Koutová, D.; Maafi, N.; Havelek, R.; Opletal, L.; Blunden, G.; Rezáčová, M.; Cahlíková, L. Chemical and biological aspects of montanine-type alkaloids isolated from plants of the *Amaryllidaceae* family. *Molecules* **2020**, *25*, 2337. [[CrossRef](#)]
9. Cedrón, J.C.; Ravelo, A.G.; León, L.G.; Padrón, J.M.; Estévez-Braun, A. Antiproliferative and structure activity relationships of Amaryllidaceae alkaloids. *Molecules* **2015**, *20*, 13854–13863. [[CrossRef](#)] [[PubMed](#)]
10. Masi, M.; van Slambrouck, S.; Gunawardana, S.; van Rensburg, M.J.; James, P.C.; Mochel, J.G.; Heliso, P.S.; Albalawi, A.S.; Cimmino, A.; van Otterlo, W.A.L.; et al. Alkaloids isolated from *Haemanthus humilis* Jacq., an indigenous South African Amaryllidaceae: Anticancer activity of coccinine and montanine. *S. Afr. J. Bot.* **2019**, *126*, 277–281. [[CrossRef](#)]
11. Evidente, A.; Andolfi, A.; Abou-Donia, A.H.; Touema, S.M.; Hammada, H.M.; Shawky, E.; Motta, A. (–)-Amarbellisine, a lycorine-type alkaloid from *Amaryllis belladonna* L. growing in Egypt. *Phytochemistry* **2004**, *65*, 2113–2118. [[CrossRef](#)]
12. Labraña, J.; Machocho, A.K.; Kricsfalussy, V.; Brun, R.; Codina, C.; Viladomat, F.; Bastida, J. Alkaloids from *Narcissus angustifolius* subsp. *transcarpathicus*. *Phytochemistry* **2002**, *60*, 847–852. [[CrossRef](#)]
13. Habartová, K.; Cahlíková, L.; Rezáčová, M.; Havelek, R. The biological activity of alkaloids from the *Amaryllidaceae*: From cholinesterases inhibition to anticancer activity. *Nat. Prod. Commun.* **2016**, *11*, 1587–1594. [[CrossRef](#)] [[PubMed](#)]
14. Havelek, R.; Seifrtová, M.; Královec, K.; Bručková, L.; Cahlíková, L.; Dalecká, M.; Vávrová, J.; Rezáčová, M.; Opletal, L.; Bilková, Z. The effect of *Amaryllidaceae* alkaloids Haemanthamine and Haemanthidine on cell cycle progression and apoptosis in p53-negative human leukemic Jurkat cells. *Phytomedicine* **2014**, *21*, 479–490. [[CrossRef](#)]
15. Guan, Y.; Zhang, H.; Pan, C.; Wang, J.; Huang, R.; Li, Q. Flexible synthesis of montanine-like alkaloids: Revisiting the structure of montabuphine. *Org. Biomol. Chem.* **2012**, *10*, 3812–3814. [[CrossRef](#)]
16. Matveenko, M.; Banwell, M.G.; Willis, A.C. A chemoenzymatic total synthesis of the structure assigned to the alkaloid (+)-montabuphine. *Org. Lett.* **2008**, *10*, 4693–4696. [[CrossRef](#)]
17. Ishizaki, M.; Hoshino, O.; Iitaka, Y. Total synthesis of montanine-type Amaryllidaceae alkaloids, which possess a 5, 11-methanomorphanthridine ring system, through cyclization with sodium bis (2-methoxyethoxy) aluminum hydride (SMEAH): The first stereoselective total syntheses of (±)-montanine, (±)-coccinine, (±)-O-acetylmontanine, (±)-pancracine, and (±)-brunsvigine. *J. Org. Chem.* **1992**, *57*, 7285–7295.
18. Bao, X.; Cao, Y.X.; Chu, W.D.; Qu, H.; Du, J.Y.; Zhao, X.H.; Ma, X.Y.; Wang, C.T.; Fan, C.A. Bioinspired total synthesis of montanine-type Amaryllidaceae alkaloids. *Angew. Chem. Int. Edit.* **2013**, *52*, 14167–14172. [[CrossRef](#)]
19. Hong, A.W.; Cheng, T.H.; Raghukumar, V.; Sha, C.K. An expedient route to montanine-type Amaryllidaceae alkaloids: Total syntheses of (–)-brunsvigine and (–)-manthine. *J. Org. Chem.* **2008**, *73*, 7580–7585. [[CrossRef](#)]
20. Pandey, G.; Gadre, S.R. Stereoselective construction of 5,11-methanomorphanthridine and 5,10b-phenanthridine structural frameworks: Total syntheses of (±)-pancracine, (±)-brunsvigine, (±)-maritidine, and (±)-crinine. *Pure Appl. Chem.* **2012**, *84*, 1597–1619. [[CrossRef](#)]
21. Inubushi, Y.; Fales, H.M.; Warnhoff, E.W.; Wildman, W.C. Structures of montanine, coccinine, and manthine. *J. Org. Chem.* **1960**, *25*, 2153–2164. [[CrossRef](#)]
22. Cedrón, J.C.; Estévez-Braun, A.; Ravelo, A.; Gutiérrez, D.; Flores, N.; Bucio, M.A.; Pérez-Hernández, N.; Joseph-Nathan, P. Bioactive montanine derivatives from halide-induced rearrangements of haemanthamine-type alkaloids. Absolute configuration by VCD. *Org. Lett.* **2009**, *11*, 1491–1494. [[CrossRef](#)]
23. Al Shammari, L.; Al Mamun, A.; Koutová, D.; Majorošová, M.; Hulcová, D.; Šafratová, M.; Breiterová, K.; Maříková, J.; Havelek, R.; Cahlíková, L. Alkaloid profiling of *Hippeastrum* cultivars by GC-MS, isolation of *Amaryllidaceae* alkaloids and evaluation of their cytotoxicity. *Rec. Nat. Prod.* **2020**, *14*, 154–159. [[CrossRef](#)]
24. Ambrosino, C.; Nebreda, A.R. Cell cycle regulation by p38 MAP kinases. *Biol. Cell* **2001**, *93*, 47–51. [[CrossRef](#)]
25. Abbastabar, M.; Kheyrollah, M.; Azizian, K.; Bagherlou, N.; Tehrani, S.S.; Maniati, M.; Karimian, A. Multiple functions of p27 in cell cycle, apoptosis, epigenetic modification and transcriptional regulation for the control of cell growth: A double-edged sword protein. *DNA Repair* **2018**, *69*, 63–72. [[CrossRef](#)] [[PubMed](#)]
26. Šalovská, B.; Janečková, H.; Fabrik, I.; Karlíková, R.; Čecháková, L.; Ondrej, M.; Link, M.; Friedecký, D.; Tichý, A. Radio-sensitizing effects of VE-821 and beyond: Distinct phosphoproteomic and metabolomic changes after ATR inhibition in irradiated MOLT-4 cells. *PLoS ONE* **2018**, *13*, e0199349. [[CrossRef](#)] [[PubMed](#)]
27. Tichý, A.; Zášková, D.; Pejchal, J.; Rezáčová, M.; Österreicher, J.; Vávrová, J.; Cerman, J. Gamma irradiation of human leukaemic cells HL-60 and MOLT-4 induces decrease in Mcl-1 and Bid, release of cytochrome c, and activation of caspase-8 and caspase-9. *Int. J. Radiat. Biol.* **2008**, *84*, 523–530. [[CrossRef](#)]
28. Muthna, D.; Vavrova, J.; Lukasova, E.; Tichy, A.; Knizek, J.; Kohlova, R.; Mazankova, N.; Rezacova, M. Valproic acid decreases the reparation capacity of irradiated MOLT-4 cells. *Mol. Biol.* **2012**, *46*, 110–116. [[CrossRef](#)]

29. Řezáčová, M.; Tichý, A.; Vávrová, J.; Vokurková, D.; Lukášová, E. Is defect in phosphorylation of Nbs1 responsible for high radiosensitivity of T-lymphocyte leukemia cells MOLT-4? *Leuk. Res.* **2008**, *32*, 1259–1267. [[CrossRef](#)]
30. Pellegrino, S.; Meyer, M.; Zorbas, C.; Bouchta, S.A.; Saraf, K.; Pelly, S.C.; Yusupova, G.; Evidente, A.; Mathieu, V.; Kornienko, A.; et al. The Amaryllidaceae alkaloid haemanthamine binds the eukaryotic ribosome to repress cancer cell growth. *Structure* **2018**, *26*, 416–425. [[CrossRef](#)]

5 DISKUZE

Zhoubná nádorová onemocnění provází lidskou společnost od nepaměti. I přes enormní úsilí špičkových vědeckých skupin se stále nepodařilo najít konečné řešení tohoto onemocnění, jež má také výrazné socioekonomické důsledky. Široká odborná veřejnost nahlíží na nádorová onemocnění komplexněji. Dávno se opustila představa nádoru jako izolované hmoty, ale je potřeba ho vnímat v kontextu jeho mikroprostředí, včetně toho nenádorového. Současně také terapie nádorových onemocnění vyžaduje komplexní přístup a multimodální léčba, zahrnující nejen klasické léčebné metody jako je radioterapie, chemoterapie a chirurgická léčba, ale také cílenou terapii a imunoterapii, včetně podpůrné a doplňkové léčby, je mnohem efektivnější. Stále je však potřeba přistupovat inovativně i k samotným dílčím léčebným postupům, kam řadíme i možnost rozšířit dostupnou chemoterapeutickou léčbu o nová cytostatika a zdokonalovat tak možnosti konvenční protinádorové léčby (Klener a Klener 2013). S ohledem na zaměření této práce a v rovině základního výzkumu se může jednat o izolaci a identifikaci nových sloučenin rostlinného původu či přípravu polosyntetických derivátů vycházejících z látek přírodního původu. V oblasti fytochemie se jedná o detailní screening biologicky aktivních molekul, především alkaloidů, jež jsou co do struktury, tak počtu významnou a rozmanitou skupinou a všechny tyto molekuly nebyly dosud zcela plně prozkoumány, ačkoliv jejich účinky byly využívány již po staletí i v lidovém léčitelství. Čeleď Amaryllidaceae obsahující řadu významných alkaloidů právem patří k těm, které jsou tomuto screeningu podrobeny. Do této čeledi lze zařadit i isochinolinové alkaloidy montaninového typu. Jejich unikátní chemická struktura, významná biologická aktivita, ale také jejich poměrně vzácný výskyt v přírodě vedly ke zvýšenému úsilí o syntézu těchto organických molekul v dostatečném množství pro potřeby biologických studií a následné použití v klinické terapii (Guan et al. 2012, Matweenko et al. 2008, Ishizaki et al. 2002, Bao et al. 2013). Dokládá to také příprava alkaloidů montaninového typu přeskupením chemické struktury typu haemanthaminového (Inubushi et al. 1960, Cedrón et al. 2009). Bohužel bez pochopení molekulárních mechanismů jejich působení není možné využít výhody jejich slibné biologické aktivity oproti jiným alkaloidům čeledi Amaryllidaceae.

Z hlediska protinádorové léčby dokládají potenciál montaninových alkaloidů hodnoty 50 % inhibiční koncentrace IC_{50} jednoho z hlavních představitelů této skupiny látek, to je pankracinu. Hodnoty IC_{50} byly stanoveny pro nádorové buněčné linie rozmanitého histotypu, A549 (adenokarcinom plic), HT-29 (adenokarcinom tlustého střeva), A2780 (karcinom ovarií),

HeLa (karcinom děložního hrdla), MCF-7 (karcinom prsu), SAOS-2 (osteosarkom), Jurkat (akutní leukémie T-lymfocytů) a MOLT-4 (akutní lymfoblastická leukémie) a pohybovaly se v nízkém mikromolárním koncentračním rozmezí od $2,29 \pm 0,43 \mu\text{mol.l}^{-1}$ do $5,15 \pm 0,34 \mu\text{mol.l}^{-1}$. Tyto hodnoty IC_{50} naměřené naší laboratoří odpovídaly hodnotám nalezeným v dřívější studii publikované Cedronem a kol., který popsal cytotoxický účinek pankracinu na nádorové buňky s hodnotami IC_{50} v rozmezí od $4,3 \pm 0,7 \mu\text{mol.l}^{-1}$ do $9,1 \pm 1,0 \mu\text{mol.l}^{-1}$ (Cedrón et al. 2015). Cytotoxický účinek montaninu se ukázal být ještě výraznější, neboť jeho hodnoty pro stejnou paletu použitých nádorových buněčných linií, na kterých byl námi testován i účinek pankracinu, byly naměřeny v rozmezí od $1,04 \pm 0,14 \mu\text{mol.l}^{-1}$ do $2,30 \pm 0,45 \mu\text{mol.l}^{-1}$. Jelikož se pankracin liší od montaninu pouze jedním substituentem na E kruhu 5,11-methanomorfantridinové struktury (na C2 má hydroxyl místo skupiny methoxy) (Koutová et al. 2020), lze předpokládat, že molekulární mechanismus účinku těchto látek bude podobný.

Strategie *in vitro* studia molekulárního mechanismu účinku byla zahájena výběrem nádorové buněčné linie rezistentní k apoptóze a nádorové buněčné linie k apoptóze sensitivní a pomocí těchto experimentálních modelů se pokusit přiblížit účinek pankracinu včetně popisu dějů, které vedou buď k zástavě buněčného cyklu nebo k indukci apoptózy.

Nádorová buněčná linie A549 představuje nemalobuněčný karcinom plic (NSCLC) s velmi špatnou prognózou vyznačující se vůči konvenční léčbě cytostatiky vysokou chemorezistencí (Ashinuma et al. 2012, Zhang et al. 2015). Silný antiproliferační účinek pankracinu stanovený metodou měření proliferace v reálném čase je plně v souladu s dříve stanovenou hodnotou IC_{50} pro buňky A549 ($2,29 \pm 0,43 \mu\text{mol.l}^{-1}$). Inhibice růstu krom jiných testovaných buněčných linií i této rezistentní nádorové linie přetrvávala po dobu 96 h. Detekce inhibice růstu byla taktéž rozšířena o test barvení pomocí Trypanové modři, která patří mezi standardní end-point metody zjištění efektu cytostatika na viabilitu a proliferaci buněk. Statisticky významný antiproliferační účinek na buňky A549 byl prokázán již s použitím koncentrace $2,5 \mu\text{mol/l}$ a to ve všech měřených časových intervalech (24, 48 a 72 h). Dopad na viabilitu buněk A549 buněk byl zanedbatelný, jelikož ani nejvyšší měřená koncentrace $20 \mu\text{mol.l}^{-1}$ nesnížila životaschopnost buněk A549 pod 80 %. Metoda monitorování buněk v reálném čase ukázala, že koncentrace pankracinu $50 \mu\text{mol.l}^{-1}$ je pro nádorovou buněčnou linii A549 ve vztahu k proliferaci a viabilitě buněk fatální. K zastavení buněčného cyklu při přechodu G1/S fáze dochází aktivací několika signálních drah. Jeden z těchto mechanismů je řízen prostřednictvím aktivace MAP kináz konkrétně fosforylací p38 MAPK, která následně

fosforyluje řadu dalších jaderných faktorů, jako je například tumor supresorový protein p53, aktivační transkripční faktor ATF-2 (activating transcription factor-2), transkripční faktor MEF-2 (members of myocyte enhance factor-2) a transkripční faktor Myc (gen izolovaný z viru ptačí myelocytomatózy) (Ambrosino a Nebreda 2001). Další možností, jak může dojít k zastavení buněčného cyklu při přechodu z G1 do S fáze je signalizace prostřednictvím kinázy Akt. Fosforylovaná Akt kináza inhibuje protein p27 (Abbastabar et al. 2018). Tento inhibitor komplexu cyklin cyklin dependentní kinázy (Cdk) brání fosforylaci tumor supresorového proteinu Rb a v důsledku toho brání oddělení transkripčního faktoru E2F od Rb, což celkově brání transkripci požadovaných genů pro přechod G1/S (Abbastabar et al. 2018). Z našich naměřených dat vyplývá, že inhibice proliferace buněk A549 je způsobena zastavením buněčného cyklu ve fázi G1 prostřednictvím upregulace fosforylované MAPK p38 po 24 h od ovlivnění pankracinem v koncentraci 10 nebo 20 $\mu\text{mol.l}^{-1}$. Zastavení buněčného cyklu způsobené výše zmíněnými mechanismy, tedy downregulací fosforylovaného proteinu pRb, upregulací p27 souběžně s hypofosforylací Akt kinázy fosforylované na Thr308 a rovněž také downregulace MAP kinázy ERK, bylo pozorováno v delším časovém intervalu (72 h) za použití stejných experimentálních podmínek. Tyto děje nevedly k iniciaci apoptózy, jak je zřejmé z kvantifikace aktivity kaspáz -3/7, -8 a -9 v buňkách A549 po aplikaci pankracinu.

MOLT-4 je T-lymfoblastická buněčná linie původně odvozená z periferní krve devatenáctiletého pacienta s akutní lymfoblastickou leukémií v relapsu. Leukemické buňky reagovaly na ovlivnění pankracinem s inhibiční koncentrací IC_{50} $2,71 \pm 0,25 \mu\text{mol.l}^{-1}$, ne příliš odlišné od hodnoty IC_{50} stanovené pro buňky A549. Statisticky významný antiproliferační účinek pankracinu, jaký byl pozorován u adenokarcinomu plic A549, byl pozorován také u leukemické linie MOLT-4. Na rozdíl od buněčné linie A549 však byl rovněž pozorován statisticky významný efekt na pokles viability leukemických buněk. Životaschopnost buněk MOLT-4 byla snížena po ovlivnění nejmenší měřené koncentrace $2,5 \mu\text{mol.l}^{-1}$, vyšší dávka $20 \mu\text{mol.l}^{-1}$ pak vedla ke snížení životaschopných buněk MOLT-4 až na 20 %. Vzhledem k významné účinnosti pankracinu na viabilitu leukemických buněk při vyšších koncentracích bylo možné použít pro detekci procent buněk v jednotlivých fázích buněčného cyklu pouze nižší koncentrace 2,5; 5 a $10 \mu\text{mol.l}^{-1}$ po 24 h od ovlivnění a 2,5 a $5 \mu\text{mol.l}^{-1}$ po 48 h od ovlivnění pankracinem. Z literatury je známo, že leukemické buňky podléhají apoptotické buněčné smrti (Šalovská et al. 2018, Tichý et al. 2008, Muthná et al. 2012). Buňky MOLT-4 odumírají apoptotickým procesem v důsledku ionizujícího záření a dalších činidel vyvolávajících poškození DNA aktivací kaspázy-8 a -9 a uvolněním cytochromu c (Tichý et al. 2008). Naše

výsledky nejsou v rozporu s tímto pozorováním. Leukemické buňky MOLT-4 umíraly v důsledku aktivace apoptózy při aplikaci pankracinu $5 \mu\text{mol.l}^{-1}$ a to zvýšením aktivity efektorové kaspázy-3/7 a kaspázy -9 odpovědné za vnitřní apoptotickou mitochondriální dráhu a kaspázy-8 odpovědnou za vnější apoptotickou dráhu iniciovanou prostřednictvím receptorů smrti. Nejen tento experiment, ale současně také detekce apoptotických buněk značených Annexinem V a propidium jodidem (PI) ukázala na statisticky významný nárůst apoptotických buněk MOLT-4 po expozici pankracinem v koncentraci $10 \mu\text{mol.l}^{-1}$ v intervalu 24 h. Při aplikaci koncentrace $20 \mu\text{mol.l}^{-1}$ bylo již 50 % buněk buď v časné nebo pozdní fázi apoptózy. Aktivace signální dráhy ATM/Chk2/p53 byla popsána v buňkách MOLT-4 po expozici ionizujícím zářením (Řezáčová et al. 2008). Dále můžeme zmínit například cytotoxický účinek kyseliny valproové, který je navíc doprovázen aktivací p21 a zvýšenou produkcí fosforylovaného p53 na Ser392 (Muthná et al. 2012). V naší práci jsme se pokusili rozkrýt pozadí dějů vedoucí k apoptóze detekcí klíčových faktorů a proteinů a pozorovali jsme zvýšení hladiny proteinu p27, proapoptotického proteinu Bax a aktivaci MAP kinázy p38 prostřednictvím fosforylace na Thr 180 a Tyr 182. Tento proces se zdá být také provázen zvýšenou hladinou tumor supresorového proteinu p53 fosforylovaného na Ser 392.

Dosud nebyla publikována jiná studie naznačující molekulární mechanismus účinku alkaloidů montaninového typu čeledi Amaryllidaceae, ale vezmeme-li v potaz biosyntézu této skupiny alkaloidů, může být užitečné nahlédnout do již experimentálně ověřených studií alkaloidů podobných chemických struktur patřící do čeledi Amaryllidaceae. Haemanthamin jakožto α -krinan také patří do skupiny isochinolinových alkaloidů čeledi Amaryllidaceae a jeho biologická aktivita byla v nedávné době intenzivně zkoumána stejně jako děje k ní vedoucí (Cahlíková et al. 2021). Haemanthamin indukoval apoptózu v koncentraci $5 \mu\text{mol.l}^{-1}$ v buněčné linii Jurkat představující akutní leukémii T-lymfocytů s deficientním proteinem p53 (Havelek et al. 2014). Alkaloidy na bázi montaninové kostry lze navíc připravit přesmykem kruhového systému struktury haemanthaminu (Inubushi et al. 1960, Cedrón et al. 2009). Podrobnější data popisující detailněji mechanismus účinku haemanthaminu byly zveřejněny v roce 2018, autoři v této studii naznačují vazbu haemanthaminu k A místu velké ribozomální podjednotky a přeskupení rRNA, což následně vede k inhibici translace a v důsledku toho k potlačení růstu nádorových buněk (Pellegrino et al. 2018). Obecně lze zhodnotit, že jsou isochinolinové alkaloidy stále v centru vědecké pozornosti, avšak pro významnější využití těchto biologicky velmi účinných molekul v klinické praxi je potřeba ještě hlubší studium.

6 ZÁVĚR

Po úspěšné izolaci dostatečného množství vybraných montaninových alkaloidů, pankracinu a montaninu, je jedním z přínosů této práce stanovení jejich 50 % inhibiční koncentrace IC_{50} v devíti nádorových buněčných liniích a v nenádorové buněčné linii lidských plicních fibroblastů. Zjištění jejich nízké mikromolární účinnosti potvrdily i následující experimenty s vybraným zástupcem montaninových alkaloidů, pankracinem. Antiproliferační aktivita pankracinu byla pozorována u adherentních linií až po dobu 96 h. Cytostatický efekt byl potvrzen i v dalších experimentech s dvěma vybranými histotypově odlišnými buněčnými kulturami, konkrétně byl potvrzen u rezistentního adenokarcinomu plic A549 a u akutní lymfoblastické leukémie MOLT-4. Na leukemickou linii pankracin rovněž působil statisticky významně cytotoxicky. Dalším benefitem a odpovědí na jeden z cílů disertační práce je popsání vlivu pankracinu na distribuci buněčné populace v jednotlivých fázích cyklu u výše zmíněných vybraných buněčných linií. Po aplikaci pankracinu, který v měřených nízkých mikromolárních koncentracích vyvolával zástavu buněčného cyklu v G1/S fázi v buňkách adenokarcinomu plic A549, docházelo k aktivaci signální dráhy Akt/p27/pRb. Statisticky významný negativní dopad na viabilitu leukemických buněk byl způsobený apoptotickou odpovědí tohoto typu buněk, dokázaný jednak zvýšenou aktivitou kaspáz, ale také stanovením fosfatidylserinu na vnější cytoplazmatické membráně buněk. Klíčový mechanismus kontrolující programovanou buněčnou smrt leukemických buněk zahrnoval zvýšení hladiny tumor supresorového proteinu p53 fosforylovaného na serinu 392 a dalších proteinů, například p27 a Bax. Všechny cíle disertační práce, jež si tato práce stanovila, a které jsou uvedené v kapitole 1, se podařilo splnit.

Závěrem lze dodat, že klíčové fázi preklinického testování nových chemoterapeutik vždy předcházelo hlubší studium molekulárních mechanismů jejich cytostatické a cytotoxické aktivity. Pankracin, se svým silným inhibičním účinkem na proliferaci a životaschopnost nádorových buněk, může být jedním z potenciálních kandidátních léčiv používaných v terapii nádorových onemocnění.

7 SEZNAM PUBLIKACÍ NEZahrnutých DO TÉMATU DISERTACE

1. Magnetic nanoparticles of Ga-substituted ϵ -Fe₂O₃ for biomedical applications: magnetic properties, transverse relaxivity, and effects of silica-coated particles on cytoskeletal networks

Královec, K., Havelek, R., Koutová, D., Veverka, P., Kubíčková, L., Brázda, P., Kohout, J., Herynek, V., Vosmanská, A., Kaman, O.

Journal of Biomedical Materials Research Part A 2020, 108(7), 1563-1578.

IF2020 3,221, Q3 dle AIS

2. Bersavine: a novel bisbenzylisoquinoline alkaloid with cytotoxic, antiproliferative and apoptosis-inducing effects on human leukemic cells

Koutova, D., Kulhava, M., Havelek, R., Majorosova, M., Královec, K., Habartova, K., Hošťálková, A., Opletal, L, Cahlikova, L., Řezáčová, M.

Molecules 2020 25(4), 964.

IF2020 3,060, Q2 dle AIS

3. Substituted piperazines as novel potential radioprotective agents

Filipova, A., Marek, J., Havelek, R., Pejchal, J., Jelicova, M., Cizkova, J., Majorosova, M., Muckova, L., Kucera, T., Prchal, L, Psoťka, M., Zivna, N., Koutova, D., Sinkorova, Z., Rezacova, M., Tichy, A.

Molecules 2020, 25(3), 532

IF2020 3,060, Q2 dle AIS

4. Semisynthetic Derivatives of Selected Amaryllidaceae Alkaloids as a New Class of Antimycobacterial Agents

Maafi, N., Mamun, A. A., Jand'ourek, O., Maříková, J., Breiterová, K., Diepolťová, A., Konečná, K., Hošťálková, A., Hulcová, D., Kuneš, J., Kohelová E., Koutová D., Šafratová, M., Nováková, L., Cahlíková, L.

Molecules 2021, 26(19), 6023.

IF2020 3,060, Q2 dle AIS

8 SEZNAM CITACÍ POUŽITÉ LITERATURY

Uvedený seznam literatury obsahuje citace, které nejsou součástí komentovaných publikací.

Abbastabar, M., Kheyrollah, M., Azizian, K., Bagherlou, N., Tehrani, S.S., Maniati, M., Karimian, A. Multiple functions of p27 in cell cycle, apoptosis, epigenetic modification and transcriptional regulation for the control of cell growth: A double-edged sword protein. *DNA Repair*, 2018, 69, 63–72.

Al-Ejeh, F., Kumar, R., Wiegmanns, A., Lakhani, S. R., Brown, M. P., Khanna, K. K. Harnessing the complexity of DNA-damage response pathways to improve cancer treatment outcomes. *Oncogene*, 2010, 29(46), 6085-6098.

Al Shammari, L., Al Mamun, A., Koutová, D., Majorošová, M., Hulcová, D., Šafratová, M., Breiterová, K., Maříková, J., Havelek, R., Cahlíková, L. Alkaloid profiling of *Hippeastrum* cultivars by GC-MS, isolation of Amaryllidaceae alkaloids and evaluation of their cytotoxicity. *Records of Natural Products*, 2020, 14, 154–159.

Ambrosino, C., Nebreda, A.R. Cell cycle regulation by p38 MAP kinases. *Biol. Cell*, 2001, 93, 47–51.

Ashinuma, H., Takiguchi, Y., Kitazono, S., Kitazono-Saitoh, M., Kitamura, A., Chiba, T., Tada, Y., Kurosu, K., Sakaida, E., Sekine, I., Tanabe, N., Iwama, A., Yokosuka, O., Tatsumi, K. Antiproliferative action of metformin in human lung cancer cell lines. *Oncology reports*, 2012, 28(1), 8-14.

Banwell, M.G., Edwards, A.J., Jolliffe, K.A., Kemmler, M. An operationally simple and fully regiocontrolled formal total synthesis of the montanine-type Amaryllidaceae alkaloid (\pm)-pancracine. *Journal of the Chemical Society, Perkin Transactions 1*, 2001, 12, 1345–1348.

Bao, X., Cao, Y.X., Chu, W.D., Qu, H., Du, J.Y., Zhao, X.H., Ma, X.Y., Wang, C.T., Fan, C.A. Bioinspired total synthesis of montanine-type Amaryllidaceae alkaloids. *Angewandte Chemie International Edition*, 2013, 52, 14167–14172.

Bartek, J., Lukas, J. Mammalian G1-and S-phase checkpoints in response to DNA damage. *Current opinion in cell biology*, 2001,13(6), 738-747.

Breiterová, K., Koutová, D., Maříková, J., Havelek, R., Kuneš, J., Majorošová, M., Opletal, L., Hošťálková, A., Jenčo, J., Řezáčová, M., Cahlíková, L. Professor Einstein and their cytotoxic activity. *Plants*, 2020, 9, 137.

Cahlíková, L., Kawano, I., Řezáčová, M., Blunden, G., Hulcová, D., Havelek, R. The Amaryllidaceae alkaloids haemanthamine, haemanthidine and their semisynthetic derivatives as potential drugs. *Phytochem. Rev.*, 2021, 20, 303–323.

Cedron, J.C., Estévez-Braun, A., Ravelo, A., Gutiérrez, D., Flores, N., Bucio, M.A., Pérez-Hernández, N., Joseph-Nathan, P. Bioactive montanine derivatives from halide-induced rearrangements of haemanthamine-type alkaloids. Absolute configuration by VCD. *Organic Letters*, 2009, 11, 1491–1494.

Cedrón, J.C., Ravelo, A.G., León, L.G., Padrón, J.M., Estévez-Braun, A. Antiproliferative and structure activity relationships of Amaryllidaceae alkaloids. *Molecules*, 2015, 20, 13854–13863.

D’Arcy, M.S. Cell death: a review of the major forms of apoptosis, necrosis and autophagy. *Cell biology international*, 2019, 43(6), 582-592.

da Silva, A.F.S., de Andrade, J.P., Bevilaqua, L.R.M., de Souza, M.M., Izquierdo, I., Henriques, A.T., Zuanazzi, J.A.S. Anxiolytic-, antidepressant- and anticonvulsant-like effects of the alkaloid montanine isolated from *Hippeastrum vittatum*. *Pharmacology Biochemistry and Behavior*, 2006, 85, 148–154.

Evidente, A., Andolfi, A., Abou-Donia, A.H., Touema, S.M., Hammada, H.M., Shawky, E., Motta, A. (-)-Amarbellisine, a lycorine-type alkaloid from *Amaryllis belladonna* L. growing in Egypt. *Phytochemistry*, 2004, 65, 2113–2118.

Faes, S., Dormond, O. PI3K and AKT: unfaithful partners in cancer. *International journal of molecular sciences*, 2015, 16(9), 21138-21152.

Farinon, M., Clarimundo, V.S., Pedrazza, G.P., Gulko, P.S., Zuanazzi, J.A., Xavier, R.M., de Oliveira, P.G. Disease modifying anti-rheumatic activity of the alkaloid montanine on experimental arthritis and fibroblast-like synoviocytes. *European Journal of Pharmacology*, 2017, 799, 180–187.

Fresno-Vara, J.A., Casado, E., de Castro, J., Cejas, P., Belda-Iniesta, C., Gonzalez-Baron, M. PI3K/Akt signalling pathway and cancer. *Cancer Treat. Rev.*, 2004, 30, 193–204.

Golias, C.H., Charalabopoulos, A., Charalabopoulos, K. Cell proliferation and cell cycle control: a mini review. *International journal of clinical practice*, 2004, 58(12), 1134-1141.

Gordaliza, M. Natural products as leads to anticancer drugs. *Clinical and Translational Oncology*, 2007, 9(12), 767-776.

Govindaraju, K., Ingels, A., Hasan, M.N., Sun, D., Mathieu, V., Masi, M., Evidente, A., Kornienko, A. Synthetic analogues of the montanine-type alkaloids with activity against apoptosis-resistant cancer cells. *Bioorganic & medicinal chemistry letters*, 2018, 28, 589–593.

Guan, Y., Zhang, H., Pan, C., Wang, J., Huang, R., Li, Q. Flexible synthesis of montanine-like alkaloids: Revisiting the structure of montabuphine. *Organic & biomolecular chemistry*, 2012, 10, 3812–3814.

Havelek, R., Seifrtová, M., Královec, K., Bručková, L., Cahlíková, L., Dalecká, M., Vávrová, J., Řezáčová, M., Opletal, L., Bílková, Z. The effect of Amaryllidaceae alkaloids Haemanthamine and Haemanthidine on cell cycle progression and apoptosis in p53-negative human leukemic Jurkat cells. *Phytomedicine*, 2014, 21, 479–490.

Hong, A.W., Cheng, T.H., Raghukumar, V., Sha, C.K. An expedient route to montanine-type Amaryllidaceae alkaloids: Total syntheses of (-)-brunsvigine and (-)-manthine. *The Journal of Organic Chemistry*, 2008, 73, 7580–7585.

Inubushi, Y., Fales, H.M., Warnhoff, E.W., Wildman, W.C. Structures of montanine, coccinine, and manthine. *The Journal of Organic Chemistry*, 1960, 25, 2153–2164.

Ishizaki, M., Hoshino, O., Iitaka, Y. Total synthesis of montanine-type Amaryllidaceae alkaloids, which possess a 5, 11-methanomorphanthridine ring system, through cyclization with sodium bis (2-methoxyethoxy) aluminum hydride (SMEAH): The first stereoselective total syntheses of (±)-montanine, (±)-coccinine, (±)-O-acetylmontanine, (±)-pancracine, and (±)-brunsvigine. *The Journal of Organic Chemistry*, 1992, 57, 7285–7295.

Jin, J., Weinreb, S.M. Application of a stereospecific intramolecular allenylsilane imino ene reaction to enantioselective total synthesis of the 5,11-methanomorphanthridine class of Amaryllidaceae alkaloids. *Journal of the American Chemical Society* 1997, 119, 5773–5784.

Klener, P., Klener, P. Principy systémové protinádorové léčby. *Grada*, 2013, 9–41. ISBN: 978-80-2474171-0.

Klener, P., Klener, P. Nová protinádorová léčiva a léčebné strategie v onkologii. *Grada*, 2010, 40-41. ISBN: 978-80-247-2808-7.

Koutová, D., Maafi, N., Havelek, R., Opletal, L., Blunden, G., Řezáčová, M., Cahlíková, L. Chemical and Biological Aspects of Montanine-Type Alkaloids Isolated from Plants of the Amaryllidaceae Family. *Molecules*, 2020, 25(10), 2337.

Koutová, D., Havelek, R., Peterová, E., Muthná, D., Královec, K., Breiterová, K., Cahlíková, L., Řezáčová, M. Pancracine, a Montanine-Type Amaryllidaceae Alkaloid, Inhibits Proliferation of A549 Lung Adenocarcinoma Cells and Induces Apoptotic Cell Death in MOLT-4 Leukemic Cells. *International journal of molecular sciences*, 2021, 22(13), 7014.

Kovář J. Buněčná proliferace a mechanismy její regulace I. *Karolinum*, 2000, 14-15. ISBN: 80-7184-429-2.

Liang, J., Slingerland, J.M. Multiple roles of the PI3K/PKB (Akt) pathway in cell cycle progression. *Cell Cycle*, 2003, 2, 339–345 (2003)

Matveenko, M., Banwell, M.G., Willis, A.C. A chemoenzymatic total synthesis of the structure assigned to the alkaloid (+)-montabuphine. *Organic Letters*, 2008, 10, 4693–4696.

Masi, M., Van Slambrouck, S., Gunawardana, S., van Rensburg, M.J., James, P.C., Mochel, J.G., Heliso, P.S., Albalawi, A.S., Cimmino, A., van Otterlo, W.A.L., Kornienko, A., Green, I.R., Evidente, A. Alkaloids isolated from *Haemanthus humilis* Jacq., an indigenous South African Amaryllidaceae: Anticancer activity of coccinine and montanine. *South African Journal of Botany*, 2019, 126, 277–281.

Mondal, A., Gandhi, A., Fimognari, C., Atanasov, A.G., Bishayee, A. Alkaloids for cancer prevention and therapy: Current progress and future perspectives. *European journal of pharmacology*, 2019, 858, 172472.

Muthna, D., Soukup, T., Vavrova, J., Mokry, J., Cmielova, J., Visek, B., Jiroutová, A., Havelek, R., Suchanek, J., Filip, S., English, D., Rezacova, M. Irradiation of adult human dental pulp stem cells provokes activation of p53, cell cycle arrest, and senescence but not apoptosis. *Stem cells and development*, 2010, 19(12), 1855-1862.

Muthna, D., Vavrova, J., Lukasova, E., Tichy, A., Knizek, J., Kohlerova, R., Mazankova, N., Rezacova, M. Valproic acid decreases the reparation capacity of irradiated MOLT-4 cells. *Mol. Biol.*, 2012, 46, 110–116.

Ondroušková, E., Vojtěšek, B. Programmed cell death in cancer cells. *Klinická onkologie: časopis České a Slovenské onkologické společnosti*, 2014, 27, S7-S14.

Qing, Z.X., Huang, J.L., Yang, X.Y., Liu, J.H., Cao, H.L., Xiang, F., Cheng, P., Zeng, J.G. Anticancer and reversing multidrug resistance activities of natural isoquinoline alkaloids and their structure-activity relationship. *Current Medicinal Chemistry*, 2017, 25(38), 5088-5114.

Pagliosa, L.B., Monteiro, S.C., Silva, K.B., De Andrade, J.P., Dutilh, J., Bastida, J., Cammarota, M., Zuanazzi, J.A.S. Effect of isoquinoline alkaloids from two *Hippeastrum* species on in vitro acetylcholinesterase activity. *Phytomedicine* 2010, 17, 698–701.

Pandey, G., Banerjee, P., Kumar, R., Puranik, V.G. Stereospecific route to 5,11-methanomorphanthridine alkaloids via intramolecular 1,3-dipolar cycloaddition of nonstabilized azomethine ylide: Formal total synthesis of (±)-pancracine. *Organic Letters*, 2005, 7, 3713–3716.

Pearson, W.H., Lian, B.W. Application of the 2-azaallyl anion cycloaddition method to an enantioselective total synthesis of (+)-coccinine. *Angewandte Chemie International Edition*, 1998, 37, 1724–1726.

Pellegrino, S., Meyer, M., Zorbas, C., Bouchta, S.A., Saraf, K., Pelly, S.C., Yusupova, G., Evidente, A., Mathieu, V., Kornienko, A. The Amaryllidaceae alkaloid haemanthamine binds the eukaryotic ribosome to repress cancer cell growth. *Structure*, 2018, 26, 416–425.

Řezáčová, M., Vávrová, J. Molekulární mechanismy účinku ionizujícího záření. *Nucleus HK[®]2000*, 40-44, 52-62. ISBN: 978-80-87009-82-6.

Řezáčová, M., Tichý, A., Vávrová, J., Vokurková, D., Lukášová, E. Is defect in phosphorylation of Nbs1 responsible for high radiosensitivity of T-lymphocyte leukemia cells MOLT-4? *Leuk. Res.*, 2008, 32, 1259–1267.

Saha, S., Panigrahi, D.P., Patil, S., Bhutia, S.K. Autophagy in health and disease: A comprehensive review. *Biomedicine & Pharmacotherapy*, 2018, 104, 485-495.

Sha, C.K., Hong, A.W., Huang, C.M. Synthesis of aza bicyclic enones via anionic cyclization: Application to the total synthesis of (–)-Brunsvigine. *Organic Letters*, 2001, 3, 2177–2179.

Silva, A.F.S, Andrade, J.P., Machado, K.R.B., Rocha, A.B., Apel, M.A., Sobral, M.E.G., Henriques, A.T., Zuanazzi, J.A.S. Screening for cytotoxic activity of extracts and isolated alkaloids from bulbs of *Hippeastrum vittatum*. *Phytomedicine*, 2008, 15(10), 882 – 885.

Šalovská, B., Janečková, H., Fabrik, I., Karlíková, R., Čecháková, L., Ondrej, M., Link, M., Friedecký, D., Tichý, A. Radio-sensitizing effects of VE-821 and beyond: Distinct phosphoproteomic and metabolomic changes after ATR inhibition in irradiated MOLT-4 cells. *PLoS ONE*, 2018, 13, e0199349.

Tichý, A., Zášková, D., Pejchal, J., Řezáčová, M., Österreicher, J., Vávrová, J., Cerman, J. Gamma irradiation of human leukaemic cells HL-60 and MOLT-4 induces decrease in Mcl-1 and Bid, release of cytochrome c, and activation of caspase-8 and caspase-9. *Int. J. Radiat. Biol.*, 2008, 84, 523–530.

Van Goiestsenoven, G., Andolfi, A., Lallemand, B., Cimmino, A., Lamoral-Theys, D., Gras, T., Abou-Donia, A., Dubois, J., Lefranc, F., Mathieu, V., Kornienko, A., Kiss, R., Evidente A. Amaryllidaceae alkaloids belonging to different structural subgroups display activity against apoptosis-resistant cancer cells. *Journal of Natural Products*, 2010, 73, 1223–1227.

Vermeulen, K., Van Bockstaele, D.R., Berneman, Z.N. The cell cycle: a review of regulation, deregulation and therapeutic targets in cancer. *Cell proliferation*, 2003, 36(3), 131-149.

Wildman, W.C., Kaufman, C.J. Alkaloids of the Amaryllidaceae. III. Isolation of five new alkaloids from *Haemanthus* species¹. *Journal of the American Chemical Society*, 1955, 77, 1248–1252.

Wildman, W.C., Olesen, B. Biosynthesis of montanine. *Journal of the Chemical Society, Chemical Communications*, 1976, 14, 551.

Yang, H., Hou, S., Tao, C., Liu, Z., Wang, C., Cheng, B., Li, Y., Zhai, H. Rhodium-catalyzed denitrogenative [3 + 2] cycloaddition: Access to functionalized hydroindolones and the framework of montanine-type Amaryllidaceae alkaloids. *Chemistry-a European Journal*, 2017, 23, 12930–12936.

Zhang, Y., Wang, X., Han, L., Zhou, Y., Sun, S. Green tea polyphenol EGCG reverse cisplatin resistance of A549/DDP cell line through candidate genes demethylation. *Biomedicine & Pharmacotherapy*, 2015, 69, 285-290.